이학석사 학위논문

Structure and Properties of Quaternary Ca-Mg Aluminosilicate Glasses and Melts in Diopside ($CaMgSi_2O_6$)-Ca-Tschermakite ($CaAl_2SiO_6$) Join: High-resolution Solid-state ^{27}Al and ^{17}O NMR Study

사성분계 비정질 Ca-Mg 알루미노 규산염의 구조와 성질 (투휘석-Ca-처마카이트 계를 중심으로): 고해상도 고상 ^{27}Al 및 ^{17}O 핵자기 공명분광분석 연구

2010 년 2 월

서울대학교 대학원

자연과학대학 지구환경과학부

박 선 영

Structure and Properties of Quaternary Ca-Mg Aluminosilicate Glasses and Melts in Diopside ($CaMgSi_2O_6$)-Ca-Tschermakite ($CaAl_2SiO_6$) Join: High-resolution Solid-state ^{27}Al and ^{17}O NMR Study

사성분계 비정질 Ca-Mg 알루미노 규산염의 구조와 성질 (투휘석 - Ca-처마카이트 계를 중심으로) : 고해상도 고상 ^{27}Al 및 ^{17}O 핵자기 공명분광분석 연구

지도교수: 이성근

이 논문을 이학석사 학위논문으로 제출함

2009 년 12 월

서울대학교 대학원
자연과학대학 지구환경과학부
박 선 영

박선영의 이학석사 학위논문을 인준함.

2010 년 2 월

위 원 장 _____ 이 인 성 (인)

부위원장 _____ 허 영 숙 (인)

위 원 _____ 이 성 근 (인)

ABSTRACT

Whereas the structure of 'multi-component' silicate glasses and melts has implication for the properties of natural silicate magmas and relevant geochemical processes, little is known about their atomic structures due to lack of suitable experimental probes of amorphous 'multi-component' oxides. Whereas most of the progress in melt structure has been made for relatively simple binary and ternary silicate glasses, recent advances in high-resolution solid-state NMR begin to provide element specific and quantitative information of atomic configurations in multi-component silicate glasses including quaternary oxide glasses. Here we report the first experimental results of the effect of composition on the atomic structure of CaO-MgO-Al_2O_3-SiO_2 (CMAS) silicate glasses in diopside ($CaMgSi_2O_6$) and Ca-Tschermakite ($CaAl_2SiO_6$) pseudobinary join, a model system for basaltic magmas, using high-resolution 1D and 2D solid-state NMR. The ^{27}Al MAS NMR spectra for the CMAS glasses show that four-coordinated Al, $^{[4]}Al$ is predominant, demonstrating that Al^{3+} is a network former. The peak position moves toward a lower frequency approximately 4.7 ppm with increasing diopside content due to a increase in $Q^4(4Si)$ fraction with decreasing Al content. The result indicates that Al is surrounded only by bridging oxygens. The ^{27}Al 3QMAS NMR spectra show well resolved $^{[4]}Al$ and $^{[5]}Al$ in CMAS glasses. The fraction of $^{[5]}Al$ species increases with increasing diopside content (and thus with increasing Mg^{2+}). The structurally relevant quadrupolar coupling constant (C_q) and full width half maximum (FWHM) of $^{[4]}Al$ decrease with increasing diopside content, suggesting a decrease in topological disorder due to bonding angle and length distributions. The ^{17}O MAS NMR spectra for CMAS glasses qualitatively suggest that the fraction of non bridging oxygen (NBO) increases with increasing diopside content, consistent with the prediction form composition. The high-resolution ^{17}O 3QMAS NMR spectra show that three types of bridging oxygens

(BO; Si-O-Si, Al-O-Al, and Si-O-Al) and two types of NBO (Ca-NBO, and mixed {Ca, Mg}−NBO) are partially resolved. The local oxygen configurations in the glasses provide previously unknown details of the chemical and topological disorders in Ca-Mg aluminosilicate glasses. The significant fraction of the Ca-NBO peak is observed around -64 ppm in the glass at intermediate compositions (e.g., diopside : Ca-Tschermakite = 50 : 50), suggesting nonrandom distributions of Ca^{2+} and Mg^{2+} around NBO and BO, characterized with preferential partitioning of Ca^{2+} into NBO; Mg^{2+} is likely to have proximity to BO including Si-O-Al at intermediate compositions thus Mg^{2+} plays a preferential role as a charge-balancing cation, while Ca^{2+} can act as a network-modifying cation in the Ca-Mg aluminosilicate glasses studied here.

The observed structural changes in the CMAS glasses can account for the changes in macroscopic properties with composition. For example, the predominance of $^{[4]}$Al and its extensive mixing with Si as evidenced by the significant fractions of $^{[4]}$Al-O-$^{[4]}$Si is consistent with a negative experimental enthalpy of mixing for silicate glasses in diopside and Ca-Tschermakite join from solution calorimetry. As viscosity of silicate melts decreases exponentially with NBO fraction, while there is no available experimental data for the viscosity of silicate melts in the diopside-anorthite join, the observed increase in NBO fraction with increasing diopside content indicates a decrease in melt viscosity toward a diopside end-member.

Finally, the preferential partitioning of Ca^{2+} and Mg^{2+} between NBO and BO may results in a variation of activity coefficient of CaO and MgO, thus controlling composition of melts generated at the Mid-Ocean Ridge or Oceanic Islands. This preference also has strong implication for dissolution mechanisms of basalts in contact with aqueous fluids. Taking into consideration of stronger bond between network modifying cations and NBO (over charge-balancing cation and BO), Mg^{2+} in the basalts is likely to be dissolved easily. The results and methods

shed light on structure of multi-component oxide glasses and provide improved understanding their structure-property relations.

Keyword: basaltic magma, multi-component silicate glass, diopside-Ca-Tschermakite join, NMR, atomic structure

TABLE OF CONTENTS

LIST OF FIGURES

Fig. 7. ^{27}Al MAS NMR spectra for CaO-MgO-Al_2O_3-SiO_2 silicate glasses in pseudobinary join (diopside and Ca-Tschermakite) at 9.4 T with varying diopside content. Di is diopside ($CaMgSi_2O_6$) and CaTs is Ca-Tschermakite ($CaAl_2SiO_6$).

Fig. 8. FWHM of $^{[4]}Al$ in MAS dimension for CaO-MgO-Al_2O_3-SiO_2 silicate glasses diopside-Ca-Tschermakite pseudobinary join. Di is diopside and CaTs is Ca-Tschermakite. X_{Di} is the mole fraction of diopside.

Fig. 9. ^{27}Al 3QMAS NMR spectra for CaO-MgO-Al_2O_3-SiO_2 silicate glasses diopside-Ca-Tschermakite pseudobinary join at 9.4 T with varying diopside content. Di is diopside ($CaMgSi_2O_6$) and CaTs is Ca-Tschermakite ($CaAl_2SiO_6$). Contour lines are drawn at 5% intervals from relative intensities of 2% to 97%.

Fig. 10. The population of $^{[5]}Al$ for CaO-MgO-Al_2O_3-SiO_2 silicate glasses diopside-Ca-Tschermakite pseudobinary join. Di is diopside and CaTs is Ca-Tschermakite.

Fig. 11. The atomic structure of diopside and Ca-Tschermakite crystals. The left one is diopside and right one is Ca-Tschermakite.

Fig. 12. Total isotropic projection of ^{27}Al 3QMAS NMR spectra for CaO-MgO-Al_2O_3-SiO_2 silicate glasses diopside-Ca-Tschermakite pseudobinary join at 9.4 T. Di is diopside and CaTs is Ca-Tschermakite. (B) is magnification of (A).

Fig. 13. FWHM of $^{[4]}$Al in total isotropic projection of ^{27}Al 3QMAS NMR spectra for CaO-MgO-Al_2O_3-SiO_2 silicate glasses diopside-Ca-Tschermakite pseudobinary join at 9.4 T. Di is diopside and CaTs is Ca-Tschermakite.

Fig. 14. Quadrupolar coupling constant (C_q) of $^{[4]}$Al in CaO-MgO-Al_2O_3-SiO_2 silicate glasses diopside-Ca-Tschermakite pseudobinary join. Di is diopside and CaTs is Ca-Tschermakite.

Fig. 15. ^{17}O MAS NMR spectra for CaO-MgO-Al_2O_3-SiO_2 silicate glasses diopside-Ca-Tschermakite pseudobinary join, (B) for diopside glass and Ca-Tschermakite glass at 9.4 T. Di is diopside and CaTs is Ca-Tschermakite.

Fig. 16. ^{17}O 3QMAS NMR spectra for model quaternary aluminosilicate glasses (CaO: MgO: Al_2O_3: SiO_2=8.8: 18.9: 21.3: 51.0 wt%) at 9.4 T. Contour lines are drawn at 5% intervals from relative intensities of 3% to 98%.

Fig. 17. ^{17}O 3QMAS NMR for CaO-MgO-Al_2O_3-SiO_2 silicate glasses diopside-Ca-Tschermakite pseudobinary join at 9.4T with varying diopside content. Di is diopside and CaTs is Ca-Tschermakite. Contour lines are drawn at 5% intervals from relative intensities of 8% to 98% with added lines at 4%.

Fig. 18. Total isotropic projection of ^{17}O 3QMAS NMR spectra for CaO-MgO-Al_2O_3-SiO_2 silicate glasses diopside-Ca-Tschermakite pseudobinary join at 9.4 T with varying diopside content. Di is diopside and CaTs is Ca-Tschermakite.

Fig. 19. ^{17}O 3QMAS NMR spectrum for intermediate composition of diopside (Di)-Ca-Tschermakite (CaTs) pseudobinary join (Di : CaTs = 50 : 50) at 9.4 T. Contour lines are drawn at 5% intervals from relative intensities of 8% to 98% with added lines at 4%. A predicted spectrum of NBO peaks (in the isotropic projection) are also shown based on composition (Ca/(Ca+Mg)=0.67) using the random model is also shown.

Fig. 20. Normalized Raman spectra at room temperature for CaO-MgO-Al_2O_3-SiO_2 silicate glasses diopside-Ca-Tschermakite pseudobinary join. Di is diopside and CaTs is Ca-Tschermakite.

Fig. A1. ^{27}Al MAS spectra for Mg-aluminosilicate,. * refers to spinning side bands.

Fig. A2. ^{27}Al 3QMAS spectra for Mg aluminosilicate glasses at 9.4 T. Contour lines are drawn from 3% to 98% of relative intensity with a 5% increment.

Fig. A3. ^{27}Al 3QMAS NMR spectra for alumina thin film. Projections on the isotropic are also shown. (Lee et al., 2009) Contour lines are drawn at 5% intervals from 12% to 97% with added lines at 6%.

LIST OF TABLES

1. INTRODUCTION

Magmatic process of earth's interior such as partial melting, mantle convection and differentiation of mantle has been a matter of common interest (Baker et al., 1995; Ohtani, 1985; Presnall et al., 2002; Tarduno et al., 2009). The major component of the earth's interior is silicate glasses thus studies of silicate melts and glasses are essential for understanding of the diverse magmatic process. It needs to study for the thermodynamic properties and transport properties like enthalpy, entropy, density, viscosity and diffusivity to demonstrate magmatic process in earth's interior. There are many methods to study about the macro properties relevant to magmatic processes; there have been three general methods. The first method is to measure the macro properties like viscosity, heat capacity, density and other thermo dynamical properties directly. For example, viscosity of silicate melts and glasses (Giordano et al., 2008a; Neuville and Richet, 1991; Richet, 1984), density (Lange and Carmichael, 1987), thermodynamic properties (Bottinga and Richet, 1978; Navrotsky et al., 1983) and so on. Second method is theoretical calculation or modeling including quantum calculation (Asimow et al., 2001; Giordano et al., 2008b; Liang et al., 1997). Third method is the calculation from microscopic origins. The atomic and molecular structure of silicate melts and glasses is related to those thermodynamic and transport properties. For example, the viscosity exponentially decreases with increasing the fraction of non bridging oxygen in silicate melts (Lee et al., 2004). And the diffusivity and activity coefficient has different pattern along degree of disorder (Lee, 2005a). Previous study have shown lots of results about measuring macroscopic properties however

there is limitation to measure the properties of mantle melt directly due to difficulty of extreme condition like high pressure and temperature. Also it can be demonstrated origin of macroscopic properties through the calculated results from microscopic origin.

In this thesis we report the atomic structure of Ca-Mg aluminosilicate glasses in diopside and Ca-Tschermakite pseudobinary join relevant to natural basaltic melts. This thesis is composed of 4 sections and appendix. In section 2, Theoretical backgrounds of NMR spectroscopy and difficulty of analysis for multi-component glasses are briefly presented. It is difficult to analyze of atomic structure of multi-component glasses due to overlapping peak site stem from increasing of the statistical chemical bond with increasing number of chemical component. The high-resolution NMR spectroscopy provides element specific information to overcome difficulty of analysis for multi-component glasses. In section 3, the atomic structure of Ca-Mg aluminosilicate glasses in diopside and Ca-Tschermakite pseudobinary join, which is the major thesis in this paper. It includes glass synthesis, ^{27}Al MAS and 3QMAS NMR, ^{17}O MAS and 3QMAS NMR results and Raman spectroscopy. Multi nuclear MAS and 3QMAS NMR spectra show the change of atomic structure with composition. It is probed the change of macroscopic properties such as enthalpy of mixing and viscosity from those atomic structure information. In section 4, we propose several works to investigate atomic structure of multi-component glasses which are ^{43}Ca NMR study and synchrotron X-ray study. In appendix, the atomic structure of Mg aluminosilicate and amorphous alumina thin film are presented.

2. THEORETICAL BACKGROUND

2.1 Brief overview of high-resolution solid state NMR

Nuclear magnetic resonance (NMR) process occurs when the nuclear magnetic moment associated with a nuclear spin is placed in an external magnetic field. Using this process, NMR spectroscopy measure interaction between rf signal and spin relaxation of material. The signal of NMR spectroscopy is determined by atomic environment of specific atom for example, coordination number, bond length, bond angle and connectivity with neighbor atoms. NMR spectrum provides dynamic information between atoms and molecules occurring from nano scale to second scale. There are several factors of protecting NMR signal, for example dipolar coupling, chemical shift anisotropy and quadrupole moment. The chemical shift anisotropy means peak broadening due to variation of chemical shift depending on orientation of molecular. Many methods are suggested to decrease effect of protecting NMR signal. One of method for increasing peak resolution is MAS (magic angle spinning), it removes dipole-dipole interaction by fixing the angle between rotating sample and external magnetic field specific value (Levitt, 2001).

Despite using MAS method the peak broadening effect still remain for quadrupolar nuclei (nuclear spin number is larger than 1, for example ^{17}O, ^{27}Al, ^{11}B, etc.) because those have quadrupolar effect which is interaction between charge in nuclei and electric gradient. Another method, 3QMAS (triple quantum magic angle spinning) deduce the second order quadrupolar anisotropy. It provides detail

information for atomic structure with high-resolution. Figure 1 shows ^{27}Al MAS and 3QMAS spectra for Mg-aluminoborate glasses ($MgO:Al_2O_3:B_2O_3 = 2:1:2$) and $AlCl_3$ liquid. The ^{27}Al MAS spectrum of Mg-aluminoborate glasses is broader than that of $AlCl_3$ liquid. As mentioned above NMR observes the configuration of spins thus the spectrum for liquid is very sharp due to offset effect for liquid whereas the spectrum for solid is very broad. Solid state NMR experiment is more challenge than liquid state NMR for those broadening effect, especially for amorphous material. Figure 1 also shows that it is difficult to peak assignment due to overlapping peak of each Al species in 1D ^{27}Al MAS NMR whereas $^{[4]}Al$, $^{[5]}Al$, $^{[6]}Al$ is partially dissolved at -40, -23, -5 ppm in isotropic dimension in 3QMAS NMR spectra. The 3QMAS NMR spectrum shows better resolution than MAS NMR spectrum.

The chemical shift is major important term in NMR spectroscopy. The chemical shift is shielding of external magnetic field by electron surround target nuclei. Though the unit of NMR spectrum is frequency like other spectroscopy, it is expressed dimensionless ppm traditionally, which is divided relative shift to reference compound (usually liquid with same isotope) by larmor frequency of investigating nuclei. The 2D NMR spectrum demonstrates each of peak having two axes (MAS and isotropic dimension), each peak is presented by a contour line. 2D NMR spectrum is demonstrated projected direction of isotropic and the resolution of isotropic projection is higher than those of MAS (Duer, 2004). It applied to spin 5/2 nuclides, such as ^{27}Al and ^{17}O, to investigate coordination number and atomic configuration in aluminosilicate glasses (Lee and Stebbins, 2000), boro-silicate glasses (Lee et al., 2005b), and alumina thin film (Lee et al., 2009b). Also MQMAS

NMR is applied to spin 7/2 nuclides such as ^{43}Ca (Angeli et al., 2007; Dupree et al., 1997; MacKenzie et al., 2007) and low gamma nuclides (e.g. ^{25}Mg) (Shimoda et al., 2007).

The magnitude of magnetic field use the unit of tesla (T), figure 2 shows ^{27}Al MAS NMR spectrum for Ca-Tschermakite ($CaAl_2SiO_6$) glass at 9.4 T and 11.7 T. The peak of $^{[4]}Al$ is better resolved at 11.7 T as compared with that of 9.4 T due to the Al is quadrupolar nuclei. The peak of quadrupolar nuclei is broad by the second-order quadrupolar interactions at low magnetic field. In order to separate peaks from spinning side band and resolve better ^{27}Al MAS NMR was performed at high field.

2.2 Difficulty in getting structural information of multi-component amorphous materials from spectroscopic and scattering studies

Figure 3 shows the relation between the number of chemical component 'n' in the composition and number of statistical chemical bonding. In case of general light scattering experiment using photon, the chemical bond increase along 'n^2' with increasing 'n'. For example, the number of measuring bond in binary system is 4 and it is increased 4 times to 16 in quaternary system. Also it is difficult to resolve peaks due to overlapping each other. One of method solving this problem is NMR. The resolution is higher in NMR spectroscopy than other spectroscopy and XRD for multi-component glasses due to it provide element specific information. In spite of measuring chemical bonds increase along $_{n+1}C_2$ $[(n^2+n)/2]$ with increasing component. This suggests that it is difficult to analyze for multi-component glasses.

In addition there is barrier resolving peaks due to inhomogeneous broadening in case of amorphous material.

Figure 4 shows the hypothetical spectra representing the change with number of component in NMR spectrum. Figure 4A is hypothetical spectrum for single component crystal, there is one sharp peak whereas the peak of single component amorphous glasses is very broad in figure 4B. Figure 4C shows a spectrum for binary amorphous material and it shows overlapping three peaks due to increasing chemical bond. It is difficult to resolve peaks in the multi component system because of overlapping peaks indicating various atomic environments like figure 4D. As mentioned above, the analysis of atomic structure for multi-component amorphous materials remained unsolved problem because there was not suitable probe to resolve it. Even though it is seriously difficult to analyze spectroscopic data for multi component system because it has been limited by inhomogeneous broadening of spectrum or diffraction pattern brings an inability to unambiguously resolve characteristic features. In addition it is difficult to know clearly the reason of peak shift because many elements in multi component could affect each other.

Here we report the atomic structure of CaO-MgO-Al_2O_3-SiO_2 (CMAS) silicate glasses in diopside-Ca-Tschermakite pseudobinary join using high-resolution ^{27}Al NMR and ^{17}O NMR. We already solved partly the structure of multi component using a new experimental method MQMAS bring the breakthroughs in spectroscopic analysis. The results of CMAS pseudobinary glasses suggest the atomic structure of natural magma. In this study, we present the detail aluminum and oxygen environments for the CMAS pseudobinary glasses with varying MgO fraction using 1-D MAS and 2-D 3QMAS solid-state NMR. We will demonstrate

structural change with composition then we discuss the microscopic origins of macroscopic properties of CMAS pseudobinary glasses.

3. PROBING ATOMIC STRUCTURE OF MULTI-COMPONENT BASALTIC GLASSES USING SOLID-STATE NMR

3.1 Introduction

The earth's materials can be divided from single component to multi component system with number of component. The multi-component silicate glasses and melts is major material of glass, ceramic, and refractory and major composition of primary melts generated from the mantle (Herzberg, 2006; Presnall et al., 2002). Thus the structure of multi-component silicate melts and glasses can provide insights into the diverse macroscopic properties of natural melts and transport of magma in the earth interior (Giordano et al., 2008a; Webb and Knoche, 1995). Among the many interesting systems relevant to generation of primary melts from the mantle, the glass composition in the CaO-MgO-Al_2O_3-SiO_2 (CMAS) quaternary system is particularly important as it reflects a major fraction of the chemical composition of the mantle melt and serves as an important model system to describe phase relationships between lherzolite minerals and primary mantle melts (Presnall et al. 2002).

Batch melting and fractional melting models are mainly used to demonstrate generation of partial melt in mantle and lower crust. Batch melting model assuming upwelling with contacting residue demonstrate melting process in equilibrium thus

the composition of rock is maintained. Whereas fractional melting model assume separating with residue thus the composition of rock is changed continually (Langmuir et al., 1992). Previous study has shown that partial melting of peridotite experiment demonstrating the melt composition changes with temperature, pressure and melt fraction. The fraction of Al_2O_3 decreases and that of MgO and FeO increases with increasing melt fraction. When partial melts are generated, the fraction of Al_2O_3 is high at first due to several reasons. One of the reason is minerals including high Al_2O_3 melt first and the other reason is the composition change to maintain equilibrium between mantle rock and melt (Kushiro, 2001). The bath melting model has limit to explain partial melting experiment result and upwelling of mantle melts thus the fractional melting is used primarily to demonstrate partial melting (Iwamori, 1993).

The mantle melt is divided mid ocean ridge basalt (MORB) and oceanic island basalt (OIB) with generating geological condition. Table 1 is the composition of MORB in mid-Atlantic ridge, East-Pacific ridge, Indian ocean ridge and OIB in Mauna Kea and West Greenland. The mole fraction of SiO_2, CaO and MgO of MORB is higher than that of OIB. In the previous study the macroscopic properties of multi-component silicate glasses and melts change with composition thus it is expected the difference of macroscopic properties between MORB and OIB.

Many studies have performed experimentally and principally about the macroscopic property of multi-component silicate glasses and melts having insight for natural melt. Figure 5 shows the enthalpy of mixing of diopside ($CaMgSi_2O_6$) and Ca-Tschermakite ($CaAl_2SiO_6$) pseudobinary crystals and glasses. The enthalpy of mixing is positive for crystal and negative for glasses (Navrotsky et al., 1983).

The entropy of diopside is higher than that of Ca-Tschermakite for crystal and those are similar for amorphous (Richet et al., 1993). Figure 6 presents the viscosity of anorthite-diopside join (Del Gaudio and Behrens, 2009; Hofmeister et al., 2009; Neuville and Richet, 1991; Urbain et al., 1982). It is normalized by T_g (glass transition temperature) and the viscosity increases several orders of magnitude and the density also increases with an increase diopside content (Barbieri et al., 2004). Many studies have been performed about macro properties of multi-component as mentioned above whereas the study of atomic structure has been performed only about binary or ternary system (Mysen BO, 2005). Recent study has shown the structure of the simplest compound Al_2O_3 made by Al and O which is common elements in crust (Lee et al., 2009b) and the structure of multi-component silicate glasses has not been well understood yet. The atomic structure of Ca-Na aluminosilicate has been performed before (Lee and Sung, 2008) though the system is limited to demonstrate melting process in earth system due to the Na^+ content is higher than natural melt.

Here we report a study for CaO-MgO-Al_2O_3-SiO_2 pseudobinary glasses, which includes the diopside (Di, $CaMgSi_2O_6$) component and Ca-Tschermakite (CaTs, $CaAl_2SiO_6$) component for end-member. The CMAS pseudobinary system is commonly used to demonstrate the change of macroscopic properties of mantle melts with composition quantitatively and systematically (Gasparik, 1984; Navrotsky et al., 1983; Richet et al., 1993). The CMAS pseudobinary glasses was used as a model system of natural basaltic melt because the melting temperature of diopside and Ca-Tschermakite join is very low. Thus CMAS pseudobinary glasses can be the model of preliminary melt.

The quantitative analysis of complex quaternary system, which is more close to real system, is particularly challenging in experimental aspect. The composition including Mg^{2+} instead of Na^{+} is used in this study. Although it is difficult to analyze atomic structure due to complexity and broadening of peak caused from higher cation field strength of Mg^{2+} than Na^{+}, the study about atomic structure of CMAS pseudobinary can provide insight about natural basaltic magma. Here we report the atomic structure of CMAS pseudobinary glasses using high-resolution ^{27}Al NMR and ^{17}O NMR break through the difficulty of analysis for multi-component glasses.

3.2. Experimental method

Sample preparation A series of CMAS pseudobinary glasses along the diopside and Ca-Tschermakite join with 0, 25, 50, 75 and 100 mol% $CaAl_2SiO_6$ component have been studied. They were synthesized from carbonate ($CaCO_3$), and oxides (MgO, Al_2O_3 and SiO_2). The compositions of pseudobinary glasses are peralkaline CMAS [$xCaO : yMgO : (x-y)Al_2O_3 : (x+y)SiO_2$ (x=4, y=0, 1, 2, 3)](see table 2). The Al_2O_3, $CaCO_3$ and SiO_2 powder were dried at 400°C for 48 hours and MgO was dried at 1200°C for 2 hours. Each weighed powder was thoroughly mixed by grinding in an agate mortar, and then it was decarbonized in a Pt crucible at 800°C for 1 hour. Due to the melting temperature of $CaMgSiO_6$ is 1391°C and about 1500°C for $CaAl_2SiO_6$ thus the sample was melted above the respective melting temperature (1550~1600°C) for 1 hour, and finally quenched into glasses by plunging the bottom of the Pt crucible in a water bath. Approximately, 0.2 wt% of

cobalt oxide was added to enhance spin-lattice relaxation. Negligible weight loss (0.2~2.6%) was measured.

The sample for ^{17}O MAS and 3QMAS NMR were synthesized from carbonates ($CaCO_3$) and oxide reagents including ^{17}O-enriched SiO_2. The latter was prepared by hydrolyzing $SiCl_4$ in 20% ^{17}O-enriched water. $CaAl_2SiO_6$ glass was synthesized by 40% ^{17}O-enriched water. Approximately, 0.2 wt% of cobalt oxide was added to enhance spin-lattice relaxation. The mixtures were then fused in a Pt crucible for 1 h at 1600°C in an Ar atmosphere. The melt was quenched by removing the crucible from the furnace and manually lowering it into water.

NMR spectroscopy The ^{27}Al MAS NMR spectra of CMAS pseudobinary glasses were collected at two static magnetic fields on a Bruker Avance DSX 500 spectrometer (11.7 T) at a Larmor frequency of 130.284 MHz using a 4mm Bruker triple-resonance probe (Seoul National University, Korea) and on a Varian Solid NMR 400 system (9.4 T) at 104.229 MHz with a 3.2 mm Varian double resonance probe (Seoul National University, Korea). The recycle delay time for ^{27}Al MAS NMR at two fields was 1s with 0.5 (11.7 T) and 0.3 (9.4 T) μs rf pulse strength. The sample spinning speeds of 15 kHz (11.7 T) and 14 kHz (9.4 T) were used for the two fields. The 3QMAS was only performed at 9.4 T using a fast-amplitude modulation (FAM)-based shifted-echo pulse sequence (consisting of two hard pulses with durations of 3.0 and 0.6 μs and a subsequent soft pulse with a duration of 15μs). Approximately 2000 to 5000 scans were averaged to achieve the signal to noise ratio shown in the ^{27}Al MAS and 3QMAS NMR spectra.

The ^{17}O MAS and 3QMAS NMR spectra of CMAS pseudobinary glasses were collected on Varian Solid NMR 400 system (9.4 T) at a Larmor frequency of 54.229 MHz using a 4 mm Doty double-resonance probe (Seoul National University, Korea). The relaxation delay times for the ^{17}O MAS NMR were 1 s and the rf pulse strength is 0.5 μs. Sample spinning speeds of 14 kHz was used. In the 3QMAS NMR experiment at 9.4 T, the FAM (Fast Amplitude Modulation)-based shifted-echo pulse sequence (with a hard pulse of duration 4.5 μs for multiple quantum excitation and two 1.1 μs pulses for single quantum reconversion, and a soft pulse with a duration of approximately 20 μs and an echo time of approximately 500 μs (integer multiple of a rotor period) was used (Baltisberger et al., 1996; Madhu et al., 1999; Zhao et al., 2001). Approximately 12960 to 20000 scans were averaged to achieve the signal to noise ratio shown in the ^{17}O 3QMAS NMR spectra. The spectra are referenced to external tap water for both the fields.

3.3 Results and discussion

3.3.1 ^{27}Al and ^{17}O NMR results

^{27}Al MAS NMR Figure 7 shows ^{27}Al MAS NMR spectra for CMAS pseudobinary glasses with varying composition at 9.4 T. Di means diopside and CaTs means Ca-Tschermakite, the number of right side indicates each percents. $^{[4]}Al$ is predominant at about 60 ppm in all samples, and the line shapes show asymmetric extra intensity at lower frequencies, which suggests that the chemical shift distribution is predominant over the quadrupolar broadening. Also inhomogeneous broadening is

observed due to structural disorder of amorphous materials. The predominant $^{[4]}$Al in all samples means that there is no structural change in nearest neighbor atom around Al due to Al^{3+} acts as a network forming cation (Allwardt et al., 2003; Barbieri et al., 2004). As the diopside content increases from 0 ($CaAl_2SiO_6$) to 75% ($CaMgSi_2O_6$), the peak position moves about 4.7 ppm from 56.2 to 51.5 ppm. This result is consistent with a trend in ternary silicate glasses from ^{27}Al MAS NMR for Ca-aluminosilicate in previous study (Lee and Stebbins, 2003) and it indicates that Q^4(4Si) increases with increasing Si fraction in CMAS pseudobinary glasses(Q^4(4Si) means that all of tetrahedral around Al is Si with all of BOs). In spite of the NBO fraction of CMAS pseudobinary glasses is dramatically changes along the composition, the coordination numbers of Al less changes. It means most of Al are surrounded BO instead of NBO (Allwardt et al., 2003).

The change of bond length and bond angle in atomic environment induce the change of peak width and it can be a degree of disorder in amorphous materials (Lee et al., 2005a; Lee and Stebbins, 1999). Figure 8 shows the full width half maximum (FWHM) of CMAS pseudobinary glasses decreases with increasing diopside content (54.5 ppm at diopside=0 and 43.9 ppm at diopside=0.75). As the fraction of Mg^{2+} increases, the degree of disorder in the system can be increasing while the trend of FWHM shows contrast results. That means 1D MAS NMR spectrum is not enough to explain change of spectrum because the quadrupolar coupling constant (C_q) affecting the peak width can be change with composition. Thus it needs to perform the supplemental experiment; 3QMAS NMR.

^{27}Al 3QMAS NMR Figure 9 shows ^{27}Al 3QMAS NMR spectra that successfully resolve the $^{[4]}$Al and $^{[5]}$Al not shown in 1D MAS NMR spectra. All spectra show that $^{[4]}$Al are major Al species and $^{[5]}$Al is clearly observed around -24 ppm in isotropic dimension. The peak shapes are very similar while the peak width in MAS dimension decreases with increasing diopside content. Figure 10 shows the population of $^{[5]}$Al changes with composition, which means that topological disorder increase in atomic structure. Ca-Tschermakite is single chain silicate thus there is $^{[4]}$Al and $^{[6]}$Al as shown figure 11 whereas $^{[4]}$Al and $^{[5]}$Al are presented in $CaAl_2SiO_6$ glasses due to topological disorder. As increasing Mg^{2+} which is a network modifying cation, the $^{[5]}$Al is generated then distance of Al-O or Al-O-Al bond angle change affecting the structure medium range order.

Figure 12 shows total isotropic projection of ^{27}Al 3QMAS NMR spectra for CMAS pseudobinary glasses. Figure 12A shows there are $^{[5]}$Al and $^{[6]}$Al in CMAS pseudobinary glasses. Figure 10B is magnification of figure 12A. The peak position of $^{[4]}$Al moves to higher frequency from -42.44 ppm ($Di_{75}CaTs_{25}$) to -46.25 ppm (CaTs). The trend in the isotropic projections provides a consistent result with MAS spectrum, the peak position shifts toward higher frequency in the 3QMAS isotropic dimension with increasing diopside content. Figure 13 shows the FWHM of $^{[4]}$Al in total isotropic dimension decrease with an increasing diopside content. It was founded that the degree of disorder decrease with an increase diopside content.

Figure 14 shows quadrupolar coupling constant (C_q) of $^{[4]}$Al for CMAS pseudobinary glasses at 9.4 T with varying composition. The C_q is one of the structurally relevant NMR parameters that denotes the magnitude of quadrupolar interactions between quadrupole moment of nuclei and electric field gradients

generated by surrounding electrons. The C_q of $^{[4]}$Al in CMAS pseudobinary glasses increases with increasing diopside content from 6.27 MHz to 6.98 MHz, suggesting larger distortion of $^{[4]}$Al polyhedral for low diopside content composition (Ghose and Tsang, 1973). As increasing diopside content, the isotropic chemical shift and FWHM of $^{[4]}$Al decreases, implying an decrease in topological entropy stemming from bond length and width distribution (Lee, 2004). These results contrast with those of population of $^{[5]}$Al in CMAS pseudobinary glasses. The population of $^{[5]}$Al suggests the Mg^{2+} perturbs the network whereas FWHM in total isotropic dimension and C_q indicate decreasing topological entropy. This means bond length and bond angle are ordered in $CaMgSi_2O_6$ than $CaAl_2SiO_6$ glasses.

^{17}O MAS NMR Figure 15 shows the ^{17}O MAS NMR spectra for CMAS pseudobinary glasses. The peak shape and position of ^{17}O NMR spectrum changes with atomic structure around oxygen, the atomic environment around oxygen is determined from that of information in multi component silicate glasses (Lee and Sung, 2008). And it can be confirmed structural changes directly from ^{17}O NMR spectra which provide the fraction of BO (e.g. Al-O-Si, Al-O-Al, Si-O-Si) and NBO (e.g., Si-O-Ca) in multi-component silicate glasses (Lee, 2005a). In spite of ^{17}O NMR experiment is very challenging because it is difficult to synthesis ^{17}O enriched sample and oxygen nuclei has low gyromagnetic ratio, ^{17}O NMR is very useful to study about earth interior because the macroscopic properties can be calculated from the atomic structure information obtained by ^{17}O NMR, such as activity coefficient topological entropy, and diffusivity involved in generation and transport of melt (Lee, 2005b). Figure 15A shows ^{17}O MAS spectra for CAMS

pseudobinary glasses and figure 15B shows tremendous change of oxygen environment with composition. ^{17}O MAS NMR spectrum shows presence of Ca-NBO at 99 ppm and the peaks of Al-O-Al overlapped with Al-O-Si in Ca-Tschermakite ($CaAl_2SiO_6$) glass. The fraction of NBO increases with increasing diopside content and there is only Si-O-Si and {Ca, Mg}-NBO in diopside ($CaMgSi_2O_6$) glass.

Both of the diopside and Ca-Tschermakite are single chain silicates (Ca^{2+}:Al^{3+} = 1:1) as shown figure 11 and NBO/T are 2 whereas previous study has shown that the NBO fraction is much high in those system (Stebbins and Xu, 1997). ^{27}Al MAS spectra in this study probe all of Al atom is surrounded by BO (Allwardt et al., 2003). From those results, the Ca-NBO in figure 15 is Ca-O-Si not Ca-O-Al. The bond preference of NBO is proved by quantum chemical calculation. The bond energy of Ca-O-Al is much higher (about 100 kJ) than Ca-O-Si (Lee and Stebbins, 2006). Recent study revealed directly the fraction of Ca-O-Al decrease with increasing Si content through a double resonance $\{^{17}O\}^{27}Al$ HMQC NMR experiment (Lee et al., 2009a). BOs and NBOs are overlapped in O-17 MAS NMR spectra except Ca-NBO in Ca-Tschermakite thus it is difficult to analyze the fraction of BO and NBO quantitatively. It needs high-resolution 2D ^{17}O 3QMAS NMR to analyze qualitatively.

^{17}O 3QMAS NMR Figure 16 shows ^{17}O 3QMAS NMR for model quaternary aluminosilicate (CaO: MgO: Al_2O_3: SiO_2=8.8: 18.9: 21.3: 51.0 wt%) resolving four different oxygen environments including Si-O-Si, Al-O-Al, Al-O-Si and {Ca, Mg}-NBO. The peak position of Si-O-Si, Al-O-Al, Al-O-Si and mixed NBO ({Ca, Mg}-

O-Si) is about -51, -17, -35 and -30 ppm in isotropic dimension, respectively (Lee et al., 2005a). The well resolved ^{17}O 3QMAS NMR spectrum for model quaternary silicate provides a ground for quantitative analysis of ^{17}O 3QMAS NMR for CMAS silicate glasses in pseudobinary join (diopside and Ca-Tschermakite).

Figure 17 shows ^{17}O 3QMAS NMR spectra for CMAS pseudobinary glasses at 9.4 T with varying diopside content providing considerably enhanced resolution among the O-atom sites as compared with ^{17}O MAS NMR spectra. The oxygen environment of CMAS pseudobinary glasses change with composition as shown Figure 17. The peak position of Al-O-Al and Al-O-Si in Ca-Tschermakite glass is about -35 and -41 ppm in isotropic dimension respectively. The proportion of each of BO is about 38 $\pm$ 5% for Al-O-Al and 62 $\pm$ 5% for Al-O-Si (Lee and Stebbins, 2002). It is note that Ca-NBO is well resolved at -63.5 ppm in isotropic dimension. The Si-O-Si peaks are shown around -51 ppm in isotropic dimension, the Al-O-Al peaks are reduced gradually and the mixed {Ca, Mg}-NBO peaks increase with an increase in X_{Di} (the mole fraction of diopside in CMAS pseudobinary glass). The chemical shielding of the mixed {Ca, Mg}-NBO peak decrease with diopside content (the peak shifts to a lower frequency in isotropic dimension). The peaks of Si-O-Si and {Ca, Mg}-NBO are remained in diopside glass (X_{Di}=1) around -40 and -51 ppm in isotropic dimension. Note that the peak assignment is based on the previous reports on binary silicates and ternary Ca-Mg aluminosilicate glasses (Allwardt and Stebbins, 2004; Lee and Stebbins, 2002). The chemical shielding of the mixed NBO peak decreases with diopside content and chemical shift dispersion increase. This result implies extensive mixing between Ca^{2+} and Mg^{2+} around the NBO (Lee and Sung, 2008). Figure 18 shows the total isotropic projection of ^{17}O

3QMAS NMR spectra for CMAS pseudobinary glasses. The resolution of ^{17}O 3QMAS NMR spectra is higher than MAS spectra however peaks are still overlapped. Ca-NBO is partially resolved in right side of spectrum and it is shown that the intensity of Si-O-Si decreases with increasing diopside content. Also Al-O-Al, Al-O-Si and Mg-NBO are partially resolved in CMAS pseudobinary glasses.

Figure 17 shows that Ca-NBO peak still remained at around -64 ppm in isotropic dimension in intermediate composition (Di : CaTs =50 : 50) of which Mg/Ca is 0.5. It means that the mixing behavior of CMAS pseudobinary glasses is nonrandom. Previous study has shown the simplest model to confirm the random mixing behavior between diopside and Ca-Tschermakite glasses. It was assumed that there are statistical distributions of three Ca and Mg cations surrounding each NBO, there are four possible species which are 3Ca-NBO, 2Ca1Mg-NBO, 1Ca2Mg-NBO, 3Mg-NBO. The peak position and width of Ca-NBO is predicted from Ca-Tschermakite, that of Mg-NBO is predicted from enstatite in previous study (Allwardt and Stebbins, 2004) and that of other species is estimated using numerical means. The predicted peak positions of each NBO are -67, -56, -46 and -36 respectively and the predicted percentages of each NBO species are

$$\begin{aligned} X_{3Ca} &= x^3 \\ X_{2CaMg} &= 3x^2(1-x) \\ X_{Ca2Mg} &= 3x(1-x)^2 \\ X_{3Mg} &= (1-x)^3 \end{aligned} \qquad (1)$$

Where x=Ca/(Ca+Mg) and this value is change from 1 to 0.5 in CMAS pseudobinary glasses. Figure 19 shows the ^{17}O 3QMAS NMR spectrum for intermediate composition of CMAS pseudobinary glasses ($Di_{50}CaTS_{50}$, diopside : Ca-Tschermakite = 50 : 50) and a hypothetical spectrum for NBO species including 3Ca-NBO, 2CaMg-NBO, Ca2Mg-NBO and 3Mg-NBO with random distribution. Ca/(Ca+Mg) change with composition from 0 to 1 in CAMS pseudobinary glasses and that is 0.67 in $Di_{50}CaTS_{50}$. The calculated percentage of each NBO using equation (1) is 29.5, 55.5 22.3 and 3.7 % in the intermediate composition as shown figure 19. The peak maximum of total NBO in hypothetical spectrum is about -56 ppm whereas that of 2D ^{17}O 3QMAS NMR spectrum is about -64 ppm as presented figure 19, suggesting nonrandom distribution of each NBO species. This ^{17}O 3QMAS NMR spectrum for $Di_{50}CaTS_{50}$ showing peak maximum at Ca-NBO site suggests two possibilities. First, there are less mixed {Ca, Mg}-NBO (2CaMg-NBO, Ca2Mg-NBO) and Mg-NBO overlapped with Al-O-Al peak. Second, Mg^{2+} prefers BO than NBO, Ca-NBO is predominant in NBO species. Assuming later possibility is correct, the preferential partitioning of Ca and Mg between NBO and BO (Al-O-Al, Al–O–Si) in CMAS pseudobinary glasses can be expressed by a quasi-equilibrium expression given below

Ca----Al-O-Al + Mg-NBO = Mg----Al-O-Al + Ca-NBO (2)

Ca----Al-O-Si + Mg-NBO = Mg----Al-O-Si + Ca-NBO (3)

The direction of above reactions is left to right basis on the preference of NBO. Ca^{2+} and Mg^{2+} compete each other and the primary role of Ca^{2+} may be as a

network-modifying cation near the NBO, while that of Mg^{2+} is as a charge-balancing cation in CMAS pseudobinary glasses.

3.3.2 Raman spectroscopy

The polymerization of silicate glasses and melts plays a critical role in their properties. Raman spectroscopy as well as NMR has been widely used to investigate changes in polymerization of silicate glasses (McMillan et al., 1982; Mysen et al., 2003; Neuville et al., 2008b). Figure 19 shows the Raman spectra of CMAS pseudobinary glasses. There are two groups of Raman mode in silicate glasses, which are Si-O-Si bending vibration between 400 and 750 cm^{-1} and Si-O stretching vibration between 800 and 110 cm^{-1}. The frequencies of stretching mode are related to the degree of polymerization Si tetrahedron, each of frequencies are 850(Q^0), 900(Q^1), 1000(Q^2) and 1100(Q^3) cm-^{1}. (McMillan, 1984) Q^n means SiO_4 tetrahedron with 'n' bridging oxygen. Figure 19 shows few change in stretching mode, while systematic change in bending mode (400~800 cm^{-1}). Q^0 and Q^1 decrease while Q^2 and Q^3 increase with decreasing diopside component, which means degree of polymerization decreases. This is because the NBO fraction increases due to perturbation of Mg^{2+} in diopside component as shown ^{17}O 3QMAS NMR spectrum. Also we observe that the frequency of Si-O-Si bending shifts to lower frequency with increasing Al_2O_3 content, which means the bond length and bond angle of Si-O-Si changes with composition. These results means that the degree of polymerization and bond length, bond angle are change with composition.

3.3.3 Implication for macroscopic properties and geophysical process

The atomic structure of CMAS pseudobinary glasses provides implications for several macroscopic properties and geophysical process. First of all, previous study has shown that the enthalpy of mixing of CMAS pseudobinary glasses is negative whereas that of crystalline materials is positive (Navrotsky et al., 1983) which means that the diopside phase and Ca-Ts phase are separated in crystal and they are mixed in glass. The Al^{3+} is in tetrahedral site and octahedral site of half rate in $CaAl_2SiO_6$ crystal. When the Ca-Tschermakite and diopside mix together, the Al^{3+} in tetrahedral in Ca-Ts is a little bit easy to exchange with Si tetrahedral whereas it is hard to exchange the Al^{3+} in octahedral site with Mg^{2+} in octahedral site in diopside because there are lattice difference due to difference of atomic distance (Al-O is 1.947 Å and Mg-O is 2.115 Å). The bond of Al^{3+} octahedral site is broken and distorted thus there are $^{[4]}$Al and $^{[5]}$Al not $^{[6]}$Al in $CaAl_2SiO_6$ glasses as shown figure 9. From this result we can conclude that it is easier to mix together in glass than crystal, the enthalpy of mixing is negative in glass. These results has implication for generation of basaltic melt. As natural basaltic melt is generated in the earth's interior, the composition of primary melt can be represented as CMAS pseudobinary glass due to the melting point of that system is the lowest. The negative enthalpy of mixing of CMAS pseudobinary glasses indicates two systems can be mixed more easily.

Second implication is about viscosity affecting the transport mantle melt in earth's interior. It has been known the viscosity decrease with increasing NBO in silicate glass and melts as mentioned above (Del Gaudio and Behrens, 2009;

Hofmeister et al., 2009; Neuville and Richet, 1991; Urbain et al., 1982), however the NBO fraction of those system is predicted by calculation. Here we report the experimental value of NBO fraction directly from ^{17}O 3QMAS NMR spectrum. We can conclude that difference of viscosity between diopside and Ca-Ts is stem from NBO fraction as shown figure 17. We can find the proportion of NBO is larger in $CaMgSi_2O_6$ than $CaAl_2SiO_6$ glasses. Thus viscosity increases with increasing diopside content in CMAS pseudobinary glasses. Viscosity is the transport property affecting melt migration thus basaltic melt in the earth's interior transport easier with composition that is high diopside content.

Third, the atomic structure has also implication for geophysical process such as dissolution of igneous rock. The rainwater or underground water infiltrate into igneous rock such as basalt then the minerals in that of rock react with waters; that is dissolution by water. There are alkaline earth's cation such as Basalt is CMAS multi component silicate Ca^{2+} extract more easily than Mg^{2+} because Ca^{2+} connects with NBO whereas Mg^{2+} connects with BO and the bond energy of BO is higher than that of NBO. The bond preference of NBO also affects the dissolution process in earth.

4. FURTHER STUDY

4.1 ^{43}Ca MAS and 3QMAS NMR

Alkaline earth cation, Ca^{2+} is abundant element in the magmatic liquids. Most studies on their chemical structures have been focused on SiO_4 and AlO_4 tetrahedral

networks, whereas the local environments around the divalent cations have been a question to understand amorphous structures. ^{27}Al and ^{17}O NMR is not enough to explain the mechanism along the changing composition. It is found that Ca^{2+} prefers NBO from ^{17}O 3QMAS NMR spectrum, however it needs obvious evidence. Also we want to know what the role of Ca^{2+} whether a network modifying cation or a charge balancing cation. We expect that ^{43}Ca NMR spectra could distinguish the network modifying Ca^{2+} and charge balancing Ca^{2+}.

NMR studies on such cation have been suppressed because of low natural abundance (0.145% for ^{43}Ca) and low gyromagnetic ratio. Despite ^{43}Ca NMR study is very challenging, through the ^{43}Ca NMR study we could obtain information of coordination number for the system (Shimoda et al., 2007). And through the coordination number or NMR parameter (e.g. C_q) we can predict Ca-O distance. From these results we could know the structure for diopside-Ca-Ts join system (Laurencin et al., 2008). Thus we want to report the Ca^{2+} environments in several geologically relevant silicate glasses using high-resolution MAS and 3QMAS NMR spectroscopy. It is expected that changing composition from diopside to Ca-Ts chemical shift of ^{43}Ca could be changed.

4.2 synchrotron study: X-ray absorption spectroscopy

Natural melts in the earth interior include about 10% FeO or Fe_2O_3 which are paramagnetic substance. Paramagnetic substances contain localized unpaired electrons, which couple to surrounding nuclei through the hyperfine interactions. Since the electron Zeeman states are unequally populated, and the electron

relaxation is very fast, the overall effect is to shift the nuclear spin resonances. (Levitt, 2001) Thus it needs another method to analyze the atomic structure of nearest composition of natural melts which include 10% FeO or Fe_2O_3. One of the effective methods is X-ray absorption spectroscopy, which provides information about atomic distance, coordination number, and local symmetry. We will perform the EXAFS (extended X-ray absorption fine structure) or XANES (X-ray absorption near edge scattering) then it will be possible to demonstrate the atomic structure of natural melts. Previous XANES study has shown there was structural rearrangement of CMAS silicate melts and glasses at high temperature (Neuville et al., 2008a) and another studies has shown XANES study about speciation of Fe in silicate glasses and melts (Wilke et al., 2007) however their system was not similar with natural basaltic melts. Thus we try to perform EXAFS or XANES experiment about CMAS pseudobinary glasses including 5~10 % FeO or Fe_2O_3. It is also expected to analysis the change of atomic structure with pressure using diamond anvil cell for multi-component silicate glasses from the atomic structure is probed using EXAFS or XANES.

5. CONCLUSION

From the experimental data presented here, an insight into multi component silicate glasses can be obtained with CMAS pseudobinary glasses in this study. The ^{27}Al MAS NMR spectra for the CMAS pseudobinary glasses show that four-coordinated Al is predominant, which demonstrate that Al^{3+} is a network forming cation. The peak position moves toward lower frequency with increasing diopside content due to an increase in Q^4(4Si) fraction with increasing Si content,

indicating that Al is surrounded only by bridging oxygen. The quadrupolar coupling constant (C_q) and FWHM of $^{[4]}$Al decreases with increasing diopside content, indicating a decrease of topological disorder. ^{17}O MAS NMR spectra for CMAS pseudobinary glasses qualitatively suggest that the NBO fraction increases with increasing diopside content. The nonrandom distribution of Ca-NBO and Mg-NBO indicates NBO prefers Ca^{2+} than Mg^{2+}. Mg^{2+} has proximity to Si-O-Al at intermediate composition thus Mg^{2+} plays a preferential role as a charge-balancing cation, while Ca^{2+} can act as a network-modifying cation in the Ca-Mg aluminosilicate glasses. The observed structural changes in the CMAS glasses can account for the changes in macroscopic properties with composition. For example, the predominance of $^{[4]}$Al and its extensive mixing with Si as evidenced by the significant fractions of $^{[4]}$Al-O-$^{[4]}$Si is consistent with a negative experimental enthalpy of mixing for silicate glasses in diopside and Ca-Tschermakite join from solution calorimetry. As viscosity of silicate melts decreases exponentially with NBO fraction, while there is no available experimental data for the viscosity of silicate melts in the diopside-anorthite join, the observed increase in NBO fraction with increasing diopside content indicates a decrease in melt viscosity toward a diopside end-member.

Finally, the preferential partitioning of Ca^{2+} and Mg^{2+} between NBO and BO may results in a variation of activity coefficient of CaO and MgO, thus controlling composition of melts generated at the Mid-Ocean Ridge or Oceanic Islands. This preference also has strong implication for dissolution mechanisms of basalts in contact with aqueous fluids. Taking into consideration of stronger bond between network modifying cations and NBO (over charge-balancing cation and BO), Mg^{2+} in the basalts is likely to be dissolved easily. The results and methods shed light on structure of multi-component oxide glasses and provide improved understanding their structure-property relations.

REFERENCE

Allwardt, J.R., Lee, S.K., and Stebbins, J.F., 2003, Bonding preferences of non-bridging O atoms: Evidence from O-17 MAS and 3QMAS NMR on calcium aluminate and low-silica Ca-aluminosilicate glasses, American Mineralogist, v. 88, p. 949-954.

Allwardt, J.R., and Stebbins, J.F., 2004, Ca-Mg and K-Mg mixing around non-bridging O atoms in silicate glasses: An investigation using O-17 MAS and 3QMAS NMR, American Mineralogist, v. 89, p. 777-784.

Angeli, F., Gaillard, M., Jollivet, P., and Charpentier, T., 2007, Contribution of Ca-43 MAS NMR for probing the structural configuration of calcium in glass, Chemical Physics Letters, v. 440, p. 324-328.

Asimow, P.D., Hirschmann, M.M., and Stolper, E.M., 2001, Calculation of peridotite partial melting from thermodynamic models of minerals and melts, IV. Adiabatic decompression and the composition and mean properties of mid-ocean ridge basalts, Journal of Petrology, v. 42, p. 963-998.

Baker, M.B., Hirschmann, M.M., Ghiorso, M.S., and Stolper, E.M., 1995, Compositions of near-solidus peridotite melts from experiments and thermodynamic calculations, Nature, v. 375, p. 308-311.

Baltisberger, J.H., Xu, Z., Stebbins, J.F., Wang, S.H., and Pines, A., 1996, Triple-quantum two-dimensional Al-27 magic-angle spinning nuclear magnetic resonance spectroscopic study of aluminosilicate and aluminate crystals and glasses, Journal of the American Chemical Society, v. 118, p. 7209-7214.

Barbieri, L., Corradi, A.B., Lancellotti, I., Leonelli, C., and Montorsi, M., 2004, Experimental and computer simulation study of glasses belonging to diopside-anorthite system, Journal of Non-Crystalline Solids, v. 345, p. 724-729.

Bottinga, Y., and Richet, P., 1978, Thermodynamics of liquid silicates, a preliminary-report, Earth and Planetary Science Letters, v. 40, p. 382-400.

Del Gaudio, P., and Behrens, H., 2009, An experimental study on the pressure dependence of viscosity in silicate melts, Journal of Chemical Physics, v. 131.

Duer, M.J., 2004, Solid-state NMR spectroscopy

Dupree, R., Howes, A.P., and Kohn, S.C., 1997, Natural abundance solid state Ca-43 NMR, Chemical Physics Letters, v. 276, p. 399-404.

Gasparik, T., 1984, Experimentally determined stability of clinopyroxene + garnet + corundum in the system CaO-MgO-Al_2O_3-SiO_2, American Mineralogist, v. 69, p. 1025-1035.

Ghose, S., and Tsang, T., 1973, Structural dependence of quadrupole coupling-constant e2qq/h for al-27 and crystal-field parameter-d for Fe^{3+} in aluminosilicates, American Mineralogist, v. 58, p. 748-755

Giordano, D., Potuzak, M., Romano, C., Dingwell, D.B., and Nowak, M., 2008a, Viscosity and glass transition temperature of hydrous melts in the system $CaAl_2Si_2O_8$-$CaMgSi_2O_6$, Chemical Geology, v. 256, p. 203-215.

Giordano, D., Russell, J.K., and Dingwell, D.B., 2008b, Viscosity of magmatic liquids, A model: Earth and Planetary Science Letters, v. 271, p. 123-134.

Hofmeister, A.M., Whittington, A.G., and Pertermann, M., 2009, Transport properties of high albite crystals, near-endmember feldspar and pyroxene glasses, and their melts to high temperature, Contributions to Mineralogy and Petrology, v. 158, p. 381-400.

Iwamori, H., 1993, A model for disequilibrium mantle melting incorporating melt transport by porous and channel flows, Nature, v. 366, p. 734-737.

Kushiro, I., 2001, Partial melting experiments on peridotite and origin of mid-ocean ridge basalt, Annual Review of Earth and Planetary Sciences, v. 29, p. 71-107.

Lange, R.A., and Carmichael, I.S.E., 1987, Densities of Na_2O-K_2O-CaO-MgO-FeO-Fe_2O_3-Al_2O_3-TiO_2-SiO_2 liquids-New measurements and derived partial molar properties, Geochimica Et Cosmochimica Acta, v. 51, p. 2931-2946.

Langmuir C.H., Klein E.M., and Plank T. (1992) Petrological systematics of mid-ocean ridge basalts: constraints on melt generation beneath ocean ridges. In: Morgan J.P., Blackman, D.K., Sinton J. (eds.) Mantle Flow and Melt Generation at Mid-Ocean Ridges, Geophys. Monogr. Ser., Vol.71, AGU, 183-280.

Laurencin, D., Wong, A., Dupree, R., and Smith, M.E., 2008, Natural abundance Ca-43 solid-state NMR characterisation of hydroxyapatite: identification of

the two calcium sites, Magnetic Resonance in Chemistry, v. 46, p. 347-350.

Lee, S.K., 2004, Structure of silicate glasses and melts at high pressure: Quantum chemical calculations and solid-state NMR, Journal of Physical Chemistry B, v. 108, p. 5889-5900.

Lee, S.K., 2005a, Microscopic origins of macroscopic properties of silicate melts and glasses at ambient and high pressure: Implications for melt generation and dynamics, Geochimica Et Cosmochimica Acta, v. 69, p. 3695-3710.

Lee, S.K., 2005b, Structure and the extent of disorder in quaternary (Ca-Mg and Ca-Na) aluminosilicate, American Mineralogist v. 90.

Lee, S.K., Cody, G.D., Fei, Y.W., and Mysen, B.O., 2004, Nature of polymerization and properties of silicate melts and glasses at high pressure, Geochimica Et Cosmochimica Acta, v. 68, p. 4189-4200.

Lee, S.K., Cody, G.D., and Mysen, B.O., 2005a, Structure and the extent of disorder in quaternary (Ca-Mg and Ca-Na) aluminosilicate glasses and melts, American Mineralogist, v. 90, p. 1393-1401.

Lee, S.K., Deschamps, M., Hiet, J., Massiot, D., and Park, S.Y., 2009a, Connectivity and Proximity between Quadrupolar Nuclides in Oxide Glasses: Insights from through-Bond and through-Space Correlations in Solid-State NMR, Journal of Physical Chemistry B, v. 113, p. 5162-5167.

Lee, S.K., Lee, S.B., Park, S.Y., Yi, Y.S., and Ahn, C.W., 2009b, Structure of Amorphous Aluminum Oxide, Physical Review Letters, v. 103.

Lee, S.K., Mibe, K., Fei, Y.W., Cody, G.D., and Mysen, B.O., 2005b, Structure of B_2O_3 glass at high pressure: A B-11 solid-state NMR study, Physical Review Letters, v. 94.

Lee, S.K., and Stebbins, J.F., 1999, The degree of aluminum avoidance in aluminosilicate glasses, American Mineralogist, v. 84, p. 937-945.

Lee, S.K., and Stebbins, J.F., 2000, The structure of aluminosilicate glasses: high-resolution O-17 and Al-27 MAS and 3QMAS, Journal of Physical Chemistry B, v. 104, p. 4091-4100.

Lee, S.K., and Stebbins, J.F., 2002, Extent of intermixing among framework units in silicate glasses and melts, Geochimica Et Cosmochimica Acta, v. 66, p. 303-309.

Lee, S.K., and Stebbins, J.F., 2003, Nature of cation mixing and ordering in Na-Ca silicate glasses and melts, Journal of Physical Chemistry B, v. 107, p. 3141-3148.

Lee, S.K., and Stebbins, J.F., 2006, Disorder and the extent of polymerization in calcium silicate and aluminosilicate glasses: O-17 NMR results and quantum chemical molecular orbital calculations, Geochimica Et Cosmochimica Acta, v. 70, p. 4275-4286.

Lee, S.K., and Sung, S., 2008, The effect of network-modifying cations on the structure and disorder in peralkaline Ca-Na aluminosilicate glasses: O-17 3QMAS NMR study, Chemical Geology, v. 256, p. 326-333.

Levin, I., and Brandon, D., 1998, Metastable alumina polymorphs: Crystal structures and transition sequences, Journal of the American Ceramic Society, v. 81, p. 1995-2012.

Levitt, M.H., 2001, Spin dynamics: Basic of nuclear magnetic resonance Chichester, England, John Wiley & Sons, Ltd.

Liang, Y., Richter, F.M., and Chamberlin, L., 1997, Diffusion in silicate melts: III. Empirical models for multicomponent diffusion, Geochimica Et Cosmochimica Acta, v. 61, p. 5295-5312.

MacKenzie, K.J.D., Smith, M.E., and Wong, A., 2007, A multinuclear MAS NMR study of calcium-containing aluminosilicate inorganic polymers, Journal of Materials Chemistry, v. 17, p. 5090-5096.

Madhu, P.K., Goldbourt, A., Frydman, L., and Vega, S., 1999, Sensitivity enhancement of the MQMAS NMR experiment by fast amplitude modulation of the pulses, Chemical Physics Letters, v. 307, p. 41-47.

McMillan, P., 1984, Structural studies of silicate-glasses and melts - applications and limitations of raman-spectroscopy, American Mineralogist, v. 69, p. 622-644.

McMillan, P., Piriou, B., and Navrotsky, A., 1982, A raman-spectroscopic study of glasses along the joins silica-calcium aluminate, silica-sodium aluminate, and silica-potassium aluminate, Geochimica Et Cosmochimica Acta, v. 46, p. 2021-2037.

Mysen, B.O., Lucier, A., and Cody, G.D., 2003, The structural behavior of Al^{3+} in

peralkaline melts and glasses in the system Na_2O-Al_2O_3-SiO_2, American Mineralogist, v. 88, p. 1668-1678.

Mysen BO, R.P., 2005, Silicate glasses and melts, Elsevier.

Navrotsky, A., Zimmermann, H.D., and Hervig, R.L., 1983, Thermochemical study of glasses in the system $CaMgSi_2O_6$-$CaAl_2SiO_6$, Geochimica Et Cosmochimica Acta, v. 47, p. 1535-1538.

Neuville, D.R., Cormier, L., De Ligny, D., Roux, J., Flank, A.M., and Lagarde, P., 2008a, Environments around Al, Si, and Ca in aluminate and aluminosilicate melts by X-ray absorption spectroscopy at high temperature: American Mineralogist, v. 93, p. 228-234.

Neuville, D.R., Cormier, L., Montouillout, V., Florian, P., Millot, F., Rifflet, J.C., and Massiot, D., 2008, Structure of Mg- and Mg/Ca aluminosilicate glasses: Al-27 NMR and Raman spectroscopy investigations, American Mineralogist, v. 93, p. 1721-1731.

Neuville, D.R., and Richet, P., 1991, Viscosity and mixing in molten (Ca, Mg) pyroxenes and garnets,

Geochimica Et Cosmochimica Acta, v. 55, p. 1011-1019.

Ohtani, E., 1985, The primordial terrestrial magma ocean and its implication for stratification of the mantle, Physics of the Earth and Planetary Interiors, v. 38, p. 70-80.

Presnall, D.C., Gudfinnsson, G.H., and Walter, M.J., 2002, Generation of mid-ocean ridge basalts at pressures from 1 to 7 GPa, Geochimica Et Cosmochimica Acta, v. 66, p. PII S0016-7037(02)00890-6.

Richet, P., 1984, Viscosity and configurational entropy of silicate melts, Geochimica Et Cosmochimica Acta, v. 48, p. 471-483.

Richet, P., Robie, R.A., and Hemingway, B.S., 1993, Entropy and structure of silicate-glasses and melts, Geochimica Et Cosmochimica Acta, v. 57, p. 2751-2766.

Shimoda, K., Tobu, Y., Shimoikeda, Y., Nemoto, T., and Saito, K., 2007, Multiple Ca2+ environments in silicate glasses by high-resolution Ca-43 MQMAS NMR technique at high and ultra-high (21.8 T) magnetic fields, Journal of Magnetic Resonance, v. 186, p. 156-159.

Stebbins, J.F., and Xu, Z., 1997, NMR evidence for excess non-bridging oxygen in an aluminosilicate glass, Nature, v. 390, p. 60-62.

Tarduno, J., Bunge, H.P., Sleep, N., and Hansen, U., 2009, The Bent Hawaiian-Emperor Hotspot Track: Inheriting the Mantle Wind, Science, v. 324, p. 50-53.

Urbain, G., Bottinga, Y., and Richet, P., 1982, Viscosity of liquid silica, silicates and alumino-silicates, Geochimica Et Cosmochimica Acta, v. 46, p. 1061-1072.

Webb, S., and Knoche, R., 1995, The glass-transition, structural relaxation and shear viscosity of silicate melts, La Petite Pierre, France, p. 165-183.

Wilke, M., Farges, F., Partzsch, G.M., Schmidt, C., and Behrens, H., 2007, Speciation of Fe in silicate glasses and melts by in-situ XANES spectroscopy: American Mineralogist, v. 92, p. 44-56.

Zhao, P., Neuhoff, P.S., and Stebbins, J.F., 2001, Comparison of FAM mixing to single-pulse mixing in O-17 3Q-and 5Q-MAS NMR of oxygen sites in zeolites, Chemical Physics Letters, v. 344, p. 325-332.

TABLES

Table 1. Composition of oceanic island basalt and mid ocean ridge basalt in mol %

	Ocean Island * (mol%)			Mid Ocean Ridge † (mol%)		
	Mauna Kea		West Greenland	Mid-Atlantic Ridge	East-Pacific Ridge	Indian-Ocean Ridge
SiO_2	46.20	45.84	46.9	56.46	56.68	56.70
TiO_2	2.01	1.83	1.29	1.04	1.25	0.83
Al_2O_3	9.93	9.90	11.6	10.24	9.92	9.98
Fe_2O_3	0.93	1.23	1.82	2.85	3.31	2.98
FeO	10.40	10.32	9.4			
MnO	0.18	0.19	0.21			
MgO	17.80	18.27	17.1	12.77	11.95	12.77
CaO	10.00	10.12	9.9	13.60	13.79	14.09
Na_2O	1.72	1.53	1.56	2.87	2.91	2.51
K_2O	0.56	0.42	0.09	0.12	0.12	0.10
P_2O_5	0.23	0.28		0.06	0.06	0.05

*(Herzberg, Nature, 2006) †(Winter J.D., 2001)

Table 2. Composition of CaO-MgO-Al_2O_3-SiO_2 silicate glasses in diopside-Ca-Tschermakite pseudobinary join.

Di-CaTs mol ratio		X_{MgO}	NBO (calculation)	CMAS mole %			
				CaO	MgO	Al_2O_3	SiO_2
0	100	0	0	33.0	0.0	33.0	33.0
25	75	0.25	0.17	30.8	7.7	23.1	38.5
50	50	0.5	0.33	28.5	14.3	14.3	42.9
75	25	0.75	0.50	26.7	20.0	6.7	46.7
100	0	1	0.67	25.0	25.0	0.0	50.0

FIGURES

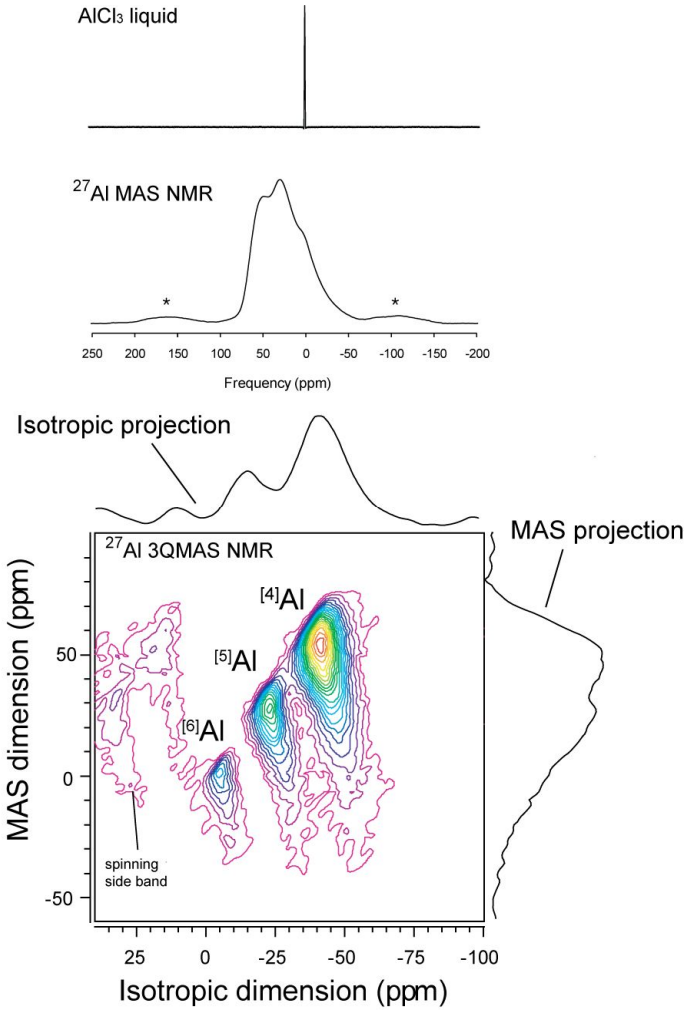

Figure 1. ^{27}Al MAS and 3QMAS NMR spectra for Mg-aluminoborate glasses ($MgO:Al_2O_3:B_2O_3$=2:1:2) at 9.4 T**.** ^{27}Al MAS spectrum for $AlCl_3$ liquid is also shown. Contour lines are drawn at 5% intervals from relative intensities of 7% to 97% with added 3%.

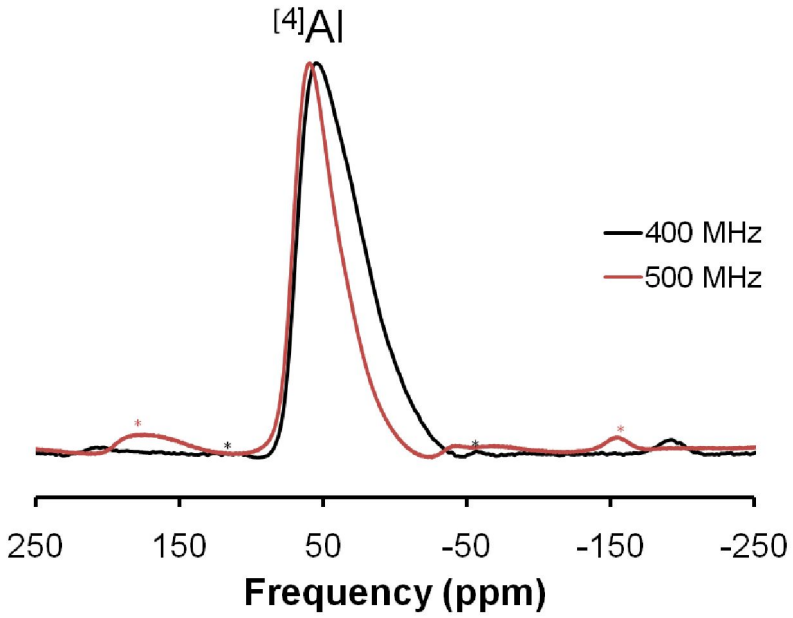

Figure 2. Comparison between ^{27}Al MAS NMR for $CaAl_2SiO_6$ glass at 9.4 T and 11.7 T. The spinning sideband is labeled '*'.

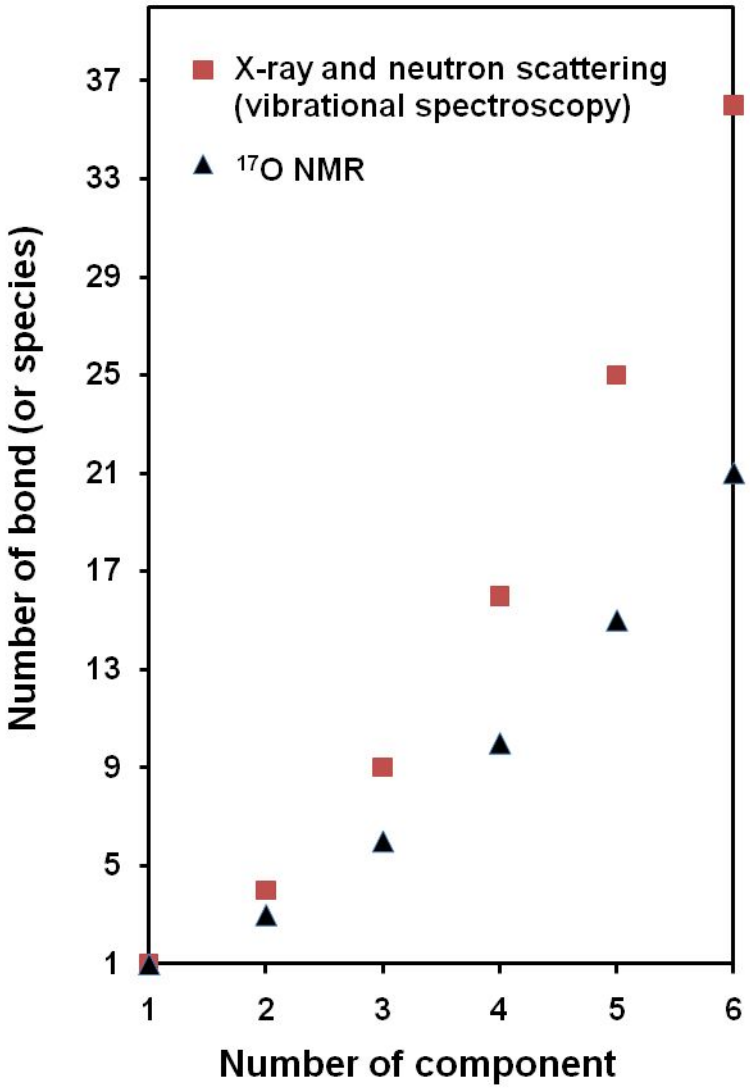

Figure 3. Effect of number of component on number of bond (or species) in oxides.

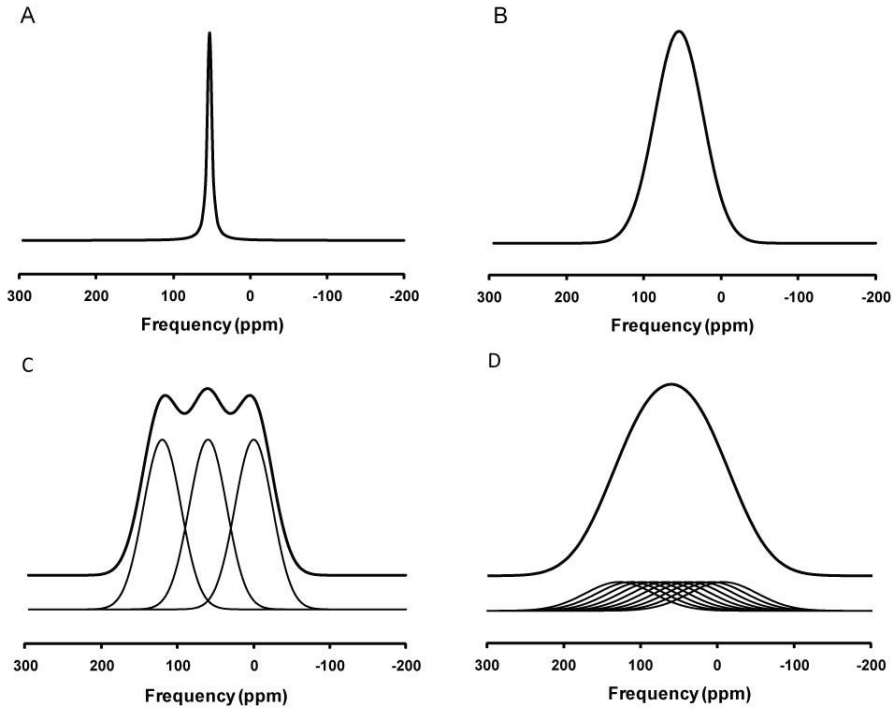

Figure 4. (A) A hypothetical NMR spectrum for single component liquid, (B) for single component amorphous material, (C) for binary amorphous material, and (D) for multi-component amorphous material.

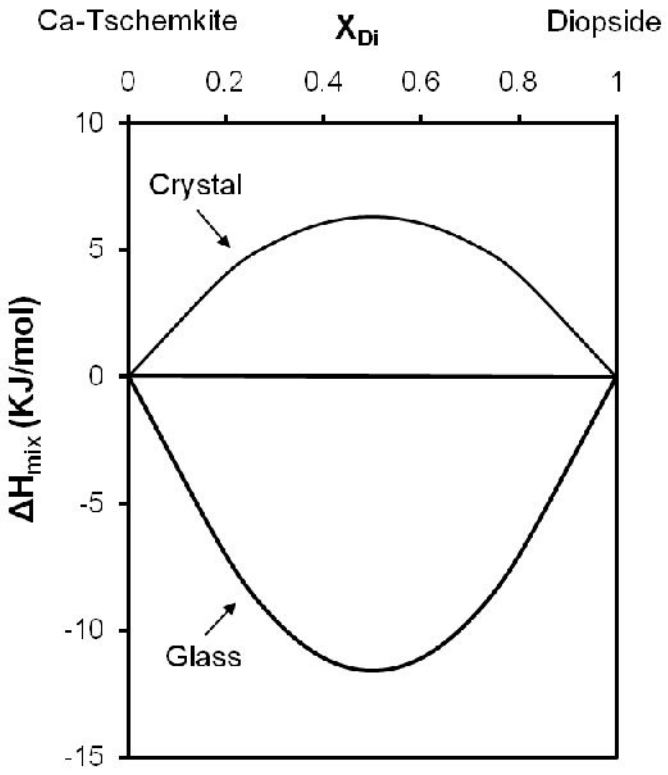

Figure 5. Enthalpy of mixing for CaO-MgO-Al_2O_3-SiO_2 silicate glasses in diopside -Ca-Tschermakite pseudobinary join. X_{Di} is the mole fraction of diopside (Navrotsky et al., 1983).

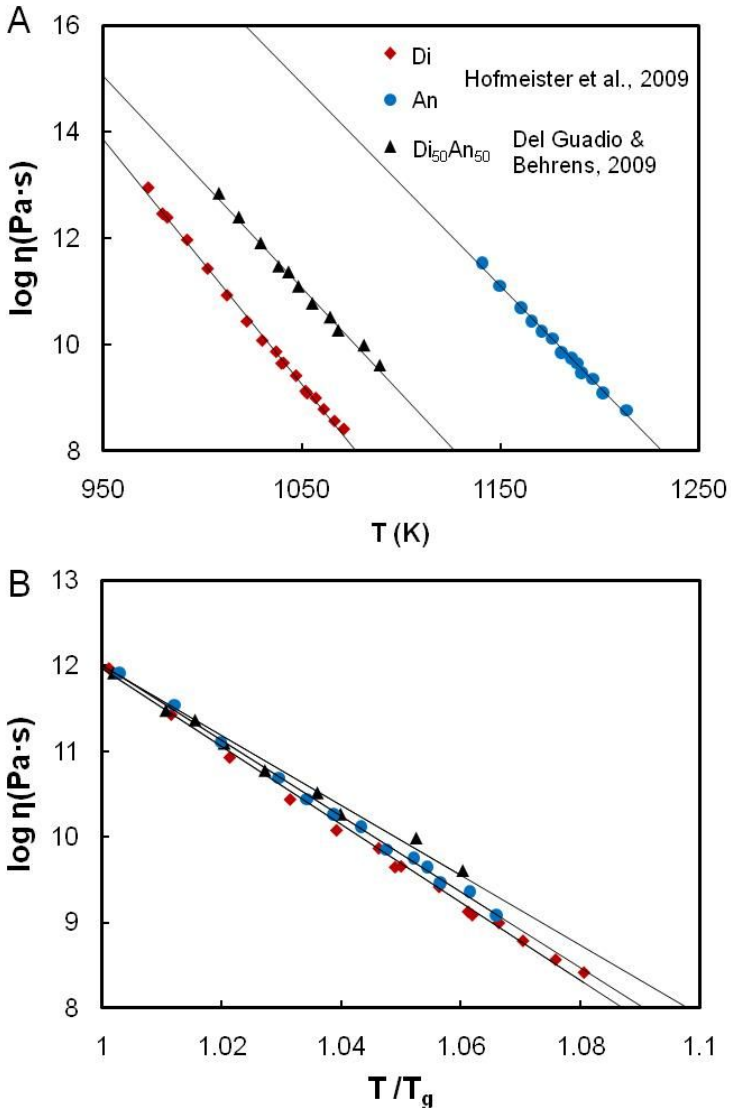

Figure 6. Viscosity of diopside (Di, $CaMgSi_2O_6$) and anorthite (An, $CaAl_2Si_2O_8$) glasses. The red diamond is viscosity of Di, the blue circle is that of An (Hofmeister et al., 2009), and the triangle is that of Di-An join (Di:An= 50:50) (Del Gaudio and Behrens, 2009). T_g is the glass transition temperature.

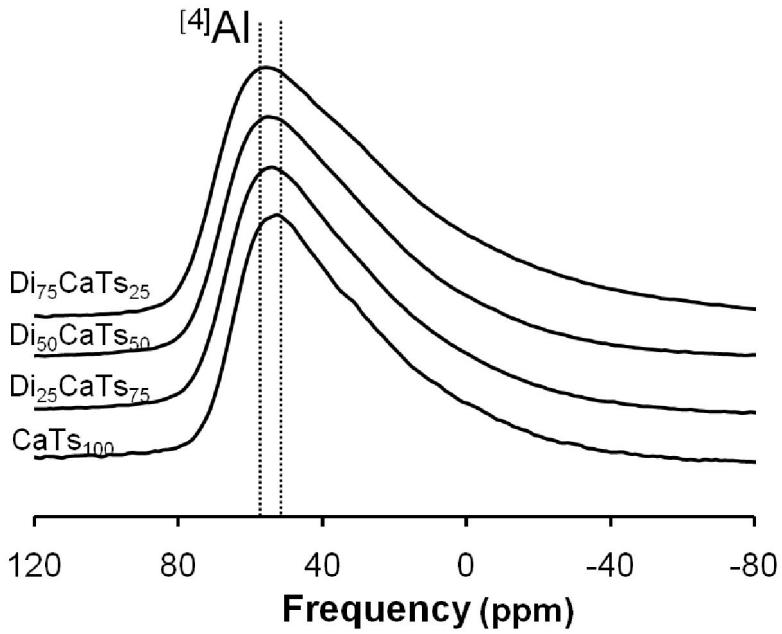

Figure 7. ^{27}Al MAS NMR spectra for CaO-MgO-Al_2O_3-SiO_2 silicate glasses in diopside -Ca-Tschermakite pseudobinary join at 9.4 T with varying diopside content. Di is diopside ($CaMgSi_2O_6$) and CaTs is Ca-Tschermakite ($CaAl_2SiO_6$).

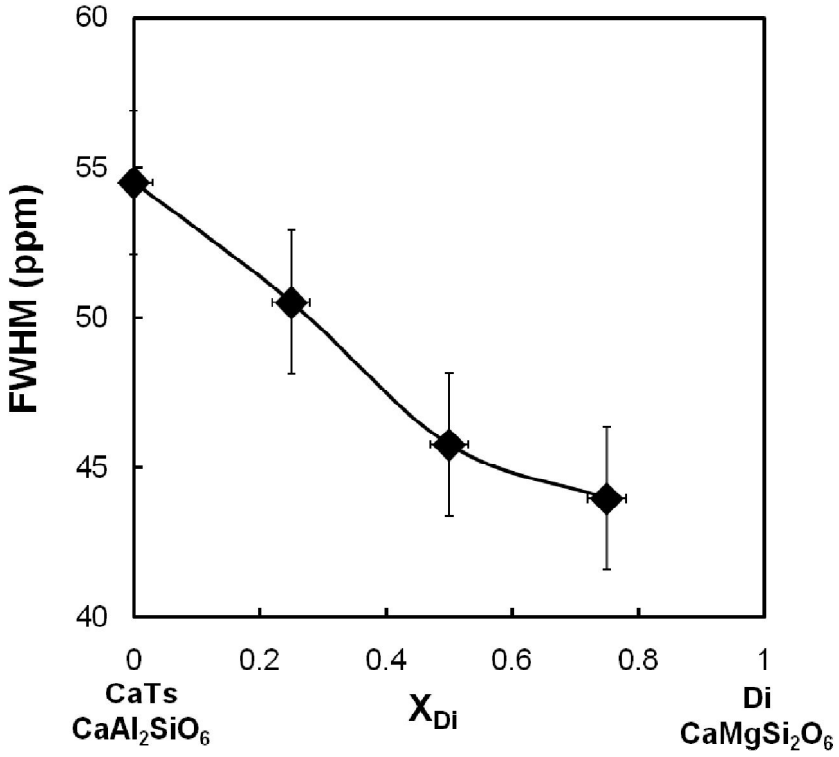

Figure 8. FWHM of $^{[4]}Al$ in MAS dimension for CaO-MgO-Al_2O_3-SiO_2 silicate glasses in diopside -Ca-Tschermakite pseudobinary join. Di is diopside and CaTs is Ca-Tschermakite. X_{Di} is the mole fraction of diopside.

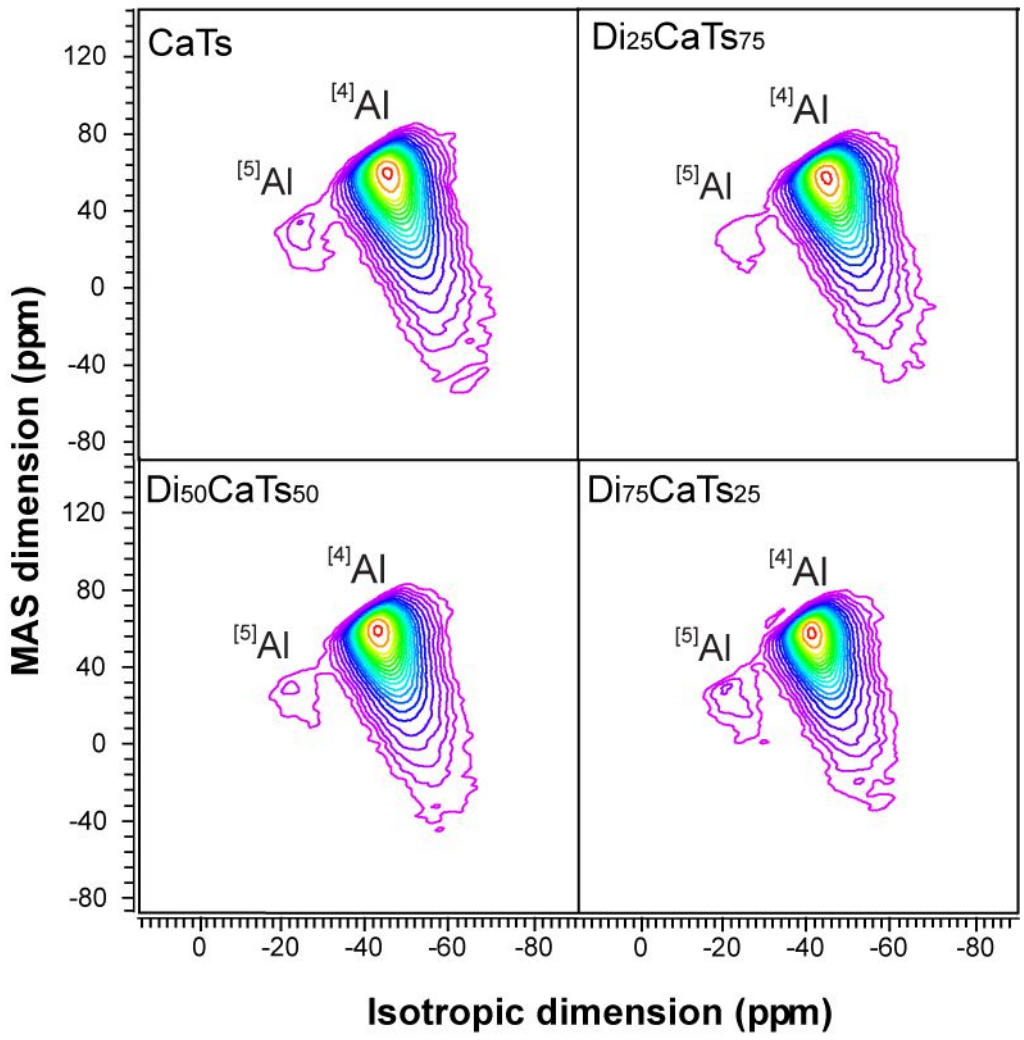

Figure 9. ^{27}Al 3QMAS NMR spectra for CaO-MgO-Al_2O_3-SiO_2 silicate glasses in diopside -Ca-Tschermakite pseudobinary join at 9.4 T with varying diopside content. Di is diopside ($CaMgSi_2O_6$) and CaTs is Ca-Tschermakite ($CaAl_2SiO_6$). Contour lines are drawn at 5% intervals from relative intensities of 2% to 97%.

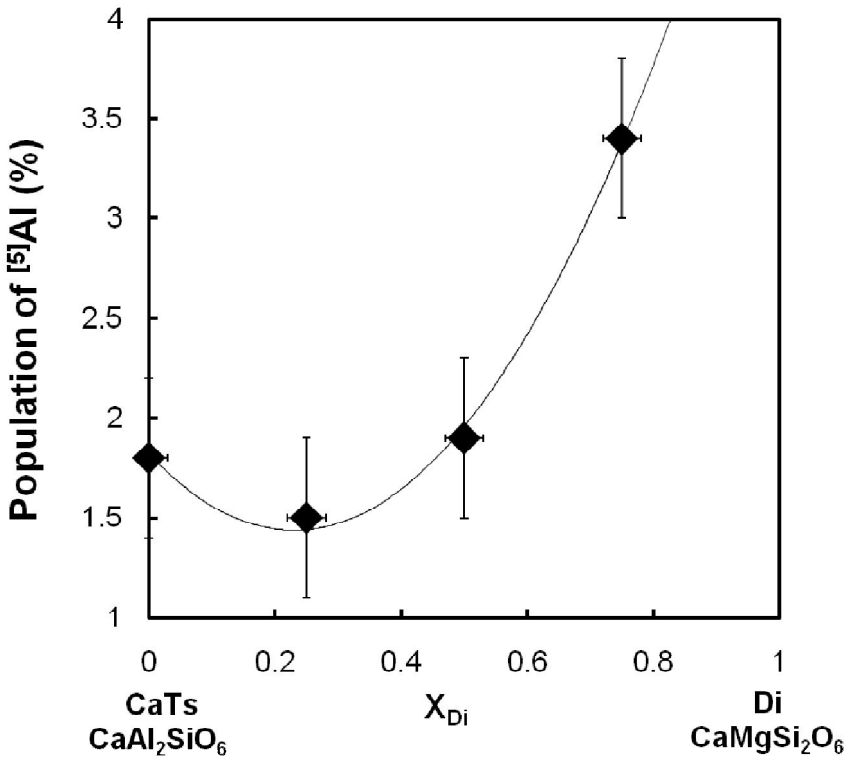

Figure 10. The population of $^{[5]}Al$ for $CaO\text{-}MgO\text{-}Al_2O_3\text{-}SiO_2$ silicate glasses in diopside -Ca-Tschermakite pseudobinary join. Di is diopside and CaTs is Ca-Tschermakite.

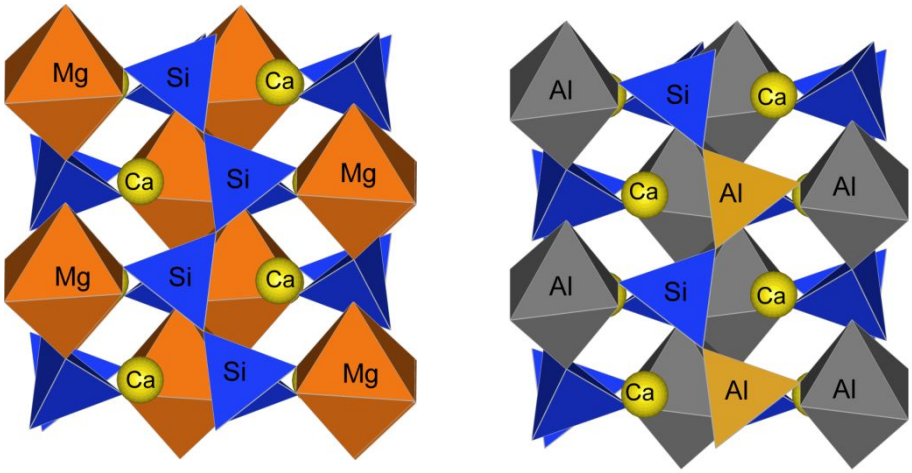

Figure 11. The atomic structure of diopside and Ca-Tschermakite crystals. The left one is diopside and right one is Ca-Tschermakite.

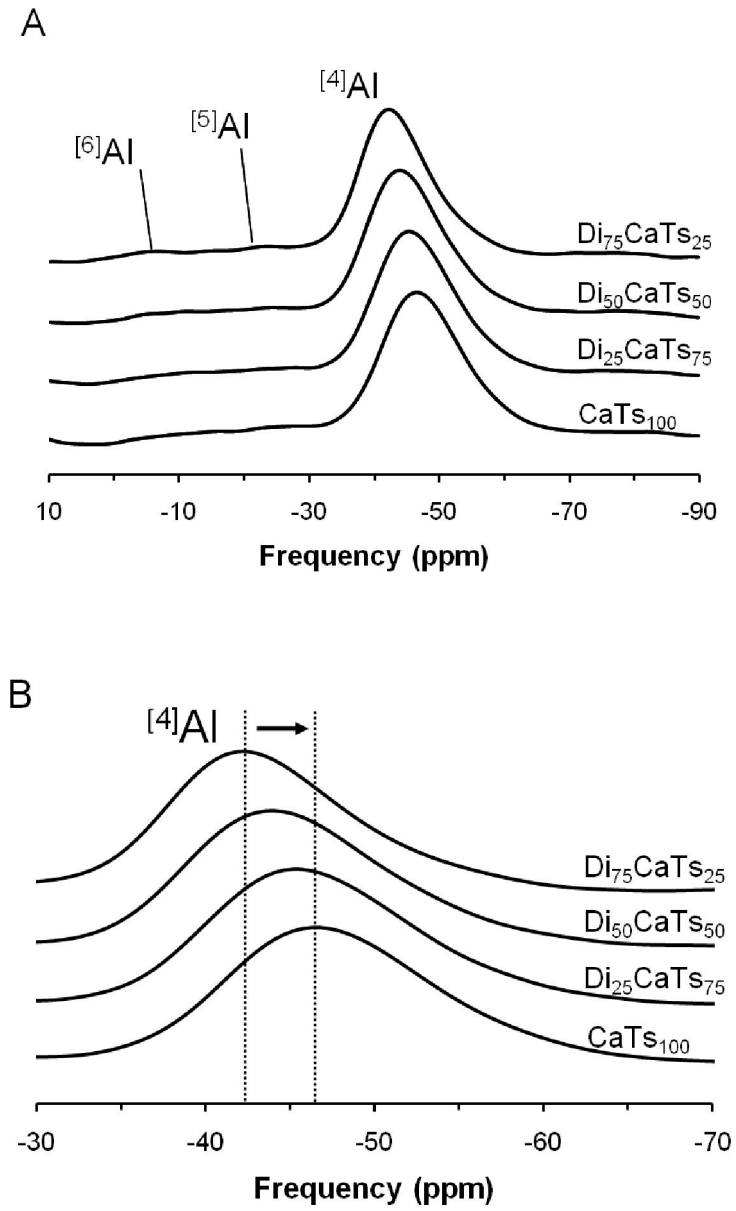

Figure 12. Total isotropic projection of ^{27}Al 3QMAS NMR spectra for CaO-MgO-Al_2O_3-SiO_2 silicate glasses in diopside -Ca-Tschermakite pseudobinary join at 9.4 T. Di is diopside and CaTs is Ca-Tschermakite. (B) is magnification of (A).

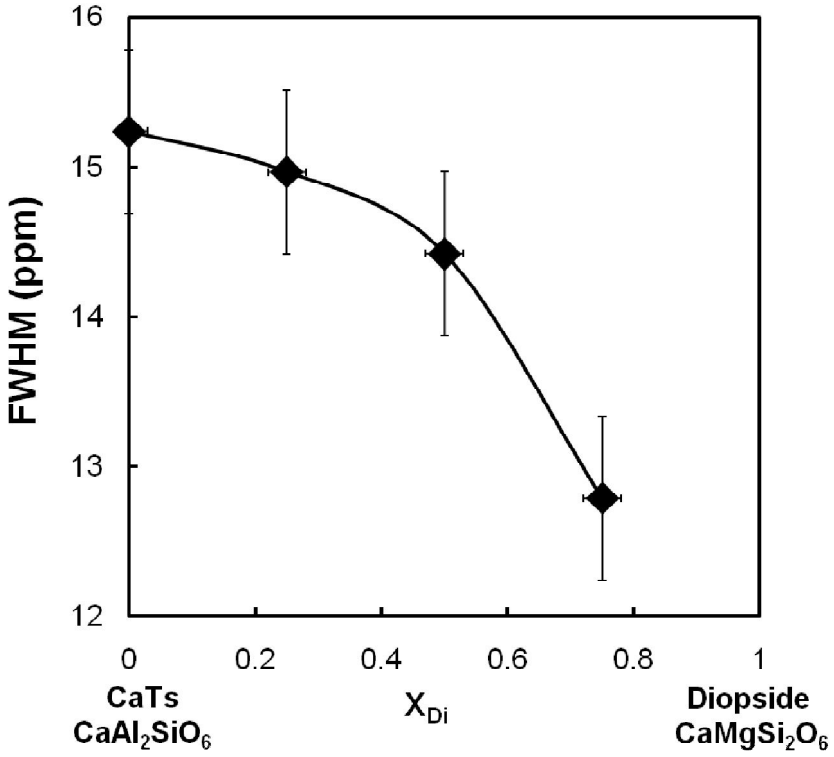

Figure 13. FWHM of $^{[4]}Al$ in total isotropic projection of ^{27}Al 3QMAS NMR spectra for CaO-MgO-Al_2O_3-SiO_2 silicate glasses in diopside -Ca-Tschermakite pseudobinary join at 9.4 T. Di is diopside and CaTs is Ca-Tschermakite.

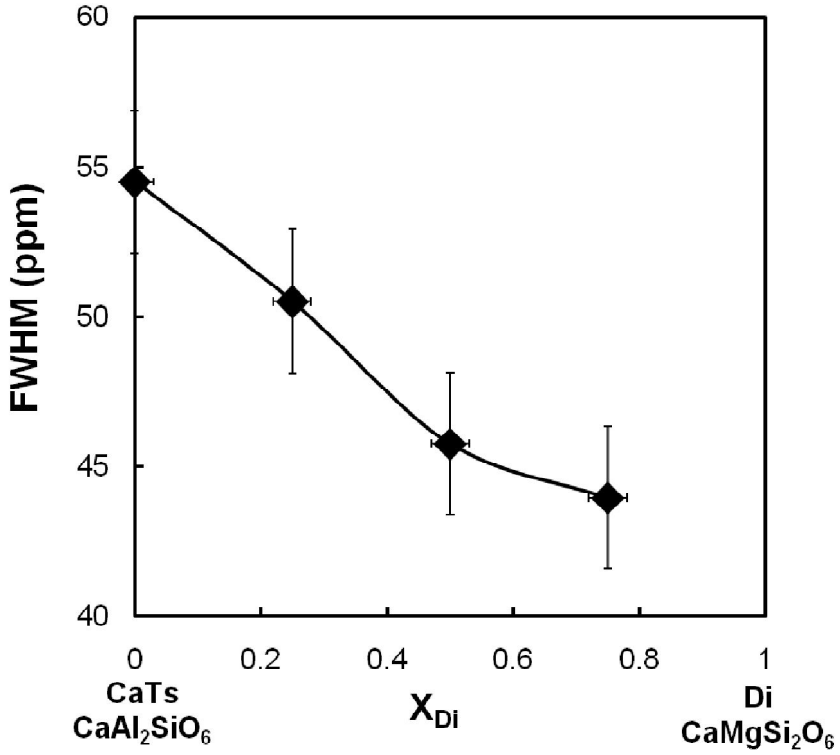

Figure 14. Quadrupolar coupling constant (C_q) of $^{[4]}Al$ in CaO-MgO-Al_2O_3-SiO_2 silicate glasses in diopside -Ca-Tschermakite pseudobinary join. Di is diopside and CaTs is Ca-Tschermakite.

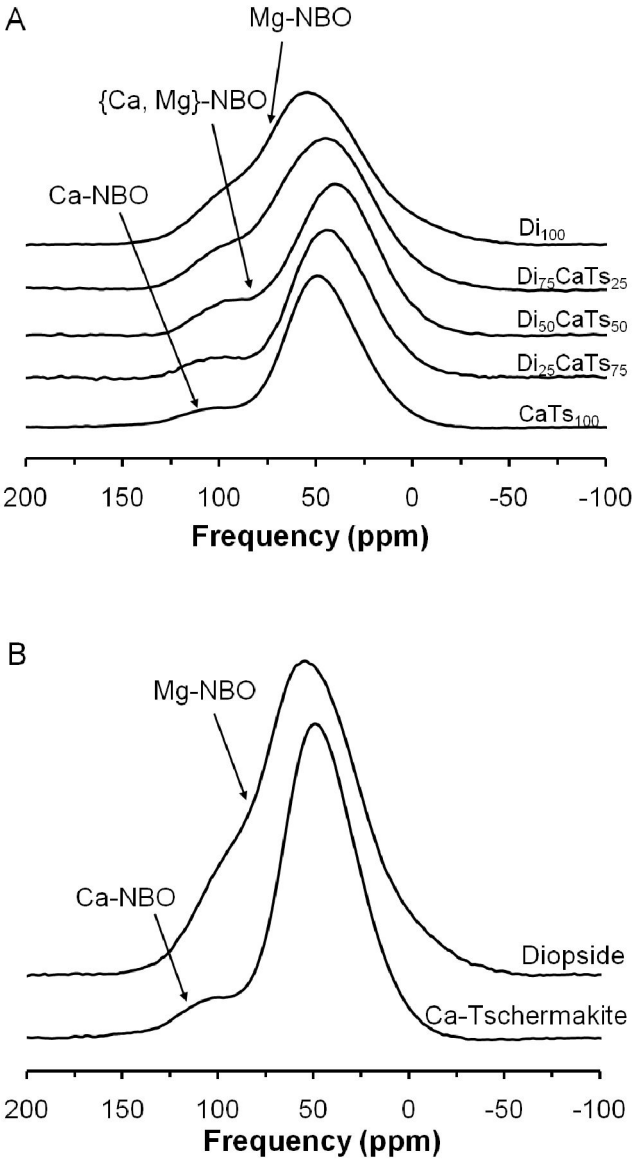

Figure 15. ^{17}O MAS NMR spectra for CaO-MgO-Al_2O_3-SiO_2 silicate glasses in diopside -Ca-Tschermakite pseudobinary join, (B) for diopside glass and Ca-Tschermakite glass at 9.4 T. Di is diopside and CaTs is Ca-Tschermakite.

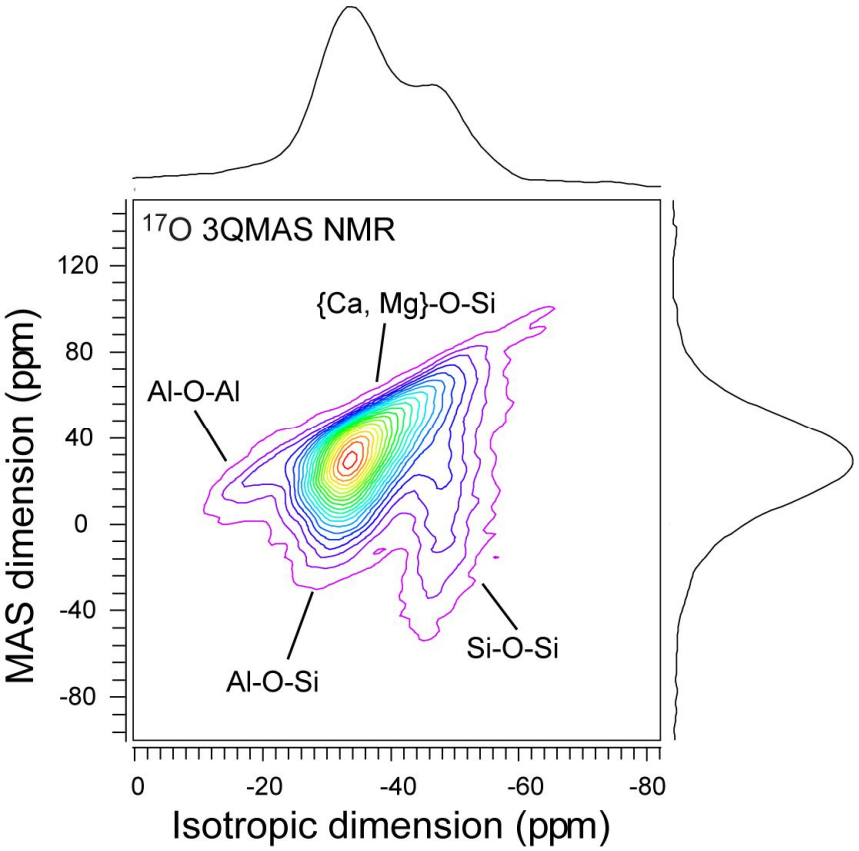

Figure 16. ^{17}O 3QMAS NMR spectra for model quaternary aluminosilicate glasses (CaO: MgO: Al_2O_3: SiO_2=8.8: 18.9: 21.3: 51.0 wt%) at 9.4 T. Contour lines are drawn at 5% intervals from relative intensities of 3% to 98%.

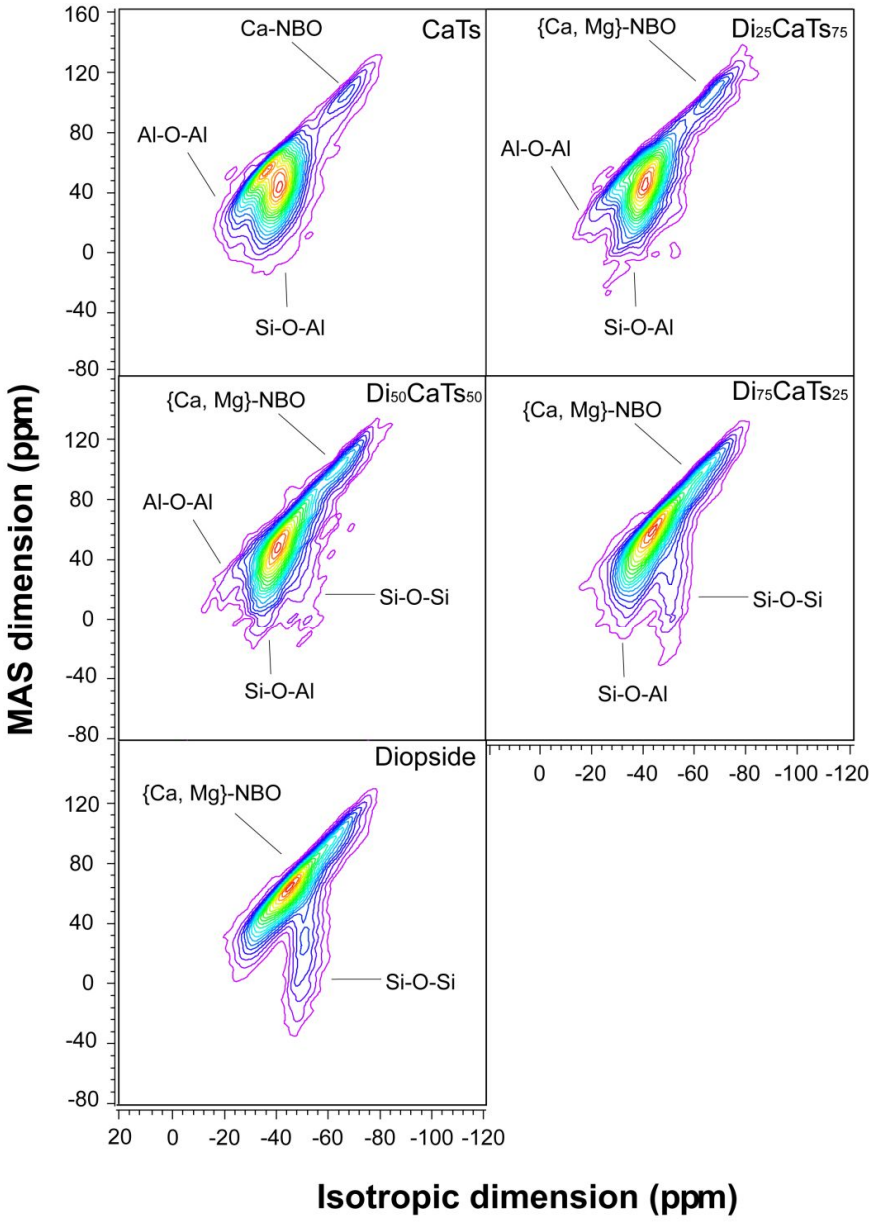

Figure 17. ^{17}O 3QMAS NMR for CaO-MgO-Al_2O_3-SiO_2 silicate glasses in diopside -Ca-Tschermakite pseudobinary join at 9.4T with varying diopside content. Di is diopside and CaTs is Ca-Tschermakite. Contour lines are drawn at 5% intervals from relative intensities of 8% to 98% with added lines at 4%.

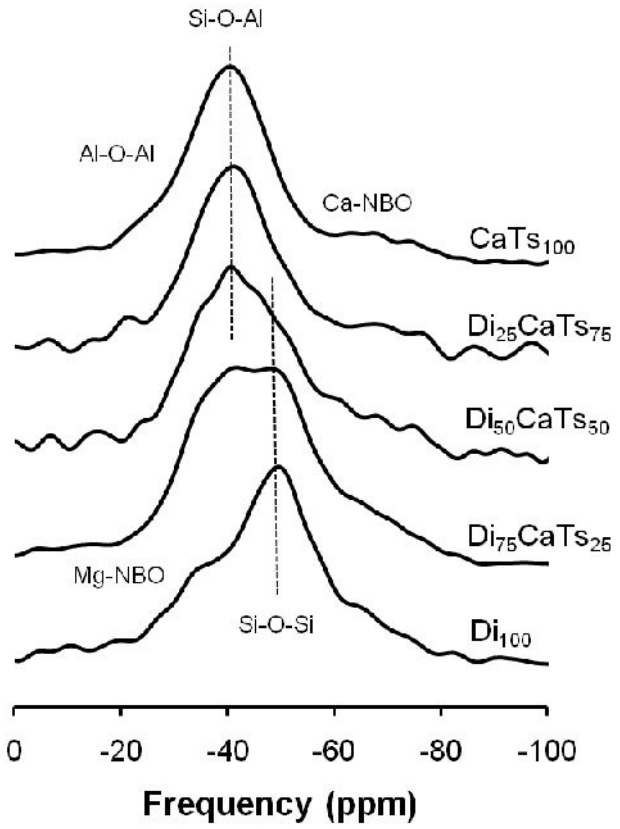

Figure 18. Total isotropic projection of ^{17}O 3QMAS NMR spectra for CaO-MgO-Al_2O_3-SiO_2 silicate glasses in diopside -Ca-Tschermakite pseudobinary join at 9.4 T with varying diopside content. Di is diopside and CaTs is Ca-Tschermakite.

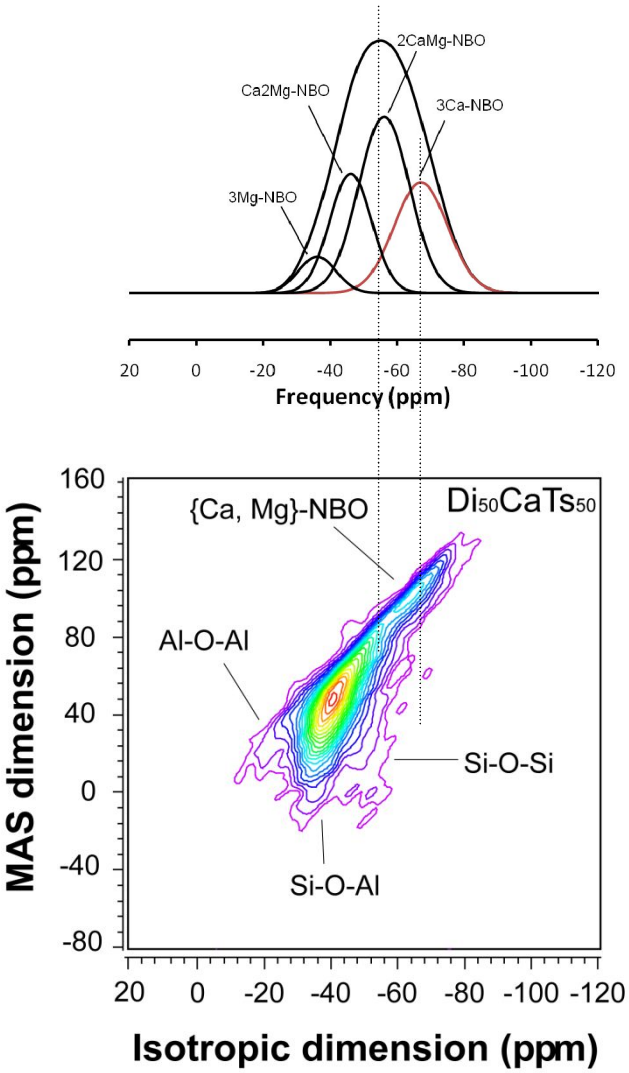

Figure 19. ^{17}O 3QMAS NMR spectrum for intermediate composition of diopside (Di)-Ca-Tschermakite (CaTs) pseudobinary join (Di : CaTs = 50 : 50) at 9.4 T. Contour lines are drawn at 5% intervals from relative intensities of 8% to 98% with added lines at 4%. A predicted spectrum of NBO peaks (in the isotropic projection) are also shown based on composition (Ca/(Ca+Mg)=0.67) using the random model is also shown.

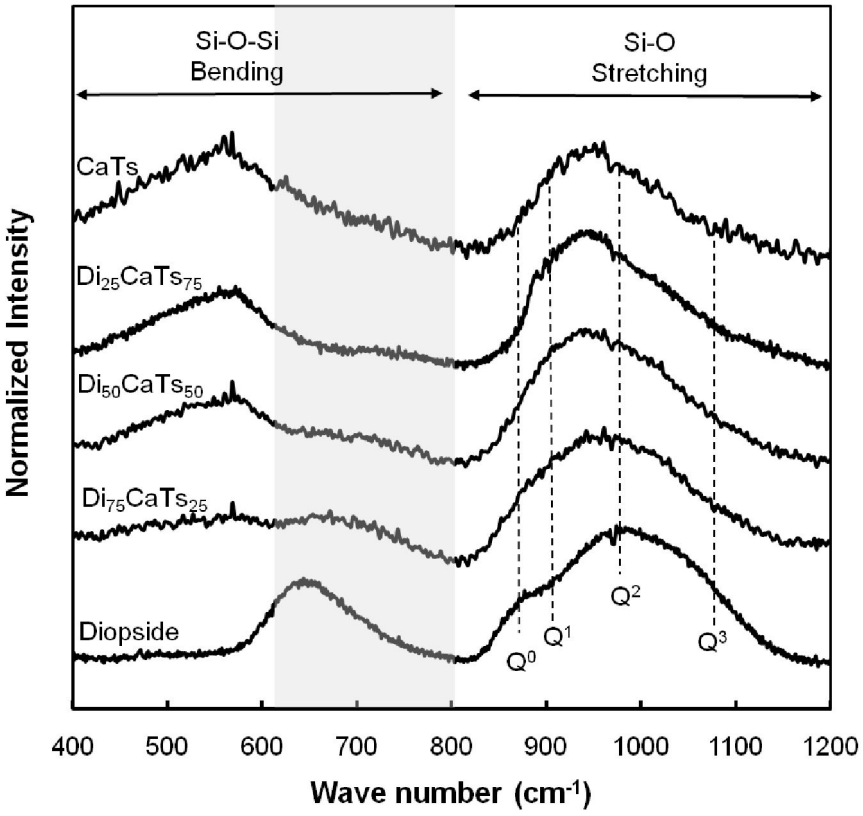

Figure 20. Normalized Raman spectra at room temperature for CaO-MgO-Al_2O_3-SiO_2 silicate glasses in diopside -Ca-Tschermakite pseudobinary join. Di is diopside and CaTs is Ca-Tschermakite.

APPENDIX 1

The effect of network modifying cation (i.e. Mg^{2+}) in Mg-aluminosilicate glass (Park et al., in preparation) Mg-aluminosilicate glass is a model silicate melts of mantle melts in the earth's interior (Lee, 2005b) In the two series of Mg-aluminosilicate glasses (i.e. $MgSiO_3$+2.5%Al_2O_3 and $MgSiO_3$ + 10% Al_2O_3), we performed ^{27}Al MAS and 3QMAS NMR experiments. The ^{27}Al NMR spectra obtained on a Varian 400 solid-state spectrometer (9.4 T) at resonance frequency of 104.229 MHz. Figure A1 shows ^{27}Al MAS NMR spectra for Mg-aluminosilicate with different alumina content, which are overlapped due to quadrupolar effect. The overlapped $^{[4]}$Al, $^{[5]}$Al, $^{[6]}$Al atomic structures are fully resolved with two-dimensional ^{27}Al 3QMAS NMR as shown figure A2. Those Al species have not been observed for other alkaline earth aluminosilicate melts and glasses. The results thus suggest significant topological and configuration disorder in the mantle melts due to the presence high field strength cation (i.e., Mg^{2+}).

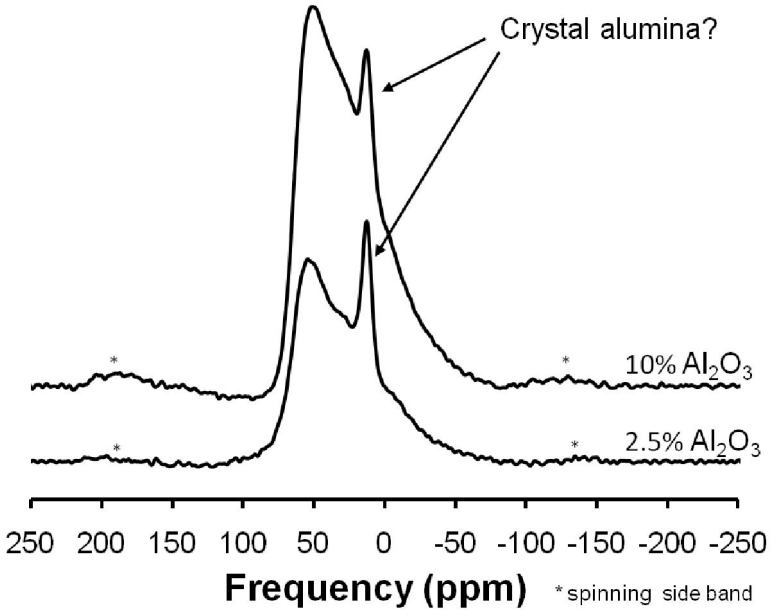

Figure A1. ^{27}Al MAS spectra for Mg-aluminosilicate glasses at 9.4 T,. * refers to spinning side bands.

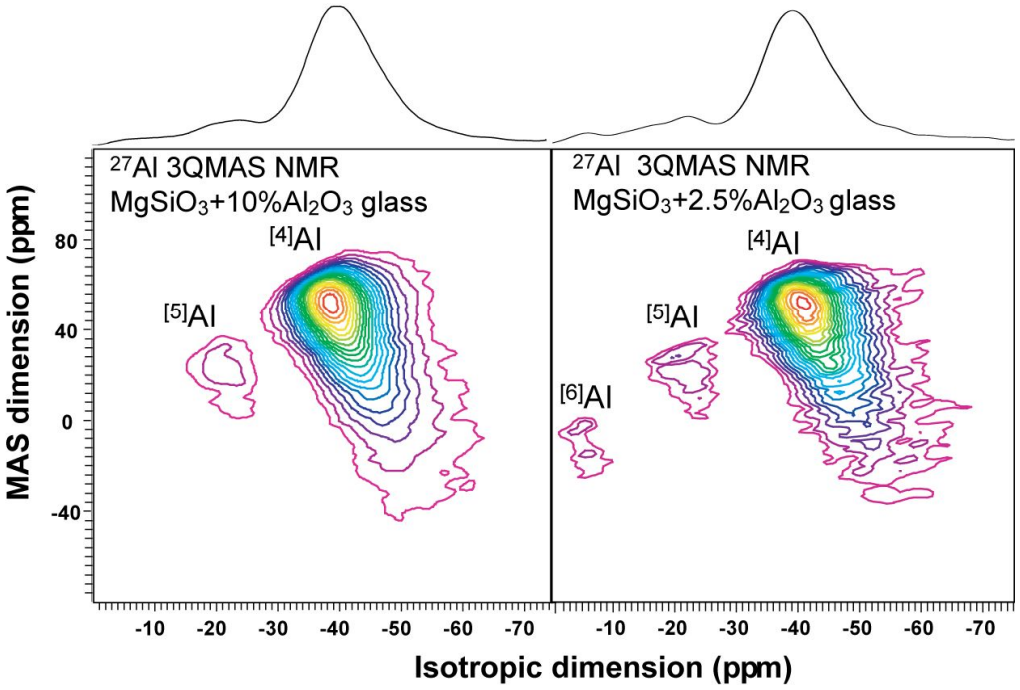

Figure A2. ^{27}Al 3QMAS spectra for Mg-aluminosilicate glasses at 9.4 T. Contour lines are drawn from 3% to 98% of relative intensity with a 5% increment.

APPENDIX 2

The atomic structure of Al_2O_3 thin film (Lee, S.K., Lee, S.B., Park, S.Y., Yi, Y.S., and Ahn, C.W., 2009, Physical Review Letter) While the structure of amorphous alumina has diverse industrial applications as catalyst, ceramics, and thin film devices, little is known about their atomic structures including its coordination states due to lack of suitable experimental probes. ^{27}Al MAS and 3QMAS NMR has proven to be extremely useful to resolve, otherwise overlapping Al species in amorphous materials. Here we extended these methods to explore the nature amorphous alumina in thin film and report the first high resolution ^{27}Al MAS and 3QMAS NMR spectra where the presence of distinct Al coordination species including $^{[4]}$Al, $^{[5]}$Al, and $^{[6]}$Al are for the first time demonstrated(figure A3. The calibrated fractions considering rotor background and other factor (i.e. C_q, quadrupolar broadening factor) for $^{[4]}$Al, $^{[5]}$Al, and $^{[6]}$Al are 55 ± 3, 42 ± 3, and 3 ± 2%, respectively. Study of alumina thin film with solid state NMR provides future directions to study single component glasses which are hard to synthesis.

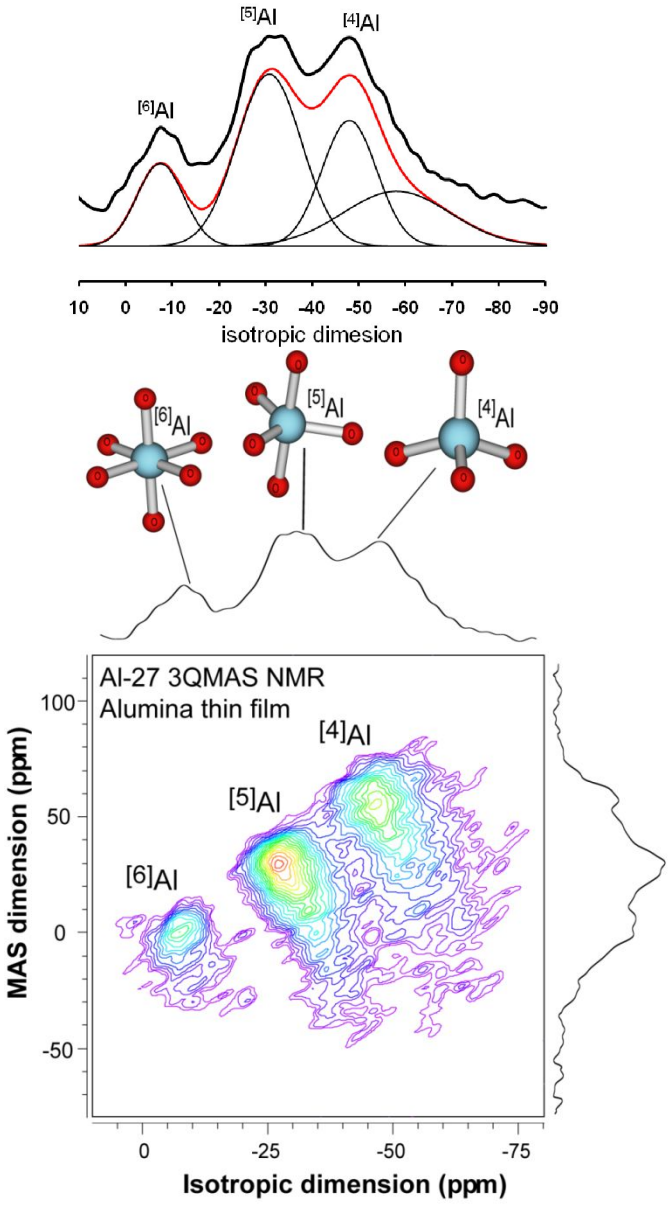

Figure A3. ^{27}Al 3QMAS NMR spectra for alumina thin film. Projections on the isotropic are also shown. (Lee et al., 2009) Contour lines are drawn at 5% intervals from 12% to 97% with added lines at 6% and 9%.

APPENDIX REFERENCE

Alvarez, L.J., Leon, L.E., Sanz, J.F., Capitan, M.J., and Odriozola, J.A., 1994, Surface-structure of cubic aluminum-oxide Physical Review B, v. 50, p. 2561-2565.

Bunker, B. C., Kirkpatrick, R. J., Brow, R. K., 1991, Local-structure of alkaline-earth boroaluminate crystals and glasses .1., crystal chemical concepts structural predictions and comparisons to known crystal-structures, Journal of the American Ceramic Society 74(6), 1425-1429.

Coster, D., Blumenfeld, A.L., and Fripiat, J.J., 1994, Lewis-acid sites and surface aluminum in alumina and zeolites- A high-resolution NMR-study, Journal of Physical Chemistry, v. 98, p. 6201-6211.

Eng, P.J., Trainor, T.P., Brown, G.E., Waychunas, G.A., Newville, M., Sutton, S.R., and Rivers, M.L., 2000, Structure of the hydrated alpha-Al2O3 (0001) surface, Science, v. 288, p. 1029-1033.

Fitzgerald, J.J., Piedra, G., Dec, S.F., Seger, M., and Maciel, G.E., 1997, Dehydration studies of a high-surface-area alumina (pseudo-boehmite) using solid-state H-1 and Al-27 NMR, Journal of the American Chemical Society, v. 119, p. 7832-7842.

Huggins, B.A., and Ellis, P.D., 1992, Al-27 nuclear magnetic resonance study of aluminas and their surfaces, Journal of the American Chemical Society, v. 114, p. 2098-2108.

Lee, S.K., 2004, Structure of silicate glasses and melts at high pressure: Quantum chemical calculations and solid-state NMR, Journal of Physical Chemistry B, v. 108, p. 5889-5900.

Lee, S.K., 2005b, Structure and the extent of disorder in quaternary (Ca-Mg and Ca-Na) aluminosilicate, American Mineralogist v. 90.

Kresse, G., Schmid, M., Napetschnig, E., Shishkin, M., Kohler, L., and Varga, P., 2005, Structure of the ultrathin aluminum oxide film on NiAl(110), Science, v. 308, p. 1440-1442.

Stierle, A., Renner, F., Streitel, R., Dosch, H., Drube, W., and Cowie, B.C., 2004, X-ray diffraction study of the ultrathin Al2O3 layer on NiAl(110), Science, v. 303, p. 1652-1656.

국 문 요 약

지구 구성 물질들은 성분의 수에 따라 단성분계에서 다성분계로 분류될 수 있다. 이 중 다성분계 비정질 규산염은 유리질, 세라믹, 내화물질의 주요 구성 물질이고 맨틀로부터 생성되는 초기 용융체(melt)의 주요 구성 성분이므로 다성분계 비정질 규산염의 원자구조와 물리 화학적 특성을 밝히는 것은 지구 내부의 마그마의 이동, 지구 시스템의 분화 등의 설명에 실마리를 제공해 준다. 특정 원자 중심의 정보를 제공해주는 고분해능 고상핵자기 공명 분광분석(NMR)은 현무암질 마그마를 포함한 대부분의 자연계의 다성분계 규산염 용융체의 원자 구조 분석에 적합하다. 본 연구에서는 일차원과 이차원 고상 NMR 을 이용하여 현무암질 마그마의 모델 시스템인 투휘석과 Ca-처마카이트를 단종으로 하는 CMAS ($CaO-MgO-Al_2O_3-SiO_2$) 비정질 규산염의 조성에 따른 원자 구조의 변화를 규명하였다. ^{27}Al MAS NMR 실험 결과 모든 조성에 대해 60 ppm 근처에서 $^{[4]}Al$ 피크가 지배적으로 나타나며 이는 Al^{3+}이 네트워크 형성 이온으로 작용한다는 것을 지시한다. 투휘석 성분이 증가함에 따라 피크 위치가 음의 방향으로 4.7 ppm 이동하는 것은 조성에서 Si 의 상대적인 양이 증가하면서 $Q^4(4Si)$가 증가하는 것을 의미하고 이를 통해 Al 주변의 산소가 모두 연결 산소(BO, bridging oxygen)임이 확인되었다. ^{27}Al 3QMAS NMR 실험 결과 1-D MAS NMR 스펙트럼에서는 구별되지 않던 $^{[4]}Al$ 와 $^{[5]}Al$ 의 피크가 분리되어 관찰되었다. 투휘석 성분이 증가하면서 $^{[5]}Al$ 의 상대적인 양이 증가하는 것이 관찰되며 이는 네트워크 교란작용을 일으키는 Mg^{2+} 가 증가하기 때문이다. Ca-Mg 알루미노규산염 내의 $^{[4]}Al$ 에 대한 C_q (quadrupolar coupling constant) 값은 투휘석 조성이 증가할수록 감소하는

경향을 보이며 이는 위상학적 무질서가 감소한 것을 의미한다. ^{17}O MAS NMR 실험 결과 Ca-Mg 알루미노규산염 내에 Ca-NBO (non bridging oxygen)인 Ca-O-Si 와 연결 산소가 ^{17}O MAS NMR 스펙트럼상에서 구별되며 투휘석 성분이 증가함에 따라 NBO 의 상대적인 양이 증가하는 것이 확인되었다. 고해상도 ^{17}O 3QMAS NMR 실험 결과 1D MAS NMR 상에서 확인되지 않던 Al-O-Al, Al-O-Si, Si-O-Si 와 Ca-NBO, {Ca, Mg}-NBO 가 부분적으로 구별되며 산소 주변의 원자환경은 투휘석과 Ca-Mg 알루미노규산염에 대해 이전에 알려지지 않았던 화학적 위상학적 무질서도에 대한 정보를 제공해준다. 투휘석과 Ca-처마카이트가 50:50 으로 섞여 있는 중간 조성에서 상당한 양의 Ca-NBO 가 -64 ppm 정도에서 분리되어 있는 것이 관찰되며 이는 Ca-NBO 와 Mg-NBO 가 생성될 때 랜덤 분포를 가지지 않고 Ca^{2+}가 NBO 를 선호한다는 것을 의미한다. Ca-Mg 알루미노 규산염 내에서 Mg^{2+}는 Si-O-Al 을 포함하는 BO 와 연결되어 전하 균형 양이온으로 작용하는 반면 Ca^{2+}는 네트워크 교란 양이온으로 작용한다. 본 연구에서의 Ca-Mg 알루미노 규산염에 대한 원자 구조는 조성에 따른 거시적 성질의 변화를 설명한다. 예를 들어 $^{[4]}Al$ 과 $^{[4]}Al\text{-}O\text{-}^{[4]}Si$ 의 존재는 비정질 투휘석과 Ca-처마카이트 유사이원계의 혼합 엔탈피가 음의 값을 가지는 것을 설명한다. 규산염 용융체의 점성도는 NBO 가 증가할수록 급격히 감소하는 것으로 알려져 있으나 투휘석과 회장석 이원계에 대해 실험적으로 NBO 의 변화를 밝힌 예는 없다. 본 연구에서는 Ca-Mg 알루미노 규산염의 산소 주변 원자환경을 통해 조성의 변화에 따라 NBO 의 상대적 양이 변하는 것을 실험적으로 증명하였으며 이는 투휘석의 상대적 양이 증가할수록 점성도가 감소하는 측정된 실험값과 일치하는 경향을 보인다.

NBO 와 BO 사이의 Ca^{2+}, Mg^{2+} 선호도는 CaO 와 MgO 의 활동도 계수에 영향을 주므로 궁극적으로 해양도와 중앙 해령에서 생성되는 용융체의 조성의 변화를 유도한다. 또한 지하수나 빗물에 의한 현무암의 용해과정에서 네트워크 교란 양이온과 NBO 사이의 강한 결합력으로 인해 Ca^{2+}에 비해 Mg^{2+}가 더 쉽게 용해된다. 본 연구에서의 결과는 다성분계 비정질 물질의 원자구조를 명확히 규명해 주며 원자구조와 성질 사이의 관계에 대한 새로운 연구 방향을 제시한다.

주요어 :현무암질 마그마, 다성분계 비정질 규산염, 투휘석−Ca−처마카이트 이원계, 핵자기 공명 분광분석, 원자구조

이학석사 학위논문

Structure and Properties of Quaternary Ca-Mg Aluminosilicate Glasses and Melts in Diopside ($CaMgSi_2O_6$)-Ca-Tschermakite ($CaAl_2SiO_6$) Join: High-resolution Solid-state ^{27}Al and ^{17}O NMR Study

사성분계 비정질 Ca-Mg 알루미노 규산염의 구조와 성질 (투휘석-Ca-처마카이트 계를 중심으로): 고해상도 고상 ^{27}Al 및 ^{17}O 핵자기 공명분광분석 연구

2010 년 2 월

서울대학교 대학원

자연과학대학 지구환경과학부

박 선 영

Structure and Properties of Quaternary Ca-Mg Aluminosilicate Glasses and Melts in Diopside ($CaMgSi_2O_6$)-Ca-Tschermakite ($CaAl_2SiO_6$) Join: High-resolution Solid-state ^{27}Al and ^{17}O NMR Study

사성분계 비정질 Ca-Mg 알루미노 규산염의 구조와 성질 (투휘석 - Ca-처마카이트 계를 중심으로) : 고해상도 고상 ^{27}Al 및 ^{17}O 핵자기 공명분광분석 연구

지도교수: 이성근

이 논문을 이학석사 학위논문으로 제출함

2009 년 12 월

서울대학교 대학원
자연과학대학 지구환경과학부
박 선 영

박선영의 이학석사 학위논문을 인준함.

2010 년 2 월

위 원 장 _____ 이 인 성 (인)

부위원장 _____ 허 영 숙 (인)

위 원 _____ 이 성 근 (인)

ABSTRACT

Whereas the structure of 'multi-component' silicate glasses and melts has implication for the properties of natural silicate magmas and relevant geochemical processes, little is known about their atomic structures due to lack of suitable experimental probes of amorphous 'multi-component' oxides. Whereas most of the progress in melt structure has been made for relatively simple binary and ternary silicate glasses, recent advances in high-resolution solid-state NMR begin to provide element specific and quantitative information of atomic configurations in multi-component silicate glasses including quaternary oxide glasses. Here we report the first experimental results of the effect of composition on the atomic structure of CaO-MgO-Al_2O_3-SiO_2 (CMAS) silicate glasses in diopside ($CaMgSi_2O_6$) and Ca-Tschermakite ($CaAl_2SiO_6$) pseudobinary join, a model system for basaltic magmas, using high-resolution 1D and 2D solid-state NMR. The ^{27}Al MAS NMR spectra for the CMAS glasses show that four-coordinated Al, $^{[4]}Al$ is predominant, demonstrating that Al^{3+} is a network former. The peak position moves toward a lower frequency approximately 4.7 ppm with increasing diopside content due to a increase in $Q^4(4Si)$ fraction with decreasing Al content. The result indicates that Al is surrounded only by bridging oxygens. The ^{27}Al 3QMAS NMR spectra show well resolved $^{[4]}Al$ and $^{[5]}Al$ in CMAS glasses. The fraction of $^{[5]}Al$ species increases with increasing diopside content (and thus with increasing Mg^{2+}). The structurally relevant quadrupolar coupling constant (C_q) and full width half maximum (FWHM) of $^{[4]}Al$ decrease with increasing diopside content, suggesting a decrease in topological disorder due to bonding angle and length distributions. The ^{17}O MAS NMR spectra for CMAS glasses qualitatively suggest that the fraction of non bridging oxygen (NBO) increases with increasing diopside content, consistent with the prediction form composition. The high-resolution ^{17}O 3QMAS NMR spectra show that three types of bridging oxygens

(BO; Si-O-Si, Al-O-Al, and Si-O-Al) and two types of NBO (Ca-NBO, and mixed {Ca, Mg}−NBO) are partially resolved. The local oxygen configurations in the glasses provide previously unknown details of the chemical and topological disorders in Ca-Mg aluminosilicate glasses. The significant fraction of the Ca-NBO peak is observed around -64 ppm in the glass at intermediate compositions (e.g., diopside : Ca-Tschermakite = 50 : 50), suggesting nonrandom distributions of Ca^{2+} and Mg^{2+} around NBO and BO, characterized with preferential partitioning of Ca^{2+} into NBO; Mg^{2+} is likely to have proximity to BO including Si-O-Al at intermediate compositions thus Mg^{2+} plays a preferential role as a charge-balancing cation, while Ca^{2+} can act as a network-modifying cation in the Ca-Mg aluminosilicate glasses studied here.

The observed structural changes in the CMAS glasses can account for the changes in macroscopic properties with composition. For example, the predominance of $^{[4]}$Al and its extensive mixing with Si as evidenced by the significant fractions of $^{[4]}$Al-O-$^{[4]}$Si is consistent with a negative experimental enthalpy of mixing for silicate glasses in diopside and Ca-Tschermakite join from solution calorimetry. As viscosity of silicate melts decreases exponentially with NBO fraction, while there is no available experimental data for the viscosity of silicate melts in the diopside-anorthite join, the observed increase in NBO fraction with increasing diopside content indicates a decrease in melt viscosity toward a diopside end-member.

Finally, the preferential partitioning of Ca^{2+} and Mg^{2+} between NBO and BO may results in a variation of activity coefficient of CaO and MgO, thus controlling composition of melts generated at the Mid-Ocean Ridge or Oceanic Islands. This preference also has strong implication for dissolution mechanisms of basalts in contact with aqueous fluids. Taking into consideration of stronger bond between network modifying cations and NBO (over charge-balancing cation and BO), Mg^{2+} in the basalts is likely to be dissolved easily. The results and methods

shed light on structure of multi-component oxide glasses and provide improved understanding their structure-property relations.

Keyword: basaltic magma, multi-component silicate glass, diopside-Ca-Tschermakite join, NMR, atomic structure

TABLE OF CONTENTS

LIST OF FIGURES

Fig. 7. ^{27}Al MAS NMR spectra for CaO-MgO-Al_2O_3-SiO_2 silicate glasses in pseudobinary join (diopside and Ca-Tschermakite) at 9.4 T with varying diopside content. Di is diopside ($CaMgSi_2O_6$) and CaTs is Ca-Tschermakite ($CaAl_2SiO_6$).

Fig. 8. FWHM of $^{[4]}Al$ in MAS dimension for CaO-MgO-Al_2O_3-SiO_2 silicate glasses diopside-Ca-Tschermakite pseudobinary join. Di is diopside and CaTs is Ca-Tschermakite. X_{Di} is the mole fraction of diopside.

Fig. 9. ^{27}Al 3QMAS NMR spectra for CaO-MgO-Al_2O_3-SiO_2 silicate glasses diopside-Ca-Tschermakite pseudobinary join at 9.4 T with varying diopside content. Di is diopside ($CaMgSi_2O_6$) and CaTs is Ca-Tschermakite ($CaAl_2SiO_6$). Contour lines are drawn at 5% intervals from relative intensities of 2% to 97%.

Fig. 10. The population of $^{[5]}Al$ for CaO-MgO-Al_2O_3-SiO_2 silicate glasses diopside-Ca-Tschermakite pseudobinary join. Di is diopside and CaTs is Ca-Tschermakite.

Fig. 11. The atomic structure of diopside and Ca-Tschermakite crystals. The left one is diopside and right one is Ca-Tschermakite.

Fig. 12. Total isotropic projection of ^{27}Al 3QMAS NMR spectra for CaO-MgO-Al_2O_3-SiO_2 silicate glasses diopside-Ca-Tschermakite pseudobinary join at 9.4 T. Di is diopside and CaTs is Ca-Tschermakite. (B) is magnification of (A).

Fig. 13. FWHM of $^{[4]}$Al in total isotropic projection of ^{27}Al 3QMAS NMR spectra for CaO-MgO-Al_2O_3-SiO_2 silicate glasses diopside-Ca-Tschermakite pseudobinary join at 9.4 T. Di is diopside and CaTs is Ca-Tschermakite.

Fig. 14. Quadrupolar coupling constant (C_q) of $^{[4]}$Al in CaO-MgO-Al_2O_3-SiO_2 silicate glasses diopside-Ca-Tschermakite pseudobinary join. Di is diopside and CaTs is Ca-Tschermakite.

Fig. 15. ^{17}O MAS NMR spectra for CaO-MgO-Al_2O_3-SiO_2 silicate glasses diopside-Ca-Tschermakite pseudobinary join, (B) for diopside glass and Ca-Tschermakite glass at 9.4 T. Di is diopside and CaTs is Ca-Tschermakite.

Fig. 16. ^{17}O 3QMAS NMR spectra for model quaternary aluminosilicate glasses (CaO: MgO: Al_2O_3: SiO_2=8.8: 18.9: 21.3: 51.0 wt%) at 9.4 T. Contour lines are drawn at 5% intervals from relative intensities of 3% to 98%.

Fig. 17. ^{17}O 3QMAS NMR for CaO-MgO-Al_2O_3-SiO_2 silicate glasses diopside-Ca-Tschermakite pseudobinary join at 9.4T with varying diopside content. Di is diopside and CaTs is Ca-Tschermakite. Contour lines are drawn at 5% intervals from relative intensities of 8% to 98% with added lines at 4%.

Fig. 18. Total isotropic projection of ^{17}O 3QMAS NMR spectra for CaO-MgO-Al_2O_3-SiO_2 silicate glasses diopside-Ca-Tschermakite pseudobinary join at 9.4 T with varying diopside content. Di is diopside and CaTs is Ca-Tschermakite.

Fig. 19. ^{17}O 3QMAS NMR spectrum for intermediate composition of diopside (Di)-Ca-Tschermakite (CaTs) pseudobinary join (Di : CaTs = 50 : 50) at 9.4 T. Contour lines are drawn at 5% intervals from relative intensities of 8% to 98% with added lines at 4%. A predicted spectrum of NBO peaks (in the isotropic projection) are also shown based on composition (Ca/(Ca+Mg)=0.67) using the random model is also shown.

Fig. 20. Normalized Raman spectra at room temperature for CaO-MgO-Al_2O_3-SiO_2 silicate glasses diopside-Ca-Tschermakite pseudobinary join. Di is diopside and CaTs is Ca-Tschermakite.

Fig. A1. ^{27}Al MAS spectra for Mg-aluminosilicate,. * refers to spinning side bands.

Fig. A2. ^{27}Al 3QMAS spectra for Mg aluminosilicate glasses at 9.4 T. Contour lines are drawn from 3% to 98% of relative intensity with a 5% increment.

Fig. A3. ^{27}Al 3QMAS NMR spectra for alumina thin film. Projections on the isotropic are also shown. (Lee et al., 2009) Contour lines are drawn at 5% intervals from 12% to 97% with added lines at 6%.

LIST OF TABLES

1. INTRODUCTION

Magmatic process of earth's interior such as partial melting, mantle convection and differentiation of mantle has been a matter of common interest (Baker et al., 1995; Ohtani, 1985; Presnall et al., 2002; Tarduno et al., 2009). The major component of the earth's interior is silicate glasses thus studies of silicate melts and glasses are essential for understanding of the diverse magmatic process. It needs to study for the thermodynamic properties and transport properties like enthalpy, entropy, density, viscosity and diffusivity to demonstrate magmatic process in earth's interior. There are many methods to study about the macro properties relevant to magmatic processes; there have been three general methods. The first method is to measure the macro properties like viscosity, heat capacity, density and other thermo dynamical properties directly. For example, viscosity of silicate melts and glasses (Giordano et al., 2008a; Neuville and Richet, 1991; Richet, 1984), density (Lange and Carmichael, 1987), thermodynamic properties (Bottinga and Richet, 1978; Navrotsky et al., 1983) and so on. Second method is theoretical calculation or modeling including quantum calculation (Asimow et al., 2001; Giordano et al., 2008b; Liang et al., 1997). Third method is the calculation from microscopic origins. The atomic and molecular structure of silicate melts and glasses is related to those thermodynamic and transport properties. For example, the viscosity exponentially decreases with increasing the fraction of non bridging oxygen in silicate melts (Lee et al., 2004). And the diffusivity and activity coefficient has different pattern along degree of disorder (Lee, 2005a). Previous study have shown lots of results about measuring macroscopic properties however

there is limitation to measure the properties of mantle melt directly due to difficulty of extreme condition like high pressure and temperature. Also it can be demonstrated origin of macroscopic properties through the calculated results from microscopic origin.

In this thesis we report the atomic structure of Ca-Mg aluminosilicate glasses in diopside and Ca-Tschermakite pseudobinary join relevant to natural basaltic melts. This thesis is composed of 4 sections and appendix. In section 2, Theoretical backgrounds of NMR spectroscopy and difficulty of analysis for multi-component glasses are briefly presented. It is difficult to analyze of atomic structure of multi-component glasses due to overlapping peak site stem from increasing of the statistical chemical bond with increasing number of chemical component. The high-resolution NMR spectroscopy provides element specific information to overcome difficulty of analysis for multi-component glasses. In section 3, the atomic structure of Ca-Mg aluminosilicate glasses in diopside and Ca-Tschermakite pseudobinary join, which is the major thesis in this paper. It includes glass synthesis, ^{27}Al MAS and 3QMAS NMR, ^{17}O MAS and 3QMAS NMR results and Raman spectroscopy. Multi nuclear MAS and 3QMAS NMR spectra show the change of atomic structure with composition. It is probed the change of macroscopic properties such as enthalpy of mixing and viscosity from those atomic structure information. In section 4, we propose several works to investigate atomic structure of multi-component glasses which are ^{43}Ca NMR study and synchrotron X-ray study. In appendix, the atomic structure of Mg aluminosilicate and amorphous alumina thin film are presented.

2. THEORETICAL BACKGROUND

2.1 Brief overview of high-resolution solid state NMR

Nuclear magnetic resonance (NMR) process occurs when the nuclear magnetic moment associated with a nuclear spin is placed in an external magnetic field. Using this process, NMR spectroscopy measure interaction between rf signal and spin relaxation of material. The signal of NMR spectroscopy is determined by atomic environment of specific atom for example, coordination number, bond length, bond angle and connectivity with neighbor atoms. NMR spectrum provides dynamic information between atoms and molecules occurring from nano scale to second scale. There are several factors of protecting NMR signal, for example dipolar coupling, chemical shift anisotropy and quadrupole moment. The chemical shift anisotropy means peak broadening due to variation of chemical shift depending on orientation of molecular. Many methods are suggested to decrease effect of protecting NMR signal. One of method for increasing peak resolution is MAS (magic angle spinning), it removes dipole-dipole interaction by fixing the angle between rotating sample and external magnetic field specific value (Levitt, 2001).

Despite using MAS method the peak broadening effect still remain for quadrupolar nuclei (nuclear spin number is larger than 1, for example ^{17}O, ^{27}Al, ^{11}B, etc.) because those have quadrupolar effect which is interaction between charge in nuclei and electric gradient. Another method, 3QMAS (triple quantum magic angle spinning) deduce the second order quadrupolar anisotropy. It provides detail

information for atomic structure with high-resolution. Figure 1 shows ^{27}Al MAS and 3QMAS spectra for Mg-aluminoborate glasses ($MgO:Al_2O_3:B_2O_3 = 2:1:2$) and $AlCl_3$ liquid. The ^{27}Al MAS spectrum of Mg-aluminoborate glasses is broader than that of $AlCl_3$ liquid. As mentioned above NMR observes the configuration of spins thus the spectrum for liquid is very sharp due to offset effect for liquid whereas the spectrum for solid is very broad. Solid state NMR experiment is more challenge than liquid state NMR for those broadening effect, especially for amorphous material. Figure 1 also shows that it is difficult to peak assignment due to overlapping peak of each Al species in 1D ^{27}Al MAS NMR whereas $^{[4]}Al$, $^{[5]}Al$, $^{[6]}Al$ is partially dissolved at -40, -23, -5 ppm in isotropic dimension in 3QMAS NMR spectra. The 3QMAS NMR spectrum shows better resolution than MAS NMR spectrum.

The chemical shift is major important term in NMR spectroscopy. The chemical shift is shielding of external magnetic field by electron surround target nuclei. Though the unit of NMR spectrum is frequency like other spectroscopy, it is expressed dimensionless ppm traditionally, which is divided relative shift to reference compound (usually liquid with same isotope) by larmor frequency of investigating nuclei. The 2D NMR spectrum demonstrates each of peak having two axes (MAS and isotropic dimension), each peak is presented by a contour line. 2D NMR spectrum is demonstrated projected direction of isotropic and the resolution of isotropic projection is higher than those of MAS (Duer, 2004). It applied to spin 5/2 nuclides, such as ^{27}Al and ^{17}O, to investigate coordination number and atomic configuration in aluminosilicate glasses (Lee and Stebbins, 2000), boro-silicate glasses (Lee et al., 2005b), and alumina thin film (Lee et al., 2009b). Also MQMAS

NMR is applied to spin 7/2 nuclides such as ^{43}Ca (Angeli et al., 2007; Dupree et al., 1997; MacKenzie et al., 2007) and low gamma nuclides (e.g. ^{25}Mg) (Shimoda et al., 2007).

The magnitude of magnetic field use the unit of tesla (T), figure 2 shows ^{27}Al MAS NMR spectrum for Ca-Tschermakite ($CaAl_2SiO_6$) glass at 9.4 T and 11.7 T. The peak of $^{[4]}Al$ is better resolved at 11.7 T as compared with that of 9.4 T due to the Al is quadrupolar nuclei. The peak of quadrupolar nuclei is broad by the second-order quadrupolar interactions at low magnetic field. In order to separate peaks from spinning side band and resolve better ^{27}Al MAS NMR was performed at high field.

2.2 Difficulty in getting structural information of multi-component amorphous materials from spectroscopic and scattering studies

Figure 3 shows the relation between the number of chemical component 'n' in the composition and number of statistical chemical bonding. In case of general light scattering experiment using photon, the chemical bond increase along 'n^2' with increasing 'n'. For example, the number of measuring bond in binary system is 4 and it is increased 4 times to 16 in quaternary system. Also it is difficult to resolve peaks due to overlapping each other. One of method solving this problem is NMR. The resolution is higher in NMR spectroscopy than other spectroscopy and XRD for multi-component glasses due to it provide element specific information. In spite of measuring chemical bonds increase along $_{n+1}C_2$ $[(n^2+n)/2]$ with increasing component. This suggests that it is difficult to analyze for multi-component glasses.

In addition there is barrier resolving peaks due to inhomogeneous broadening in case of amorphous material.

Figure 4 shows the hypothetical spectra representing the change with number of component in NMR spectrum. Figure 4A is hypothetical spectrum for single component crystal, there is one sharp peak whereas the peak of single component amorphous glasses is very broad in figure 4B. Figure 4C shows a spectrum for binary amorphous material and it shows overlapping three peaks due to increasing chemical bond. It is difficult to resolve peaks in the multi component system because of overlapping peaks indicating various atomic environments like figure 4D. As mentioned above, the analysis of atomic structure for multi-component amorphous materials remained unsolved problem because there was not suitable probe to resolve it. Even though it is seriously difficult to analyze spectroscopic data for multi component system because it has been limited by inhomogeneous broadening of spectrum or diffraction pattern brings an inability to unambiguously resolve characteristic features. In addition it is difficult to know clearly the reason of peak shift because many elements in multi component could affect each other.

Here we report the atomic structure of CaO-MgO-Al_2O_3-SiO_2 (CMAS) silicate glasses in diopside-Ca-Tschermakite pseudobinary join using high-resolution ^{27}Al NMR and ^{17}O NMR. We already solved partly the structure of multi component using a new experimental method MQMAS bring the breakthroughs in spectroscopic analysis. The results of CMAS pseudobinary glasses suggest the atomic structure of natural magma. In this study, we present the detail aluminum and oxygen environments for the CMAS pseudobinary glasses with varying MgO fraction using 1-D MAS and 2-D 3QMAS solid-state NMR. We will demonstrate

structural change with composition then we discuss the microscopic origins of macroscopic properties of CMAS pseudobinary glasses.

3. PROBING ATOMIC STRUCTURE OF MULTI-COMPONENT BASALTIC GLASSES USING SOLID-STATE NMR

3.1 Introduction

The earth's materials can be divided from single component to multi component system with number of component. The multi-component silicate glasses and melts is major material of glass, ceramic, and refractory and major composition of primary melts generated from the mantle (Herzberg, 2006; Presnall et al., 2002). Thus the structure of multi-component silicate melts and glasses can provide insights into the diverse macroscopic properties of natural melts and transport of magma in the earth interior (Giordano et al., 2008a; Webb and Knoche, 1995). Among the many interesting systems relevant to generation of primary melts from the mantle, the glass composition in the CaO-MgO-Al_2O_3-SiO_2 (CMAS) quaternary system is particularly important as it reflects a major fraction of the chemical composition of the mantle melt and serves as an important model system to describe phase relationships between lherzolite minerals and primary mantle melts (Presnall et al. 2002).

Batch melting and fractional melting models are mainly used to demonstrate generation of partial melt in mantle and lower crust. Batch melting model assuming upwelling with contacting residue demonstrate melting process in equilibrium thus

the composition of rock is maintained. Whereas fractional melting model assume separating with residue thus the composition of rock is changed continually (Langmuir et al., 1992). Previous study has shown that partial melting of peridotite experiment demonstrating the melt composition changes with temperature, pressure and melt fraction. The fraction of Al_2O_3 decreases and that of MgO and FeO increases with increasing melt fraction. When partial melts are generated, the fraction of Al_2O_3 is high at first due to several reasons. One of the reason is minerals including high Al_2O_3 melt first and the other reason is the composition change to maintain equilibrium between mantle rock and melt (Kushiro, 2001). The bath melting model has limit to explain partial melting experiment result and upwelling of mantle melts thus the fractional melting is used primarily to demonstrate partial melting (Iwamori, 1993).

The mantle melt is divided mid ocean ridge basalt (MORB) and oceanic island basalt (OIB) with generating geological condition. Table 1 is the composition of MORB in mid-Atlantic ridge, East-Pacific ridge, Indian ocean ridge and OIB in Mauna Kea and West Greenland. The mole fraction of SiO_2, CaO and MgO of MORB is higher than that of OIB. In the previous study the macroscopic properties of multi-component silicate glasses and melts change with composition thus it is expected the difference of macroscopic properties between MORB and OIB.

Many studies have performed experimentally and principally about the macroscopic property of multi-component silicate glasses and melts having insight for natural melt. Figure 5 shows the enthalpy of mixing of diopside ($CaMgSi_2O_6$) and Ca-Tschermakite ($CaAl_2SiO_6$) pseudobinary crystals and glasses. The enthalpy of mixing is positive for crystal and negative for glasses (Navrotsky et al., 1983).

The entropy of diopside is higher than that of Ca-Tschermakite for crystal and those are similar for amorphous (Richet et al., 1993). Figure 6 presents the viscosity of anorthite-diopside join (Del Gaudio and Behrens, 2009; Hofmeister et al., 2009; Neuville and Richet, 1991; Urbain et al., 1982). It is normalized by T_g (glass transition temperature) and the viscosity increases several orders of magnitude and the density also increases with an increase diopside content (Barbieri et al., 2004). Many studies have been performed about macro properties of multi-component as mentioned above whereas the study of atomic structure has been performed only about binary or ternary system (Mysen BO, 2005). Recent study has shown the structure of the simplest compound Al_2O_3 made by Al and O which is common elements in crust (Lee et al., 2009b) and the structure of multi-component silicate glasses has not been well understood yet. The atomic structure of Ca-Na aluminosilicate has been performed before (Lee and Sung, 2008) though the system is limited to demonstrate melting process in earth system due to the Na^+ content is higher than natural melt.

Here we report a study for CaO-MgO-Al_2O_3-SiO_2 pseudobinary glasses, which includes the diopside (Di, $CaMgSi_2O_6$) component and Ca-Tschermakite (CaTs, $CaAl_2SiO_6$) component for end-member. The CMAS pseudobinary system is commonly used to demonstrate the change of macroscopic properties of mantle melts with composition quantitatively and systematically (Gasparik, 1984; Navrotsky et al., 1983; Richet et al., 1993). The CMAS pseudobinary glasses was used as a model system of natural basaltic melt because the melting temperature of diopside and Ca-Tschermakite join is very low. Thus CMAS pseudobinary glasses can be the model of preliminary melt.

The quantitative analysis of complex quaternary system, which is more close to real system, is particularly challenging in experimental aspect. The composition including Mg^{2+} instead of Na^{+} is used in this study. Although it is difficult to analyze atomic structure due to complexity and broadening of peak caused from higher cation field strength of Mg^{2+} than Na^{+}, the study about atomic structure of CMAS pseudobinary can provide insight about natural basaltic magma. Here we report the atomic structure of CMAS pseudobinary glasses using high-resolution ^{27}Al NMR and ^{17}O NMR break through the difficulty of analysis for multi-component glasses.

3.2. Experimental method

Sample preparation A series of CMAS pseudobinary glasses along the diopside and Ca-Tschermakite join with 0, 25, 50, 75 and 100 mol% $CaAl_2SiO_6$ component have been studied. They were synthesized from carbonate ($CaCO_3$), and oxides (MgO, Al_2O_3 and SiO_2). The compositions of pseudobinary glasses are peralkaline CMAS [$xCaO : yMgO : (x-y)Al_2O_3 : (x+y)SiO_2$ (x=4, y=0, 1, 2, 3)](see table 2). The Al_2O_3, $CaCO_3$ and SiO_2 powder were dried at 400°C for 48 hours and MgO was dried at 1200°C for 2 hours. Each weighed powder was thoroughly mixed by grinding in an agate mortar, and then it was decarbonized in a Pt crucible at 800°C for 1 hour. Due to the melting temperature of $CaMgSiO_6$ is 1391°C and about 1500°C for $CaAl_2SiO_6$ thus the sample was melted above the respective melting temperature (1550~1600°C) for 1 hour, and finally quenched into glasses by plunging the bottom of the Pt crucible in a water bath. Approximately, 0.2 wt% of

cobalt oxide was added to enhance spin-lattice relaxation. Negligible weight loss (0.2~2.6%) was measured.

The sample for ^{17}O MAS and 3QMAS NMR were synthesized from carbonates ($CaCO_3$) and oxide reagents including ^{17}O-enriched SiO_2. The latter was prepared by hydrolyzing $SiCl_4$ in 20% ^{17}O-enriched water. $CaAl_2SiO_6$ glass was synthesized by 40% ^{17}O-enriched water. Approximately, 0.2 wt% of cobalt oxide was added to enhance spin-lattice relaxation. The mixtures were then fused in a Pt crucible for 1 h at 1600°C in an Ar atmosphere. The melt was quenched by removing the crucible from the furnace and manually lowering it into water.

NMR spectroscopy The ^{27}Al MAS NMR spectra of CMAS pseudobinary glasses were collected at two static magnetic fields on a Bruker Avance DSX 500 spectrometer (11.7 T) at a Larmor frequency of 130.284 MHz using a 4mm Bruker triple-resonance probe (Seoul National University, Korea) and on a Varian Solid NMR 400 system (9.4 T) at 104.229 MHz with a 3.2 mm Varian double resonance probe (Seoul National University, Korea). The recycle delay time for ^{27}Al MAS NMR at two fields was 1s with 0.5 (11.7 T) and 0.3 (9.4 T) μs rf pulse strength. The sample spinning speeds of 15 kHz (11.7 T) and 14 kHz (9.4 T) were used for the two fields. The 3QMAS was only performed at 9.4 T using a fast-amplitude modulation (FAM)-based shifted-echo pulse sequence (consisting of two hard pulses with durations of 3.0 and 0.6 μs and a subsequent soft pulse with a duration of 15μs). Approximately 2000 to 5000 scans were averaged to achieve the signal to noise ratio shown in the ^{27}Al MAS and 3QMAS NMR spectra.

The ^{17}O MAS and 3QMAS NMR spectra of CMAS pseudobinary glasses were collected on Varian Solid NMR 400 system (9.4 T) at a Larmor frequency of 54.229 MHz using a 4 mm Doty double-resonance probe (Seoul National University, Korea). The relaxation delay times for the ^{17}O MAS NMR were 1 s and the rf pulse strength is 0.5 μs. Sample spinning speeds of 14 kHz was used. In the 3QMAS NMR experiment at 9.4 T, the FAM (Fast Amplitude Modulation)-based shifted-echo pulse sequence (with a hard pulse of duration 4.5 μs for multiple quantum excitation and two 1.1 μs pulses for single quantum reconversion, and a soft pulse with a duration of approximately 20 μs and an echo time of approximately 500 μs (integer multiple of a rotor period) was used (Baltisberger et al., 1996; Madhu et al., 1999; Zhao et al., 2001). Approximately 12960 to 20000 scans were averaged to achieve the signal to noise ratio shown in the ^{17}O 3QMAS NMR spectra. The spectra are referenced to external tap water for both the fields.

3.3 Results and discussion

3.3.1 ^{27}Al and ^{17}O NMR results

^{27}Al MAS NMR Figure 7 shows ^{27}Al MAS NMR spectra for CMAS pseudobinary glasses with varying composition at 9.4 T. Di means diopside and CaTs means Ca-Tschermakite, the number of right side indicates each percents. $^{[4]}Al$ is predominant at about 60 ppm in all samples, and the line shapes show asymmetric extra intensity at lower frequencies, which suggests that the chemical shift distribution is predominant over the quadrupolar broadening. Also inhomogeneous broadening is

observed due to structural disorder of amorphous materials. The predominant $^{[4]}$Al in all samples means that there is no structural change in nearest neighbor atom around Al due to Al^{3+} acts as a network forming cation (Allwardt et al., 2003; Barbieri et al., 2004). As the diopside content increases from 0 ($CaAl_2SiO_6$) to 75% ($CaMgSi_2O_6$), the peak position moves about 4.7 ppm from 56.2 to 51.5 ppm. This result is consistent with a trend in ternary silicate glasses from ^{27}Al MAS NMR for Ca-aluminosilicate in previous study (Lee and Stebbins, 2003) and it indicates that Q^4(4Si) increases with increasing Si fraction in CMAS pseudobinary glasses(Q^4(4Si) means that all of tetrahedral around Al is Si with all of BOs). In spite of the NBO fraction of CMAS pseudobinary glasses is dramatically changes along the composition, the coordination numbers of Al less changes. It means most of Al are surrounded BO instead of NBO (Allwardt et al., 2003).

The change of bond length and bond angle in atomic environment induce the change of peak width and it can be a degree of disorder in amorphous materials (Lee et al., 2005a; Lee and Stebbins, 1999). Figure 8 shows the full width half maximum (FWHM) of CMAS pseudobinary glasses decreases with increasing diopside content (54.5 ppm at diopside=0 and 43.9 ppm at diopside=0.75). As the fraction of Mg^{2+} increases, the degree of disorder in the system can be increasing while the trend of FWHM shows contrast results. That means 1D MAS NMR spectrum is not enough to explain change of spectrum because the quadrupolar coupling constant (C_q) affecting the peak width can be change with composition. Thus it needs to perform the supplemental experiment; 3QMAS NMR.

^{27}Al 3QMAS NMR Figure 9 shows ^{27}Al 3QMAS NMR spectra that successfully resolve the $^{[4]}$Al and $^{[5]}$Al not shown in 1D MAS NMR spectra. All spectra show that $^{[4]}$Al are major Al species and $^{[5]}$Al is clearly observed around -24 ppm in isotropic dimension. The peak shapes are very similar while the peak width in MAS dimension decreases with increasing diopside content. Figure 10 shows the population of $^{[5]}$Al changes with composition, which means that topological disorder increase in atomic structure. Ca-Tschermakite is single chain silicate thus there is $^{[4]}$Al and $^{[6]}$Al as shown figure 11 whereas $^{[4]}$Al and $^{[5]}$Al are presented in $CaAl_2SiO_6$ glasses due to topological disorder. As increasing Mg^{2+} which is a network modifying cation, the $^{[5]}$Al is generated then distance of Al-O or Al-O-Al bond angle change affecting the structure medium range order.

Figure 12 shows total isotropic projection of ^{27}Al 3QMAS NMR spectra for CMAS pseudobinary glasses. Figure 12A shows there are $^{[5]}$Al and $^{[6]}$Al in CMAS pseudobinary glasses. Figure 10B is magnification of figure 12A. The peak position of $^{[4]}$Al moves to higher frequency from -42.44 ppm ($Di_{75}CaTs_{25}$) to -46.25 ppm (CaTs). The trend in the isotropic projections provides a consistent result with MAS spectrum, the peak position shifts toward higher frequency in the 3QMAS isotropic dimension with increasing diopside content. Figure 13 shows the FWHM of $^{[4]}$Al in total isotropic dimension decrease with an increasing diopside content. It was founded that the degree of disorder decrease with an increase diopside content.

Figure 14 shows quadrupolar coupling constant (C_q) of $^{[4]}$Al for CMAS pseudobinary glasses at 9.4 T with varying composition. The C_q is one of the structurally relevant NMR parameters that denotes the magnitude of quadrupolar interactions between quadrupole moment of nuclei and electric field gradients

generated by surrounding electrons. The C_q of $^{[4]}$Al in CMAS pseudobinary glasses increases with increasing diopside content from 6.27 MHz to 6.98 MHz, suggesting larger distortion of $^{[4]}$Al polyhedral for low diopside content composition (Ghose and Tsang, 1973). As increasing diopside content, the isotropic chemical shift and FWHM of $^{[4]}$Al decreases, implying an decrease in topological entropy stemming from bond length and width distribution (Lee, 2004). These results contrast with those of population of $^{[5]}$Al in CMAS pseudobinary glasses. The population of $^{[5]}$Al suggests the Mg^{2+} perturbs the network whereas FWHM in total isotropic dimension and C_q indicate decreasing topological entropy. This means bond length and bond angle are ordered in $CaMgSi_2O_6$ than $CaAl_2SiO_6$ glasses.

^{17}O MAS NMR Figure 15 shows the ^{17}O MAS NMR spectra for CMAS pseudobinary glasses. The peak shape and position of ^{17}O NMR spectrum changes with atomic structure around oxygen, the atomic environment around oxygen is determined from that of information in multi component silicate glasses (Lee and Sung, 2008). And it can be confirmed structural changes directly from ^{17}O NMR spectra which provide the fraction of BO (e.g. Al-O-Si, Al-O-Al, Si-O-Si) and NBO (e.g., Si-O-Ca) in multi-component silicate glasses (Lee, 2005a). In spite of ^{17}O NMR experiment is very challenging because it is difficult to synthesis ^{17}O enriched sample and oxygen nuclei has low gyromagnetic ratio, ^{17}O NMR is very useful to study about earth interior because the macroscopic properties can be calculated from the atomic structure information obtained by ^{17}O NMR, such as activity coefficient topological entropy, and diffusivity involved in generation and transport of melt (Lee, 2005b). Figure 15A shows ^{17}O MAS spectra for CAMS

pseudobinary glasses and figure 15B shows tremendous change of oxygen environment with composition. ^{17}O MAS NMR spectrum shows presence of Ca-NBO at 99 ppm and the peaks of Al-O-Al overlapped with Al-O-Si in Ca-Tschermakite ($CaAl_2SiO_6$) glass. The fraction of NBO increases with increasing diopside content and there is only Si-O-Si and {Ca, Mg}-NBO in diopside ($CaMgSi_2O_6$) glass.

Both of the diopside and Ca-Tschermakite are single chain silicates (Ca^{2+}:Al^{3+} = 1:1) as shown figure 11 and NBO/T are 2 whereas previous study has shown that the NBO fraction is much high in those system (Stebbins and Xu, 1997). ^{27}Al MAS spectra in this study probe all of Al atom is surrounded by BO (Allwardt et al., 2003). From those results, the Ca-NBO in figure 15 is Ca-O-Si not Ca-O-Al. The bond preference of NBO is proved by quantum chemical calculation. The bond energy of Ca-O-Al is much higher (about 100 kJ) than Ca-O-Si (Lee and Stebbins, 2006). Recent study revealed directly the fraction of Ca-O-Al decrease with increasing Si content through a double resonance $\{^{17}O\}^{27}Al$ HMQC NMR experiment (Lee et al., 2009a). BOs and NBOs are overlapped in O-17 MAS NMR spectra except Ca-NBO in Ca-Tschermakite thus it is difficult to analyze the fraction of BO and NBO quantitatively. It needs high-resolution 2D ^{17}O 3QMAS NMR to analyze qualitatively.

^{17}O 3QMAS NMR Figure 16 shows ^{17}O 3QMAS NMR for model quaternary aluminosilicate (CaO: MgO: Al_2O_3: SiO_2=8.8: 18.9: 21.3: 51.0 wt%) resolving four different oxygen environments including Si-O-Si, Al-O-Al, Al-O-Si and {Ca, Mg}-NBO. The peak position of Si-O-Si, Al-O-Al, Al-O-Si and mixed NBO ({Ca, Mg}-

O-Si) is about -51, -17, -35 and -30 ppm in isotropic dimension, respectively (Lee et al., 2005a). The well resolved ^{17}O 3QMAS NMR spectrum for model quaternary silicate provides a ground for quantitative analysis of ^{17}O 3QMAS NMR for CMAS silicate glasses in pseudobinary join (diopside and Ca-Tschermakite).

Figure 17 shows ^{17}O 3QMAS NMR spectra for CMAS pseudobinary glasses at 9.4 T with varying diopside content providing considerably enhanced resolution among the O-atom sites as compared with ^{17}O MAS NMR spectra. The oxygen environment of CMAS pseudobinary glasses change with composition as shown Figure 17. The peak position of Al-O-Al and Al-O-Si in Ca-Tschermakite glass is about -35 and -41 ppm in isotropic dimension respectively. The proportion of each of BO is about 38 $\pm$ 5% for Al-O-Al and 62 $\pm$ 5% for Al-O-Si (Lee and Stebbins, 2002). It is note that Ca-NBO is well resolved at -63.5 ppm in isotropic dimension. The Si-O-Si peaks are shown around -51 ppm in isotropic dimension, the Al-O-Al peaks are reduced gradually and the mixed {Ca, Mg}-NBO peaks increase with an increase in X_{Di} (the mole fraction of diopside in CMAS pseudobinary glass). The chemical shielding of the mixed {Ca, Mg}-NBO peak decrease with diopside content (the peak shifts to a lower frequency in isotropic dimension). The peaks of Si-O-Si and {Ca, Mg}-NBO are remained in diopside glass (X_{Di}=1) around -40 and -51 ppm in isotropic dimension. Note that the peak assignment is based on the previous reports on binary silicates and ternary Ca-Mg aluminosilicate glasses (Allwardt and Stebbins, 2004; Lee and Stebbins, 2002). The chemical shielding of the mixed NBO peak decreases with diopside content and chemical shift dispersion increase. This result implies extensive mixing between Ca^{2+} and Mg^{2+} around the NBO (Lee and Sung, 2008). Figure 18 shows the total isotropic projection of ^{17}O

3QMAS NMR spectra for CMAS pseudobinary glasses. The resolution of ^{17}O 3QMAS NMR spectra is higher than MAS spectra however peaks are still overlapped. Ca-NBO is partially resolved in right side of spectrum and it is shown that the intensity of Si-O-Si decreases with increasing diopside content. Also Al-O-Al, Al-O-Si and Mg-NBO are partially resolved in CMAS pseudobinary glasses.

Figure 17 shows that Ca-NBO peak still remained at around -64 ppm in isotropic dimension in intermediate composition (Di : CaTs =50 : 50) of which Mg/Ca is 0.5. It means that the mixing behavior of CMAS pseudobinary glasses is nonrandom. Previous study has shown the simplest model to confirm the random mixing behavior between diopside and Ca-Tschermakite glasses. It was assumed that there are statistical distributions of three Ca and Mg cations surrounding each NBO, there are four possible species which are 3Ca-NBO, 2Ca1Mg-NBO, 1Ca2Mg-NBO, 3Mg-NBO. The peak position and width of Ca-NBO is predicted from Ca-Tschermakite, that of Mg-NBO is predicted from enstatite in previous study (Allwardt and Stebbins, 2004) and that of other species is estimated using numerical means. The predicted peak positions of each NBO are -67, -56, -46 and -36 respectively and the predicted percentages of each NBO species are

$$\begin{aligned} X_{3Ca} &= x^3 \\ X_{2CaMg} &= 3x^2(1-x) \\ X_{Ca2Mg} &= 3x(1-x)^2 \\ X_{3Mg} &= (1-x)^3 \end{aligned} \qquad (1)$$

Where x=Ca/(Ca+Mg) and this value is change from 1 to 0.5 in CMAS pseudobinary glasses. Figure 19 shows the ^{17}O 3QMAS NMR spectrum for intermediate composition of CMAS pseudobinary glasses ($Di_{50}CaTS_{50}$, diopside : Ca-Tschermakite = 50 : 50) and a hypothetical spectrum for NBO species including 3Ca-NBO, 2CaMg-NBO, Ca2Mg-NBO and 3Mg-NBO with random distribution. Ca/(Ca+Mg) change with composition from 0 to 1 in CAMS pseudobinary glasses and that is 0.67 in $Di_{50}CaTS_{50}$. The calculated percentage of each NBO using equation (1) is 29.5, 55.5 22.3 and 3.7 % in the intermediate composition as shown figure 19. The peak maximum of total NBO in hypothetical spectrum is about -56 ppm whereas that of 2D ^{17}O 3QMAS NMR spectrum is about -64 ppm as presented figure 19, suggesting nonrandom distribution of each NBO species. This ^{17}O 3QMAS NMR spectrum for $Di_{50}CaTS_{50}$ showing peak maximum at Ca-NBO site suggests two possibilities. First, there are less mixed {Ca, Mg}-NBO (2CaMg-NBO, Ca2Mg-NBO) and Mg-NBO overlapped with Al-O-Al peak. Second, Mg^{2+} prefers BO than NBO, Ca-NBO is predominant in NBO species. Assuming later possibility is correct, the preferential partitioning of Ca and Mg between NBO and BO (Al-O-Al, Al–O–Si) in CMAS pseudobinary glasses can be expressed by a quasi-equilibrium expression given below

Ca----Al-O-Al + Mg-NBO = Mg----Al-O-Al + Ca-NBO (2)

Ca----Al-O-Si + Mg-NBO = Mg----Al-O-Si + Ca-NBO (3)

The direction of above reactions is left to right basis on the preference of NBO. Ca^{2+} and Mg^{2+} compete each other and the primary role of Ca^{2+} may be as a

network-modifying cation near the NBO, while that of Mg^{2+} is as a charge-balancing cation in CMAS pseudobinary glasses.

3.3.2 Raman spectroscopy

The polymerization of silicate glasses and melts plays a critical role in their properties. Raman spectroscopy as well as NMR has been widely used to investigate changes in polymerization of silicate glasses (McMillan et al., 1982; Mysen et al., 2003; Neuville et al., 2008b). Figure 19 shows the Raman spectra of CMAS pseudobinary glasses. There are two groups of Raman mode in silicate glasses, which are Si-O-Si bending vibration between 400 and 750 cm^{-1} and Si-O stretching vibration between 800 and 110 cm^{-1}. The frequencies of stretching mode are related to the degree of polymerization Si tetrahedron, each of frequencies are 850(Q^0), 900(Q^1), 1000(Q^2) and 1100(Q^3) cm-^{1}. (McMillan, 1984) Q^n means SiO_4 tetrahedron with 'n' bridging oxygen. Figure 19 shows few change in stretching mode, while systematic change in bending mode (400~800 cm^{-1}). Q^0 and Q^1 decrease while Q^2 and Q^3 increase with decreasing diopside component, which means degree of polymerization decreases. This is because the NBO fraction increases due to perturbation of Mg^{2+} in diopside component as shown ^{17}O 3QMAS NMR spectrum. Also we observe that the frequency of Si-O-Si bending shifts to lower frequency with increasing Al_2O_3 content, which means the bond length and bond angle of Si-O-Si changes with composition. These results means that the degree of polymerization and bond length, bond angle are change with composition.

3.3.3 Implication for macroscopic properties and geophysical process

The atomic structure of CMAS pseudobinary glasses provides implications for several macroscopic properties and geophysical process. First of all, previous study has shown that the enthalpy of mixing of CMAS pseudobinary glasses is negative whereas that of crystalline materials is positive (Navrotsky et al., 1983) which means that the diopside phase and Ca-Ts phase are separated in crystal and they are mixed in glass. The Al^{3+} is in tetrahedral site and octahedral site of half rate in $CaAl_2SiO_6$ crystal. When the Ca-Tschermakite and diopside mix together, the Al^{3+} in tetrahedral in Ca-Ts is a little bit easy to exchange with Si tetrahedral whereas it is hard to exchange the Al^{3+} in octahedral site with Mg^{2+} in octahedral site in diopside because there are lattice difference due to difference of atomic distance (Al-O is 1.947 Å and Mg-O is 2.115 Å). The bond of Al^{3+} octahedral site is broken and distorted thus there are $^{[4]}$Al and $^{[5]}$Al not $^{[6]}$Al in $CaAl_2SiO_6$ glasses as shown figure 9. From this result we can conclude that it is easier to mix together in glass than crystal, the enthalpy of mixing is negative in glass. These results has implication for generation of basaltic melt. As natural basaltic melt is generated in the earth's interior, the composition of primary melt can be represented as CMAS pseudobinary glass due to the melting point of that system is the lowest. The negative enthalpy of mixing of CMAS pseudobinary glasses indicates two systems can be mixed more easily.

Second implication is about viscosity affecting the transport mantle melt in earth's interior. It has been known the viscosity decrease with increasing NBO in silicate glass and melts as mentioned above (Del Gaudio and Behrens, 2009;

Hofmeister et al., 2009; Neuville and Richet, 1991; Urbain et al., 1982), however the NBO fraction of those system is predicted by calculation. Here we report the experimental value of NBO fraction directly from ^{17}O 3QMAS NMR spectrum. We can conclude that difference of viscosity between diopside and Ca-Ts is stem from NBO fraction as shown figure 17. We can find the proportion of NBO is larger in $CaMgSi_2O_6$ than $CaAl_2SiO_6$ glasses. Thus viscosity increases with increasing diopside content in CMAS pseudobinary glasses. Viscosity is the transport property affecting melt migration thus basaltic melt in the earth's interior transport easier with composition that is high diopside content.

Third, the atomic structure has also implication for geophysical process such as dissolution of igneous rock. The rainwater or underground water infiltrate into igneous rock such as basalt then the minerals in that of rock react with waters; that is dissolution by water. There are alkaline earth's cation such as Basalt is CMAS multi component silicate Ca^{2+} extract more easily than Mg^{2+} because Ca^{2+} connects with NBO whereas Mg^{2+} connects with BO and the bond energy of BO is higher than that of NBO. The bond preference of NBO also affects the dissolution process in earth.

4. FURTHER STUDY

4.1 ^{43}Ca MAS and 3QMAS NMR

Alkaline earth cation, Ca^{2+} is abundant element in the magmatic liquids. Most studies on their chemical structures have been focused on SiO_4 and AlO_4 tetrahedral

networks, whereas the local environments around the divalent cations have been a question to understand amorphous structures. ^{27}Al and ^{17}O NMR is not enough to explain the mechanism along the changing composition. It is found that Ca^{2+} prefers NBO from ^{17}O 3QMAS NMR spectrum, however it needs obvious evidence. Also we want to know what the role of Ca^{2+} whether a network modifying cation or a charge balancing cation. We expect that ^{43}Ca NMR spectra could distinguish the network modifying Ca^{2+} and charge balancing Ca^{2+}.

NMR studies on such cation have been suppressed because of low natural abundance (0.145% for ^{43}Ca) and low gyromagnetic ratio. Despite ^{43}Ca NMR study is very challenging, through the ^{43}Ca NMR study we could obtain information of coordination number for the system (Shimoda et al., 2007). And through the coordination number or NMR parameter (e.g. C_q) we can predict Ca-O distance. From these results we could know the structure for diopside-Ca-Ts join system (Laurencin et al., 2008). Thus we want to report the Ca^{2+} environments in several geologically relevant silicate glasses using high-resolution MAS and 3QMAS NMR spectroscopy. It is expected that changing composition from diopside to Ca-Ts chemical shift of ^{43}Ca could be changed.

4.2 synchrotron study: X-ray absorption spectroscopy

Natural melts in the earth interior include about 10% FeO or Fe_2O_3 which are paramagnetic substance. Paramagnetic substances contain localized unpaired electrons, which couple to surrounding nuclei through the hyperfine interactions. Since the electron Zeeman states are unequally populated, and the electron

relaxation is very fast, the overall effect is to shift the nuclear spin resonances. (Levitt, 2001) Thus it needs another method to analyze the atomic structure of nearest composition of natural melts which include 10% FeO or Fe_2O_3. One of the effective methods is X-ray absorption spectroscopy, which provides information about atomic distance, coordination number, and local symmetry. We will perform the EXAFS (extended X-ray absorption fine structure) or XANES (X-ray absorption near edge scattering) then it will be possible to demonstrate the atomic structure of natural melts. Previous XANES study has shown there was structural rearrangement of CMAS silicate melts and glasses at high temperature (Neuville et al., 2008a) and another studies has shown XANES study about speciation of Fe in silicate glasses and melts (Wilke et al., 2007) however their system was not similar with natural basaltic melts. Thus we try to perform EXAFS or XANES experiment about CMAS pseudobinary glasses including 5~10 % FeO or Fe_2O_3. It is also expected to analysis the change of atomic structure with pressure using diamond anvil cell for multi-component silicate glasses from the atomic structure is probed using EXAFS or XANES.

5. CONCLUSION

From the experimental data presented here, an insight into multi component silicate glasses can be obtained with CMAS pseudobinary glasses in this study. The ^{27}Al MAS NMR spectra for the CMAS pseudobinary glasses show that four-coordinated Al is predominant, which demonstrate that Al^{3+} is a network forming cation. The peak position moves toward lower frequency with increasing diopside content due to an increase in Q^4(4Si) fraction with increasing Si content,

indicating that Al is surrounded only by bridging oxygen. The quadrupolar coupling constant (C_q) and FWHM of $^{[4]}$Al decreases with increasing diopside content, indicating a decrease of topological disorder. ^{17}O MAS NMR spectra for CMAS pseudobinary glasses qualitatively suggest that the NBO fraction increases with increasing diopside content. The nonrandom distribution of Ca-NBO and Mg-NBO indicates NBO prefers Ca^{2+} than Mg^{2+}. Mg^{2+} has proximity to Si-O-Al at intermediate composition thus Mg^{2+} plays a preferential role as a charge-balancing cation, while Ca^{2+} can act as a network-modifying cation in the Ca-Mg aluminosilicate glasses. The observed structural changes in the CMAS glasses can account for the changes in macroscopic properties with composition. For example, the predominance of $^{[4]}$Al and its extensive mixing with Si as evidenced by the significant fractions of $^{[4]}$Al-O-$^{[4]}$Si is consistent with a negative experimental enthalpy of mixing for silicate glasses in diopside and Ca-Tschermakite join from solution calorimetry. As viscosity of silicate melts decreases exponentially with NBO fraction, while there is no available experimental data for the viscosity of silicate melts in the diopside-anorthite join, the observed increase in NBO fraction with increasing diopside content indicates a decrease in melt viscosity toward a diopside end-member.

Finally, the preferential partitioning of Ca^{2+} and Mg^{2+} between NBO and BO may results in a variation of activity coefficient of CaO and MgO, thus controlling composition of melts generated at the Mid-Ocean Ridge or Oceanic Islands. This preference also has strong implication for dissolution mechanisms of basalts in contact with aqueous fluids. Taking into consideration of stronger bond between network modifying cations and NBO (over charge-balancing cation and BO), Mg^{2+} in the basalts is likely to be dissolved easily. The results and methods shed light on structure of multi-component oxide glasses and provide improved understanding their structure-property relations.

REFERENCE

Allwardt, J.R., Lee, S.K., and Stebbins, J.F., 2003, Bonding preferences of non-bridging O atoms: Evidence from O-17 MAS and 3QMAS NMR on calcium aluminate and low-silica Ca-aluminosilicate glasses, American Mineralogist, v. 88, p. 949-954.

Allwardt, J.R., and Stebbins, J.F., 2004, Ca-Mg and K-Mg mixing around non-bridging O atoms in silicate glasses: An investigation using O-17 MAS and 3QMAS NMR, American Mineralogist, v. 89, p. 777-784.

Angeli, F., Gaillard, M., Jollivet, P., and Charpentier, T., 2007, Contribution of Ca-43 MAS NMR for probing the structural configuration of calcium in glass, Chemical Physics Letters, v. 440, p. 324-328.

Asimow, P.D., Hirschmann, M.M., and Stolper, E.M., 2001, Calculation of peridotite partial melting from thermodynamic models of minerals and melts, IV. Adiabatic decompression and the composition and mean properties of mid-ocean ridge basalts, Journal of Petrology, v. 42, p. 963-998.

Baker, M.B., Hirschmann, M.M., Ghiorso, M.S., and Stolper, E.M., 1995, Compositions of near-solidus peridotite melts from experiments and thermodynamic calculations, Nature, v. 375, p. 308-311.

Baltisberger, J.H., Xu, Z., Stebbins, J.F., Wang, S.H., and Pines, A., 1996, Triple-quantum two-dimensional Al-27 magic-angle spinning nuclear magnetic resonance spectroscopic study of aluminosilicate and aluminate crystals and glasses, Journal of the American Chemical Society, v. 118, p. 7209-7214.

Barbieri, L., Corradi, A.B., Lancellotti, I., Leonelli, C., and Montorsi, M., 2004, Experimental and computer simulation study of glasses belonging to diopside-anorthite system, Journal of Non-Crystalline Solids, v. 345, p. 724-729.

Bottinga, Y., and Richet, P., 1978, Thermodynamics of liquid silicates, a preliminary-report, Earth and Planetary Science Letters, v. 40, p. 382-400.

Del Gaudio, P., and Behrens, H., 2009, An experimental study on the pressure dependence of viscosity in silicate melts, Journal of Chemical Physics, v. 131.

Duer, M.J., 2004, Solid-state NMR spectroscopy

Dupree, R., Howes, A.P., and Kohn, S.C., 1997, Natural abundance solid state Ca-43 NMR, Chemical Physics Letters, v. 276, p. 399-404.

Gasparik, T., 1984, Experimentally determined stability of clinopyroxene + garnet + corundum in the system CaO-MgO-Al_2O_3-SiO_2, American Mineralogist, v. 69, p. 1025-1035.

Ghose, S., and Tsang, T., 1973, Structural dependence of quadrupole coupling-constant e2qq/h for al-27 and crystal-field parameter-d for Fe^{3+} in aluminosilicates, American Mineralogist, v. 58, p. 748-755

Giordano, D., Potuzak, M., Romano, C., Dingwell, D.B., and Nowak, M., 2008a, Viscosity and glass transition temperature of hydrous melts in the system $CaAl_2Si_2O_8$-$CaMgSi_2O_6$, Chemical Geology, v. 256, p. 203-215.

Giordano, D., Russell, J.K., and Dingwell, D.B., 2008b, Viscosity of magmatic liquids, A model: Earth and Planetary Science Letters, v. 271, p. 123-134.

Hofmeister, A.M., Whittington, A.G., and Pertermann, M., 2009, Transport properties of high albite crystals, near-endmember feldspar and pyroxene glasses, and their melts to high temperature, Contributions to Mineralogy and Petrology, v. 158, p. 381-400.

Iwamori, H., 1993, A model for disequilibrium mantle melting incorporating melt transport by porous and channel flows, Nature, v. 366, p. 734-737.

Kushiro, I., 2001, Partial melting experiments on peridotite and origin of mid-ocean ridge basalt, Annual Review of Earth and Planetary Sciences, v. 29, p. 71-107.

Lange, R.A., and Carmichael, I.S.E., 1987, Densities of Na_2O-K_2O-CaO-MgO-FeO-Fe_2O_3-Al_2O_3-TiO_2-SiO_2 liquids-New measurements and derived partial molar properties, Geochimica Et Cosmochimica Acta, v. 51, p. 2931-2946.

Langmuir C.H., Klein E.M., and Plank T. (1992) Petrological systematics of mid-ocean ridge basalts: constraints on melt generation beneath ocean ridges. In: Morgan J.P., Blackman, D.K., Sinton J. (eds.) Mantle Flow and Melt Generation at Mid-Ocean Ridges, Geophys. Monogr. Ser., Vol.71, AGU, 183-280.

Laurencin, D., Wong, A., Dupree, R., and Smith, M.E., 2008, Natural abundance Ca-43 solid-state NMR characterisation of hydroxyapatite: identification of

the two calcium sites, Magnetic Resonance in Chemistry, v. 46, p. 347-350.

Lee, S.K., 2004, Structure of silicate glasses and melts at high pressure: Quantum chemical calculations and solid-state NMR, Journal of Physical Chemistry B, v. 108, p. 5889-5900.

Lee, S.K., 2005a, Microscopic origins of macroscopic properties of silicate melts and glasses at ambient and high pressure: Implications for melt generation and dynamics, Geochimica Et Cosmochimica Acta, v. 69, p. 3695-3710.

Lee, S.K., 2005b, Structure and the extent of disorder in quaternary (Ca-Mg and Ca-Na) aluminosilicate, American Mineralogist v. 90.

Lee, S.K., Cody, G.D., Fei, Y.W., and Mysen, B.O., 2004, Nature of polymerization and properties of silicate melts and glasses at high pressure, Geochimica Et Cosmochimica Acta, v. 68, p. 4189-4200.

Lee, S.K., Cody, G.D., and Mysen, B.O., 2005a, Structure and the extent of disorder in quaternary (Ca-Mg and Ca-Na) aluminosilicate glasses and melts, American Mineralogist, v. 90, p. 1393-1401.

Lee, S.K., Deschamps, M., Hiet, J., Massiot, D., and Park, S.Y., 2009a, Connectivity and Proximity between Quadrupolar Nuclides in Oxide Glasses: Insights from through-Bond and through-Space Correlations in Solid-State NMR, Journal of Physical Chemistry B, v. 113, p. 5162-5167.

Lee, S.K., Lee, S.B., Park, S.Y., Yi, Y.S., and Ahn, C.W., 2009b, Structure of Amorphous Aluminum Oxide, Physical Review Letters, v. 103.

Lee, S.K., Mibe, K., Fei, Y.W., Cody, G.D., and Mysen, B.O., 2005b, Structure of B_2O_3 glass at high pressure: A B-11 solid-state NMR study, Physical Review Letters, v. 94.

Lee, S.K., and Stebbins, J.F., 1999, The degree of aluminum avoidance in aluminosilicate glasses, American Mineralogist, v. 84, p. 937-945.

Lee, S.K., and Stebbins, J.F., 2000, The structure of aluminosilicate glasses: high-resolution O-17 and Al-27 MAS and 3QMAS, Journal of Physical Chemistry B, v. 104, p. 4091-4100.

Lee, S.K., and Stebbins, J.F., 2002, Extent of intermixing among framework units in silicate glasses and melts, Geochimica Et Cosmochimica Acta, v. 66, p. 303-309.

Lee, S.K., and Stebbins, J.F., 2003, Nature of cation mixing and ordering in Na-Ca silicate glasses and melts, Journal of Physical Chemistry B, v. 107, p. 3141-3148.

Lee, S.K., and Stebbins, J.F., 2006, Disorder and the extent of polymerization in calcium silicate and aluminosilicate glasses: O-17 NMR results and quantum chemical molecular orbital calculations, Geochimica Et Cosmochimica Acta, v. 70, p. 4275-4286.

Lee, S.K., and Sung, S., 2008, The effect of network-modifying cations on the structure and disorder in peralkaline Ca-Na aluminosilicate glasses: O-17 3QMAS NMR study, Chemical Geology, v. 256, p. 326-333.

Levin, I., and Brandon, D., 1998, Metastable alumina polymorphs: Crystal structures and transition sequences, Journal of the American Ceramic Society, v. 81, p. 1995-2012.

Levitt, M.H., 2001, Spin dynamics: Basic of nuclear magnetic resonance Chichester, England, John Wiley & Sons, Ltd.

Liang, Y., Richter, F.M., and Chamberlin, L., 1997, Diffusion in silicate melts: III. Empirical models for multicomponent diffusion, Geochimica Et Cosmochimica Acta, v. 61, p. 5295-5312.

MacKenzie, K.J.D., Smith, M.E., and Wong, A., 2007, A multinuclear MAS NMR study of calcium-containing aluminosilicate inorganic polymers, Journal of Materials Chemistry, v. 17, p. 5090-5096.

Madhu, P.K., Goldbourt, A., Frydman, L., and Vega, S., 1999, Sensitivity enhancement of the MQMAS NMR experiment by fast amplitude modulation of the pulses, Chemical Physics Letters, v. 307, p. 41-47.

McMillan, P., 1984, Structural studies of silicate-glasses and melts - applications and limitations of raman-spectroscopy, American Mineralogist, v. 69, p. 622-644.

McMillan, P., Piriou, B., and Navrotsky, A., 1982, A raman-spectroscopic study of glasses along the joins silica-calcium aluminate, silica-sodium aluminate, and silica-potassium aluminate, Geochimica Et Cosmochimica Acta, v. 46, p. 2021-2037.

Mysen, B.O., Lucier, A., and Cody, G.D., 2003, The structural behavior of Al^{3+} in

peralkaline melts and glasses in the system Na_2O-Al_2O_3-SiO_2, American Mineralogist, v. 88, p. 1668-1678.

Mysen BO, R.P., 2005, Silicate glasses and melts, Elsevier.

Navrotsky, A., Zimmermann, H.D., and Hervig, R.L., 1983, Thermochemical study of glasses in the system $CaMgSi_2O_6$-$CaAl_2SiO_6$, Geochimica Et Cosmochimica Acta, v. 47, p. 1535-1538.

Neuville, D.R., Cormier, L., De Ligny, D., Roux, J., Flank, A.M., and Lagarde, P., 2008a, Environments around Al, Si, and Ca in aluminate and aluminosilicate melts by X-ray absorption spectroscopy at high temperature: American Mineralogist, v. 93, p. 228-234.

Neuville, D.R., Cormier, L., Montouillout, V., Florian, P., Millot, F., Rifflet, J.C., and Massiot, D., 2008, Structure of Mg- and Mg/Ca aluminosilicate glasses: Al-27 NMR and Raman spectroscopy investigations, American Mineralogist, v. 93, p. 1721-1731.

Neuville, D.R., and Richet, P., 1991, Viscosity and mixing in molten (Ca, Mg) pyroxenes and garnets,

Geochimica Et Cosmochimica Acta, v. 55, p. 1011-1019.

Ohtani, E., 1985, The primordial terrestrial magma ocean and its implication for stratification of the mantle, Physics of the Earth and Planetary Interiors, v. 38, p. 70-80.

Presnall, D.C., Gudfinnsson, G.H., and Walter, M.J., 2002, Generation of mid-ocean ridge basalts at pressures from 1 to 7 GPa, Geochimica Et Cosmochimica Acta, v. 66, p. PII S0016-7037(02)00890-6.

Richet, P., 1984, Viscosity and configurational entropy of silicate melts, Geochimica Et Cosmochimica Acta, v. 48, p. 471-483.

Richet, P., Robie, R.A., and Hemingway, B.S., 1993, Entropy and structure of silicate-glasses and melts, Geochimica Et Cosmochimica Acta, v. 57, p. 2751-2766.

Shimoda, K., Tobu, Y., Shimoikeda, Y., Nemoto, T., and Saito, K., 2007, Multiple Ca2+ environments in silicate glasses by high-resolution Ca-43 MQMAS NMR technique at high and ultra-high (21.8 T) magnetic fields, Journal of Magnetic Resonance, v. 186, p. 156-159.

Stebbins, J.F., and Xu, Z., 1997, NMR evidence for excess non-bridging oxygen in an aluminosilicate glass, Nature, v. 390, p. 60-62.

Tarduno, J., Bunge, H.P., Sleep, N., and Hansen, U., 2009, The Bent Hawaiian-Emperor Hotspot Track: Inheriting the Mantle Wind, Science, v. 324, p. 50-53.

Urbain, G., Bottinga, Y., and Richet, P., 1982, Viscosity of liquid silica, silicates and alumino-silicates, Geochimica Et Cosmochimica Acta, v. 46, p. 1061-1072.

Webb, S., and Knoche, R., 1995, The glass-transition, structural relaxation and shear viscosity of silicate melts, La Petite Pierre, France, p. 165-183.

Wilke, M., Farges, F., Partzsch, G.M., Schmidt, C., and Behrens, H., 2007, Speciation of Fe in silicate glasses and melts by in-situ XANES spectroscopy: American Mineralogist, v. 92, p. 44-56.

Zhao, P., Neuhoff, P.S., and Stebbins, J.F., 2001, Comparison of FAM mixing to single-pulse mixing in O-17 3Q-and 5Q-MAS NMR of oxygen sites in zeolites, Chemical Physics Letters, v. 344, p. 325-332.

TABLES

Table 1. Composition of oceanic island basalt and mid ocean ridge basalt in mol %

	Ocean Island * (mol%)			Mid Ocean Ridge † (mol%)		
	Mauna Kea		West Greenland	Mid-Atlantic Ridge	East-Pacific Ridge	Indian-Ocean Ridge
SiO_2	46.20	45.84	46.9	56.46	56.68	56.70
TiO_2	2.01	1.83	1.29	1.04	1.25	0.83
Al_2O_3	9.93	9.90	11.6	10.24	9.92	9.98
Fe_2O_3	0.93	1.23	1.82	2.85	3.31	2.98
FeO	10.40	10.32	9.4			
MnO	0.18	0.19	0.21			
MgO	17.80	18.27	17.1	12.77	11.95	12.77
CaO	10.00	10.12	9.9	13.60	13.79	14.09
Na_2O	1.72	1.53	1.56	2.87	2.91	2.51
K_2O	0.56	0.42	0.09	0.12	0.12	0.10
P_2O_5	0.23	0.28		0.06	0.06	0.05

*(Herzberg, Nature, 2006) †(Winter J.D., 2001)

Table 2. Composition of CaO-MgO-Al_2O_3-SiO_2 silicate glasses in diopside-Ca-Tschermakite pseudobinary join.

Di-CaTs mol ratio		X_{MgO}	NBO (calculation)	CMAS mole %			
				CaO	MgO	Al_2O_3	SiO_2
0	100	0	0	33.0	0.0	33.0	33.0
25	75	0.25	0.17	30.8	7.7	23.1	38.5
50	50	0.5	0.33	28.5	14.3	14.3	42.9
75	25	0.75	0.50	26.7	20.0	6.7	46.7
100	0	1	0.67	25.0	25.0	0.0	50.0

FIGURES

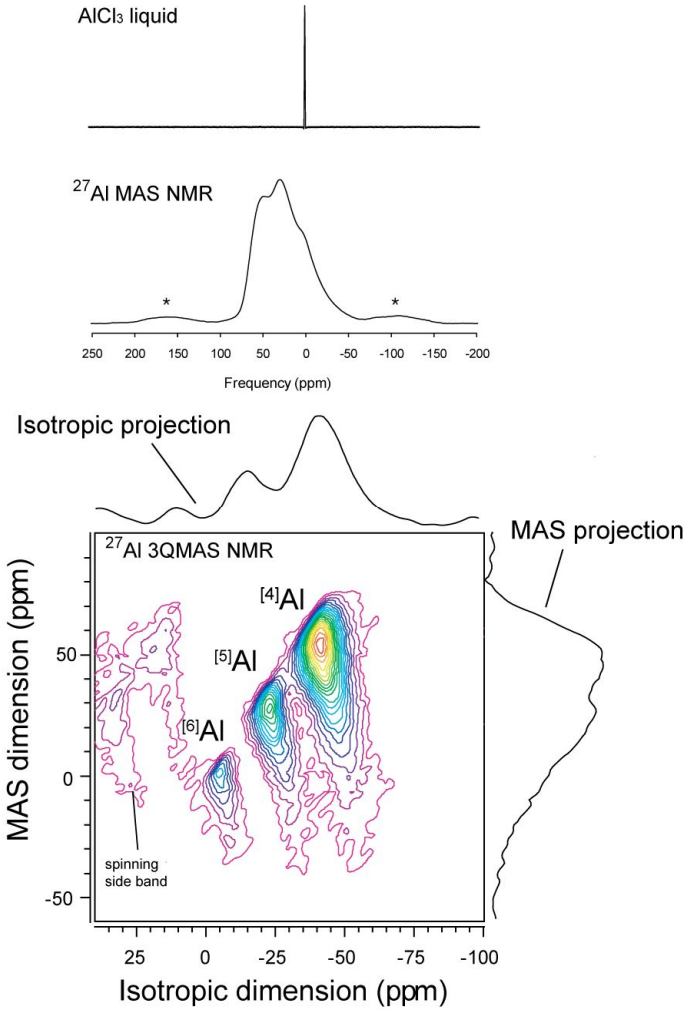

Figure 1. ^{27}Al MAS and 3QMAS NMR spectra for Mg-aluminoborate glasses ($MgO:Al_2O_3:B_2O_3$=2:1:2) at 9.4 T**.** ^{27}Al MAS spectrum for $AlCl_3$ liquid is also shown. Contour lines are drawn at 5% intervals from relative intensities of 7% to 97% with added 3%.

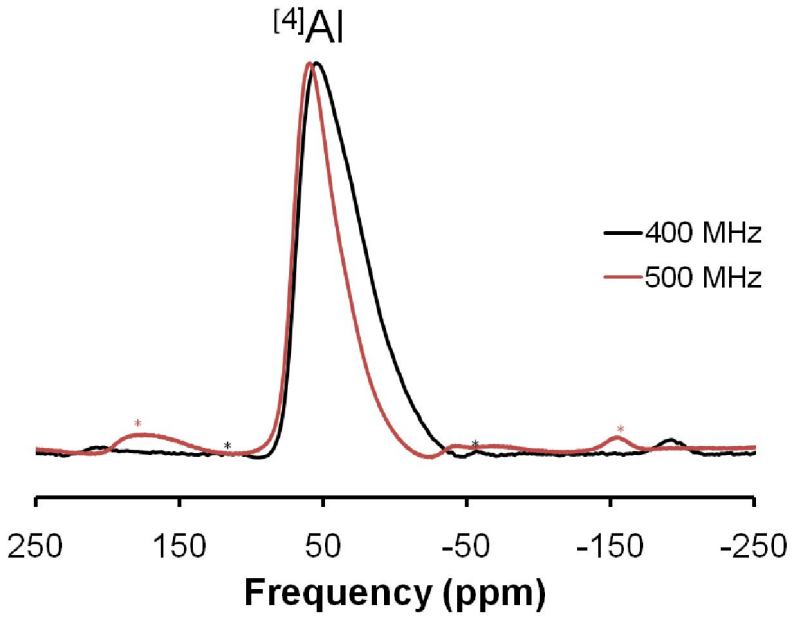

Figure 2. Comparison between ^{27}Al MAS NMR for $CaAl_2SiO_6$ glass at 9.4 T and 11.7 T. The spinning sideband is labeled '*'.

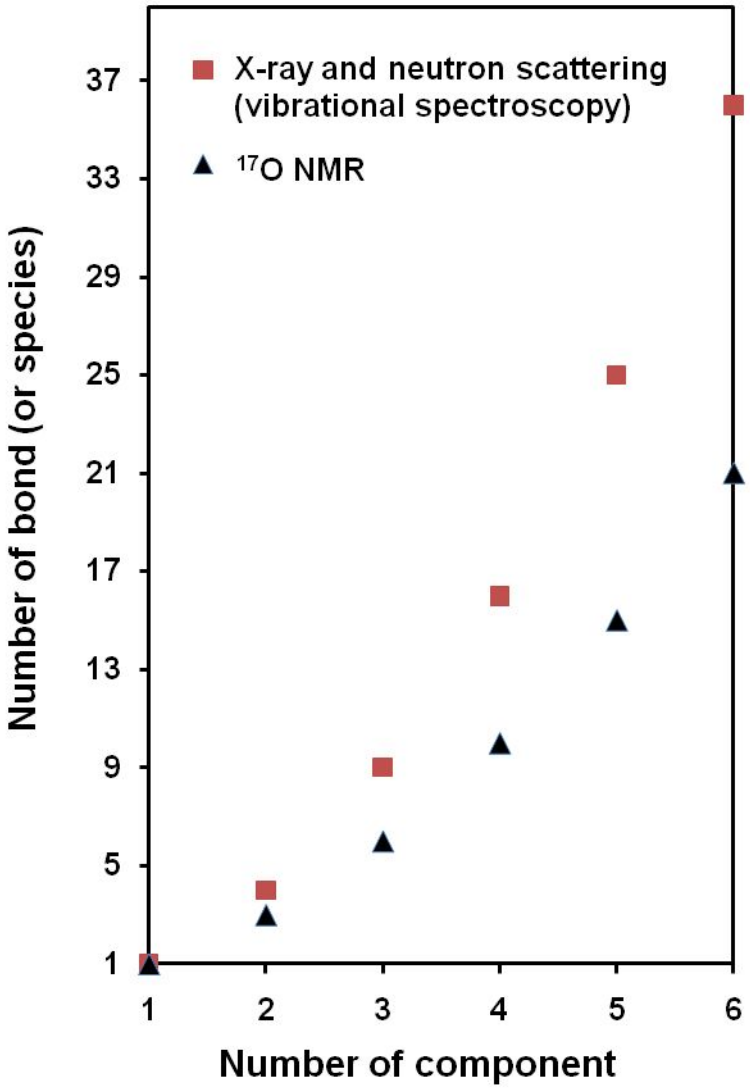

Figure 3. Effect of number of component on number of bond (or species) in oxides.

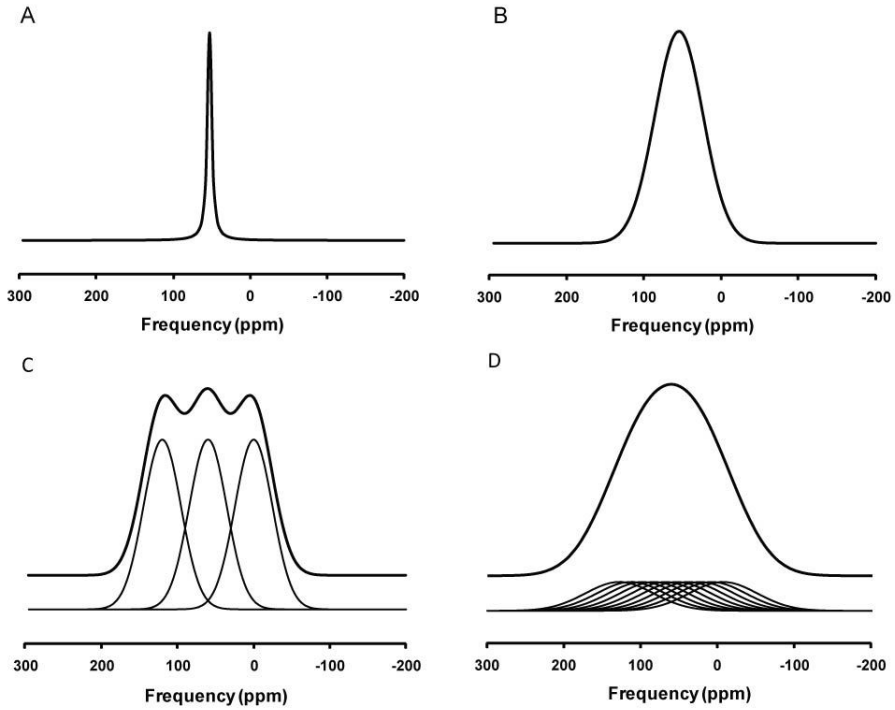

Figure 4. (A) A hypothetical NMR spectrum for single component liquid, (B) for single component amorphous material, (C) for binary amorphous material, and (D) for multi-component amorphous material.

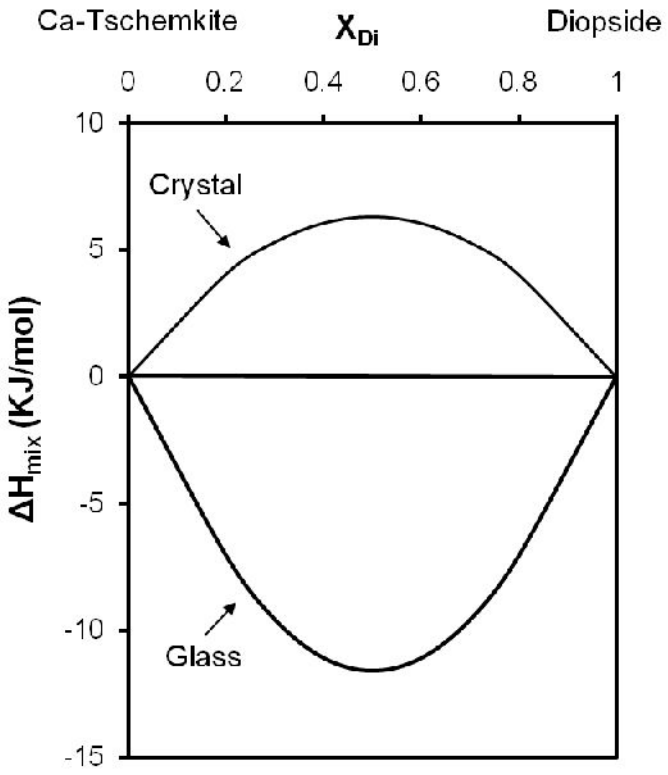

Figure 5. Enthalpy of mixing for CaO-MgO-Al_2O_3-SiO_2 silicate glasses in diopside -Ca-Tschermakite pseudobinary join. X_{Di} is the mole fraction of diopside (Navrotsky et al., 1983).

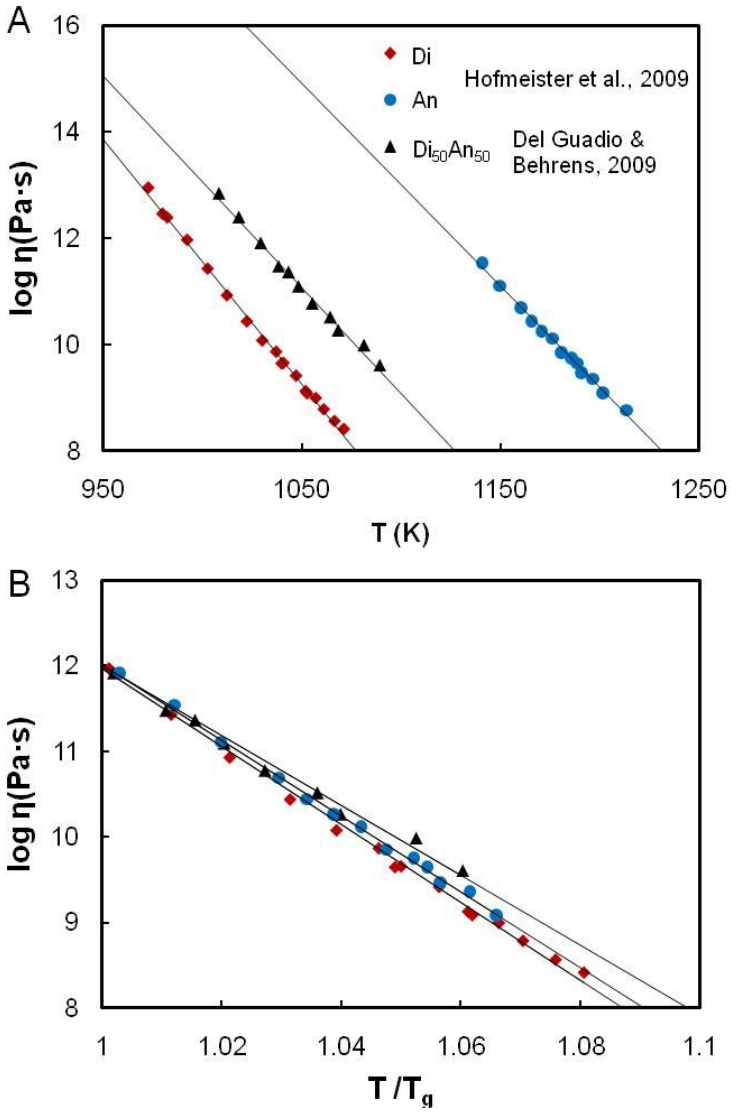

Figure 6. Viscosity of diopside (Di, $CaMgSi_2O_6$) and anorthite (An, $CaAl_2Si_2O_8$) glasses. The red diamond is viscosity of Di, the blue circle is that of An (Hofmeister et al., 2009), and the triangle is that of Di-An join (Di:An= 50:50) (Del Gaudio and Behrens, 2009). T_g is the glass transition temperature.

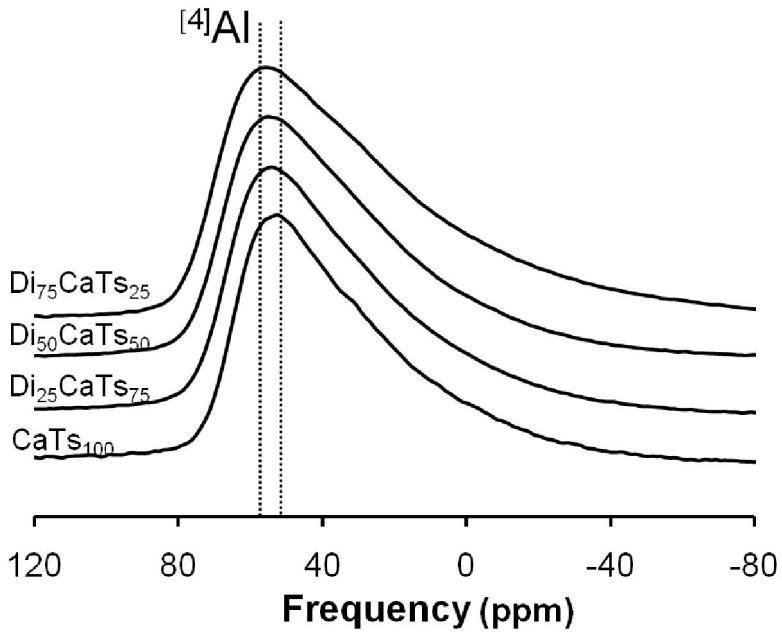

Figure 7. ^{27}Al MAS NMR spectra for CaO-MgO-Al_2O_3-SiO_2 silicate glasses in diopside -Ca-Tschermakite pseudobinary join at 9.4 T with varying diopside content. Di is diopside ($CaMgSi_2O_6$) and CaTs is Ca-Tschermakite ($CaAl_2SiO_6$).

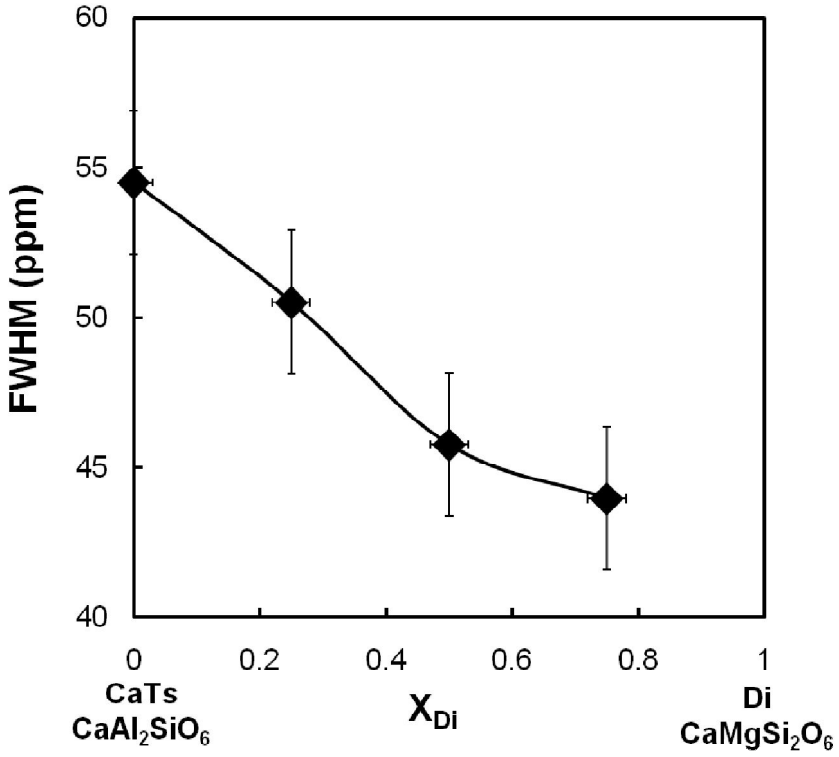

Figure 8. FWHM of $^{[4]}Al$ in MAS dimension for CaO-MgO-Al_2O_3-SiO_2 silicate glasses in diopside -Ca-Tschermakite pseudobinary join. Di is diopside and CaTs is Ca-Tschermakite. X_{Di} is the mole fraction of diopside.

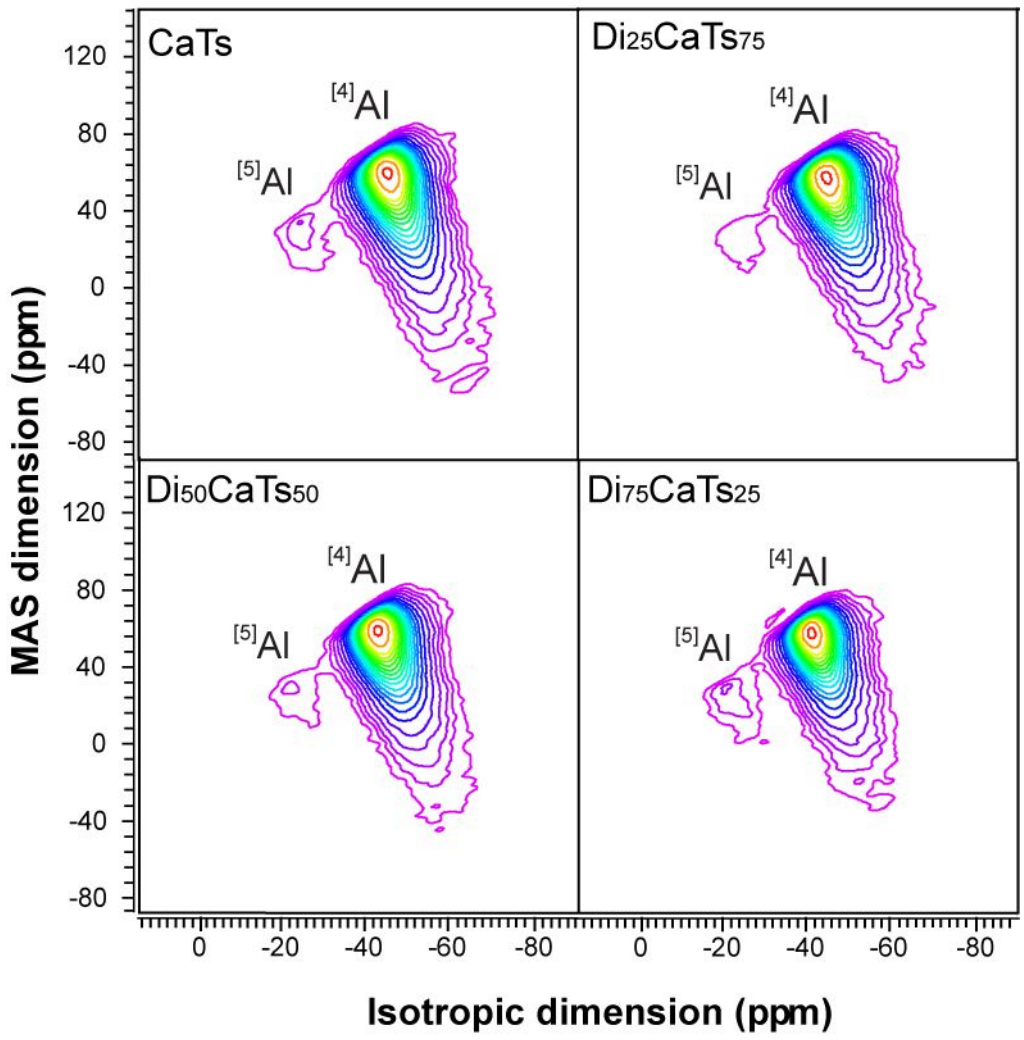

Figure 9. ^{27}Al 3QMAS NMR spectra for CaO-MgO-Al_2O_3-SiO_2 silicate glasses in diopside -Ca-Tschermakite pseudobinary join at 9.4 T with varying diopside content. Di is diopside ($CaMgSi_2O_6$) and CaTs is Ca-Tschermakite ($CaAl_2SiO_6$). Contour lines are drawn at 5% intervals from relative intensities of 2% to 97%.

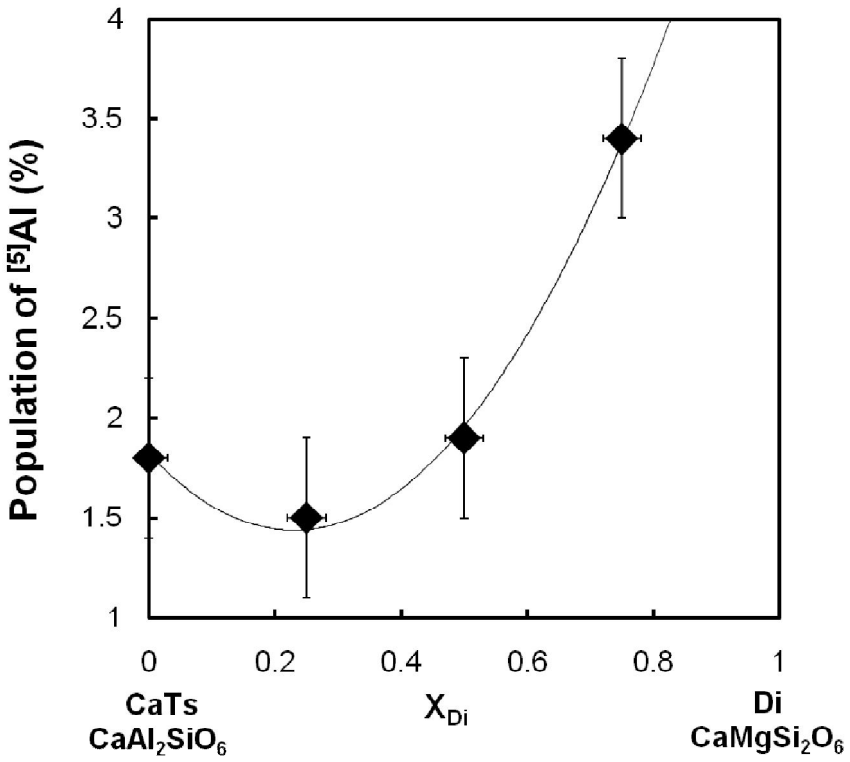

Figure 10. The population of $^{[5]}Al$ for $CaO\text{-}MgO\text{-}Al_2O_3\text{-}SiO_2$ silicate glasses in diopside -Ca-Tschermakite pseudobinary join. Di is diopside and CaTs is Ca-Tschermakite.

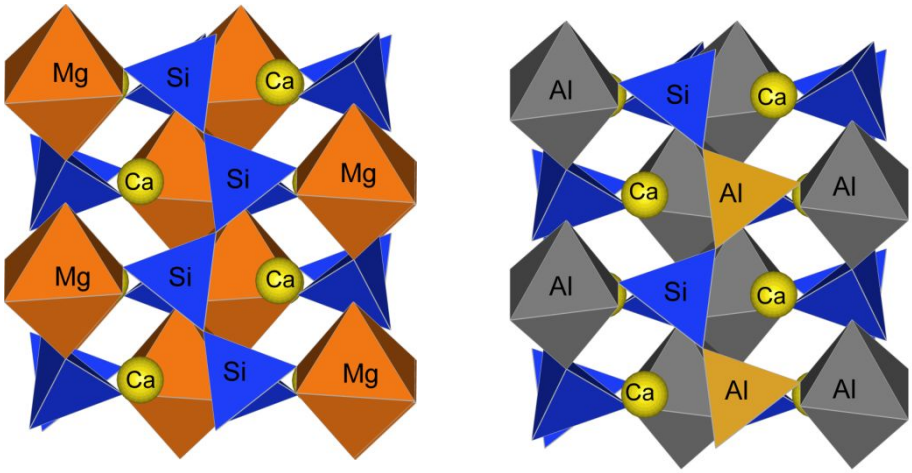

Figure 11. The atomic structure of diopside and Ca-Tschermakite crystals. The left one is diopside and right one is Ca-Tschermakite.

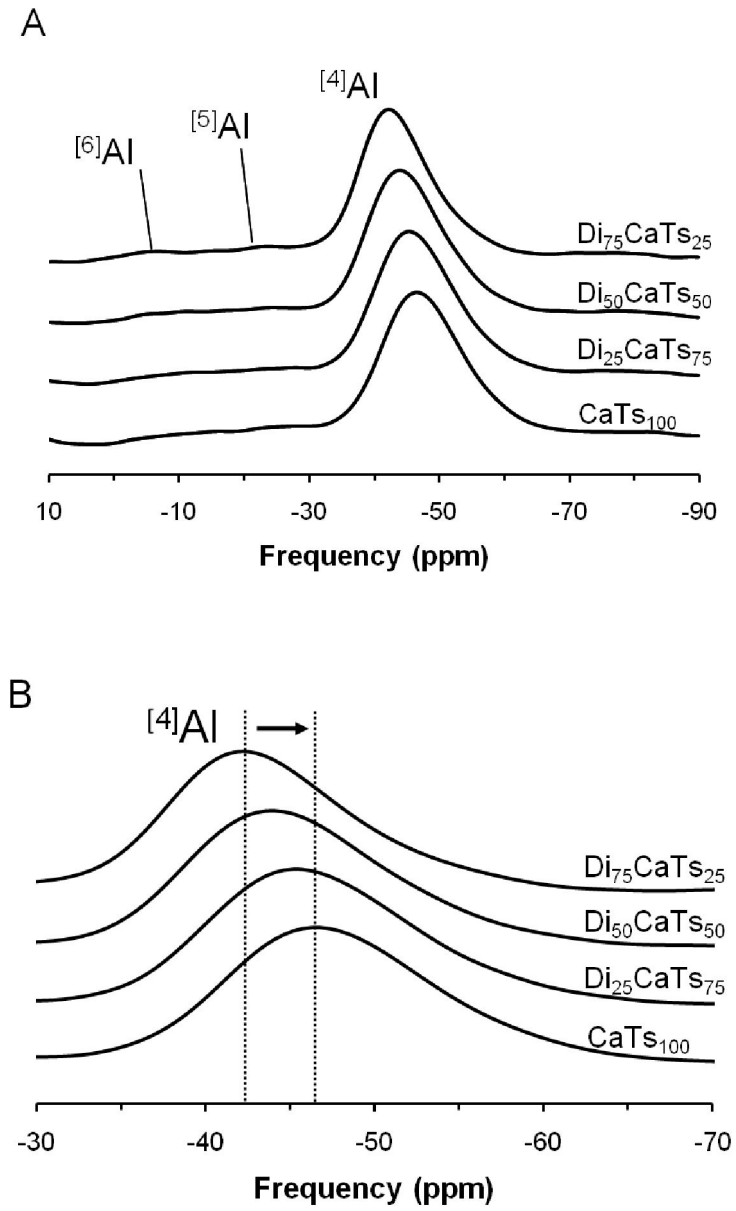

Figure 12. Total isotropic projection of ^{27}Al 3QMAS NMR spectra for CaO-MgO-Al_2O_3-SiO_2 silicate glasses in diopside -Ca-Tschermakite pseudobinary join at 9.4 T. Di is diopside and CaTs is Ca-Tschermakite. (B) is magnification of (A).

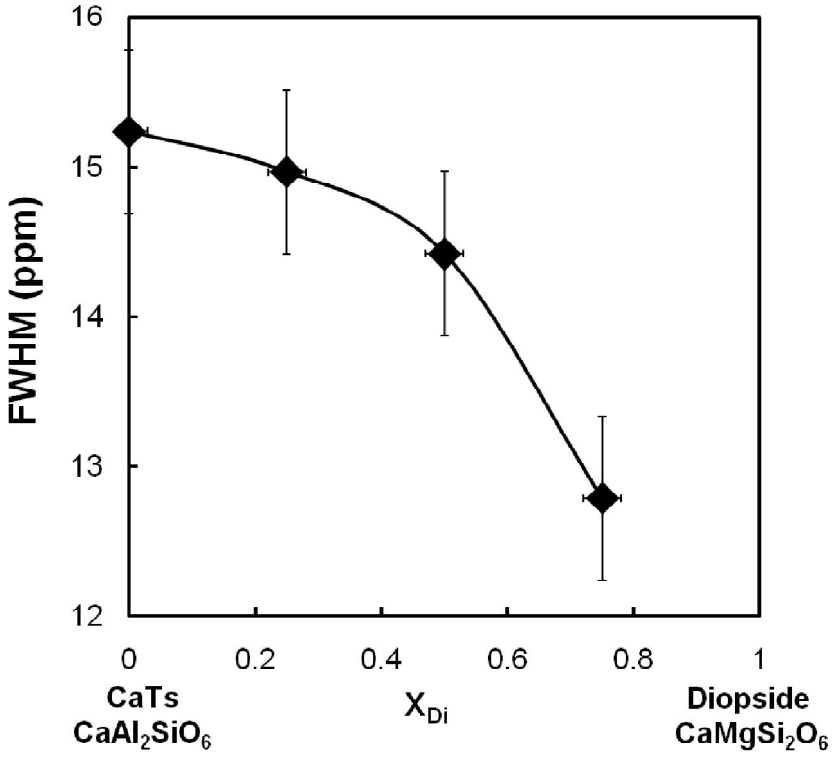

Figure 13. FWHM of $^{[4]}Al$ in total isotropic projection of ^{27}Al 3QMAS NMR spectra for CaO-MgO-Al_2O_3-SiO_2 silicate glasses in diopside -Ca-Tschermakite pseudobinary join at 9.4 T. Di is diopside and CaTs is Ca-Tschermakite.

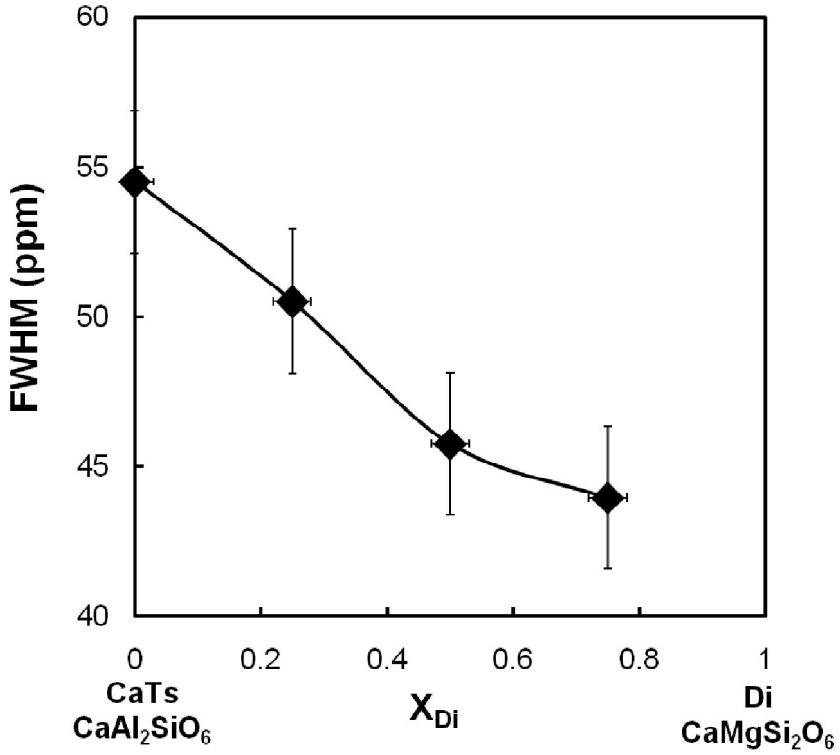

Figure 14. Quadrupolar coupling constant (C_q) of $^{[4]}Al$ in CaO-MgO-Al_2O_3-SiO_2 silicate glasses in diopside -Ca-Tschermakite pseudobinary join. Di is diopside and CaTs is Ca-Tschermakite.

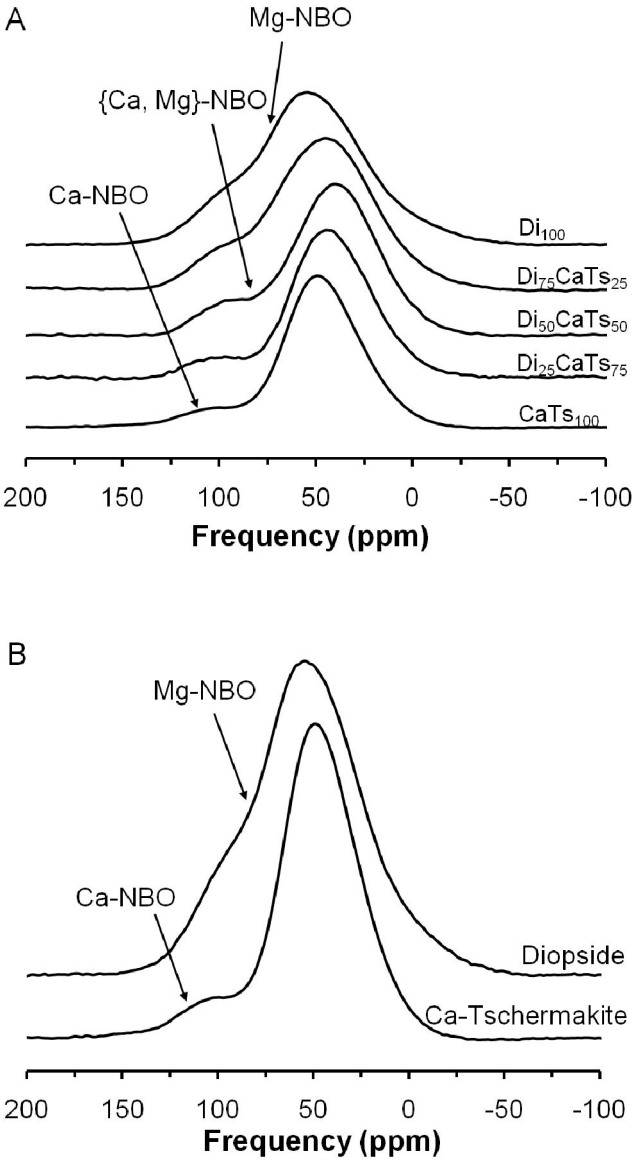

Figure 15. ^{17}O MAS NMR spectra for CaO-MgO-Al_2O_3-SiO_2 silicate glasses in diopside -Ca-Tschermakite pseudobinary join, (B) for diopside glass and Ca-Tschermakite glass at 9.4 T. Di is diopside and CaTs is Ca-Tschermakite.

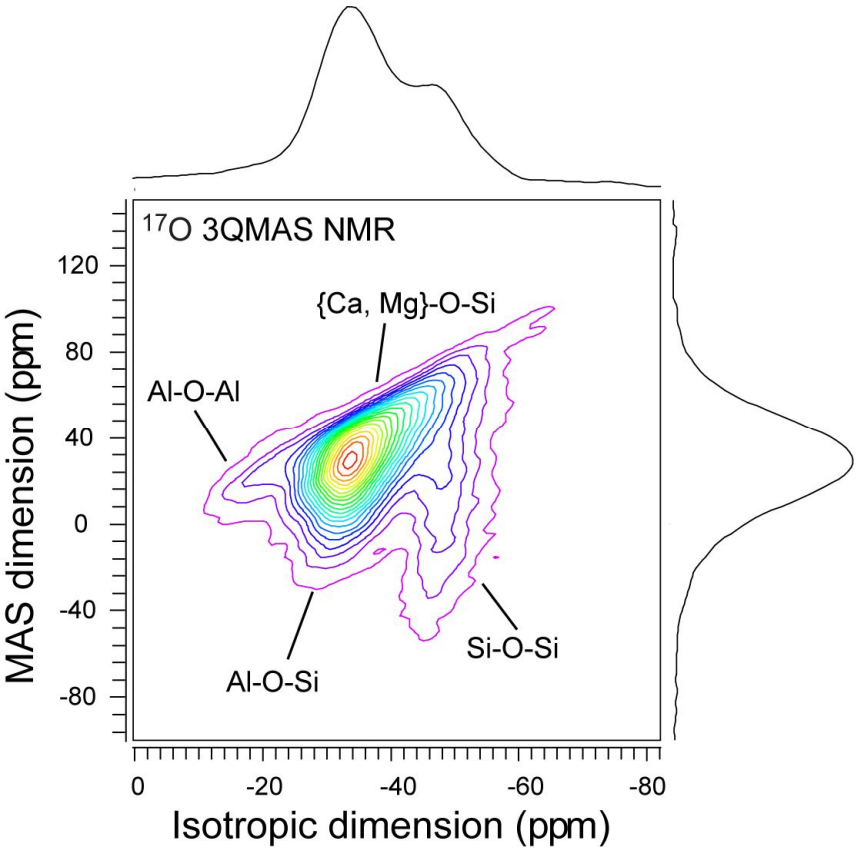

Figure 16. ^{17}O 3QMAS NMR spectra for model quaternary aluminosilicate glasses (CaO: MgO: Al_2O_3: SiO_2=8.8: 18.9: 21.3: 51.0 wt%) at 9.4 T. Contour lines are drawn at 5% intervals from relative intensities of 3% to 98%.

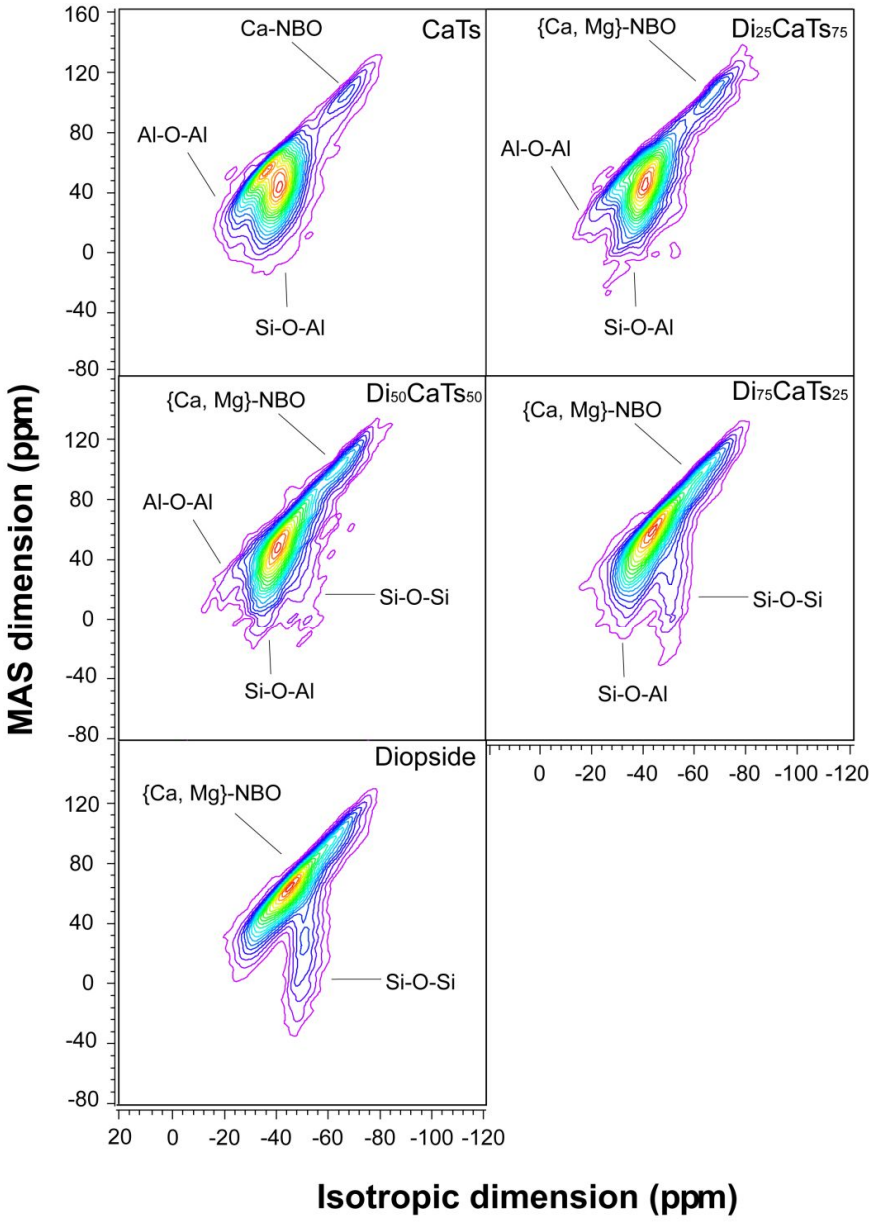

Figure 17. ^{17}O 3QMAS NMR for CaO-MgO-Al_2O_3-SiO_2 silicate glasses in diopside -Ca-Tschermakite pseudobinary join at 9.4T with varying diopside content. Di is diopside and CaTs is Ca-Tschermakite. Contour lines are drawn at 5% intervals from relative intensities of 8% to 98% with added lines at 4%.

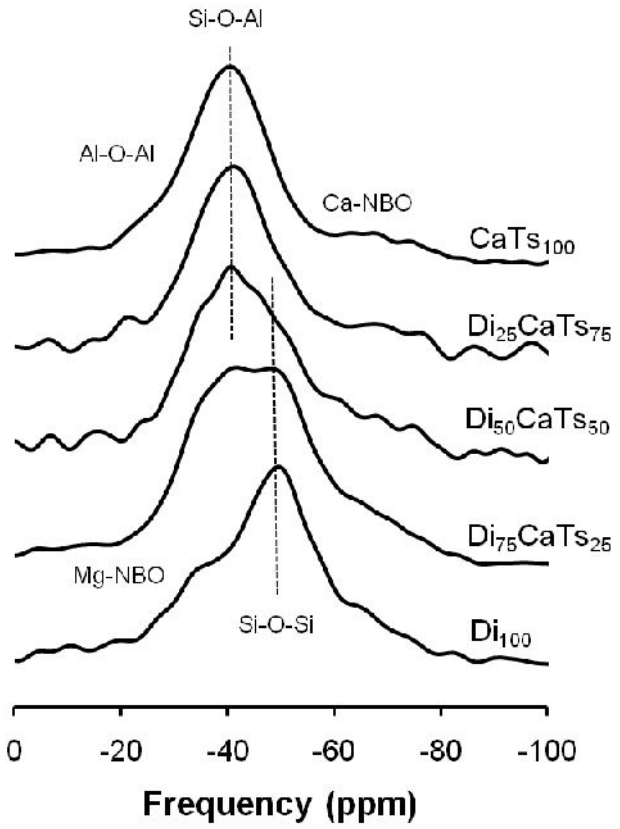

Figure 18. Total isotropic projection of ^{17}O 3QMAS NMR spectra for CaO-MgO-Al_2O_3-SiO_2 silicate glasses in diopside -Ca-Tschermakite pseudobinary join at 9.4 T with varying diopside content. Di is diopside and CaTs is Ca-Tschermakite.

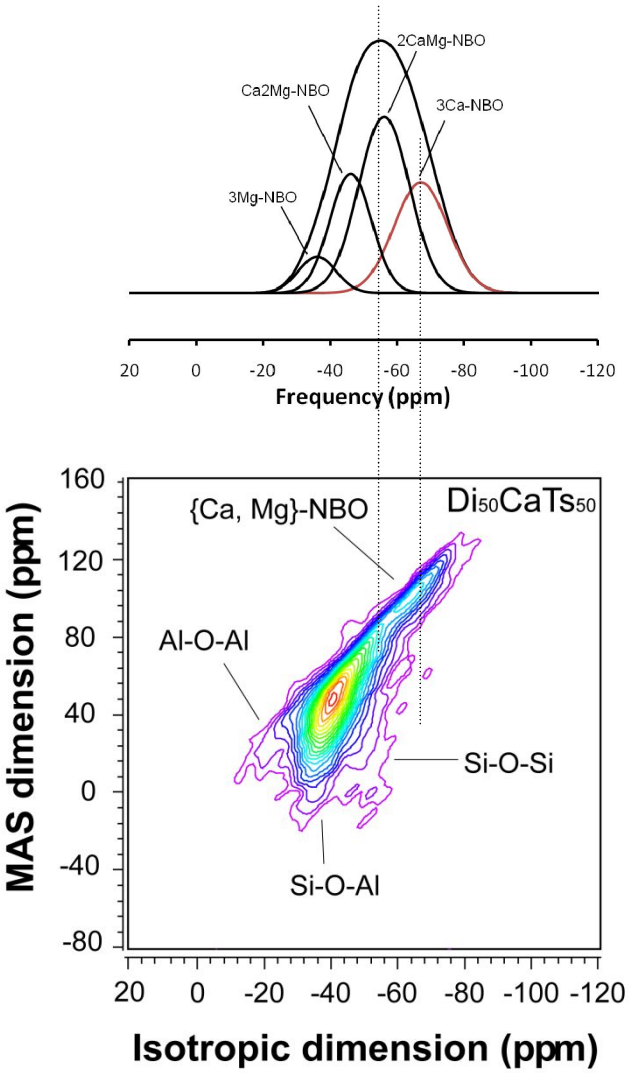

Figure 19. ^{17}O 3QMAS NMR spectrum for intermediate composition of diopside (Di)-Ca-Tschermakite (CaTs) pseudobinary join (Di : CaTs = 50 : 50) at 9.4 T. Contour lines are drawn at 5% intervals from relative intensities of 8% to 98% with added lines at 4%. A predicted spectrum of NBO peaks (in the isotropic projection) are also shown based on composition (Ca/(Ca+Mg)=0.67) using the random model is also shown.

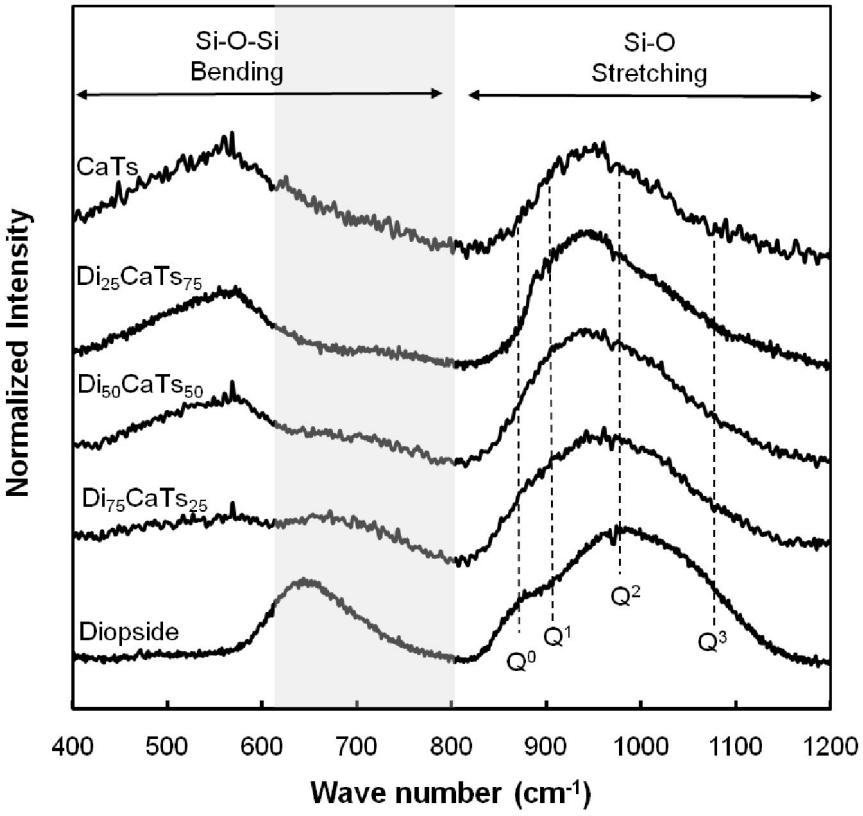

Figure 20. Normalized Raman spectra at room temperature for CaO-MgO-Al_2O_3-SiO_2 silicate glasses in diopside -Ca-Tschermakite pseudobinary join. Di is diopside and CaTs is Ca-Tschermakite.

APPENDIX 1

The effect of network modifying cation (i.e. Mg^{2+}) in Mg-aluminosilicate glass (Park et al., in preparation) Mg-aluminosilicate glass is a model silicate melts of mantle melts in the earth's interior (Lee, 2005b) In the two series of Mg-aluminosilicate glasses (i.e. $MgSiO_3$+2.5%Al_2O_3 and $MgSiO_3$ + 10% Al_2O_3), we performed ^{27}Al MAS and 3QMAS NMR experiments. The ^{27}Al NMR spectra obtained on a Varian 400 solid-state spectrometer (9.4 T) at resonance frequency of 104.229 MHz. Figure A1 shows ^{27}Al MAS NMR spectra for Mg-aluminosilicate with different alumina content, which are overlapped due to quadrupolar effect. The overlapped $^{[4]}$Al, $^{[5]}$Al, $^{[6]}$Al atomic structures are fully resolved with two-dimensional ^{27}Al 3QMAS NMR as shown figure A2. Those Al species have not been observed for other alkaline earth aluminosilicate melts and glasses. The results thus suggest significant topological and configuration disorder in the mantle melts due to the presence high field strength cation (i.e., Mg^{2+}).

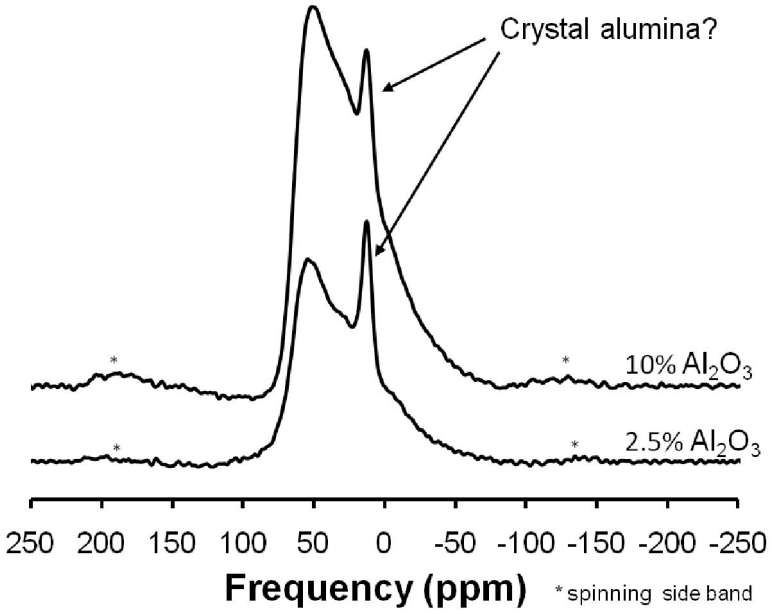

Figure A1. ^{27}Al MAS spectra for Mg-aluminosilicate glasses at 9.4 T,. * refers to spinning side bands.

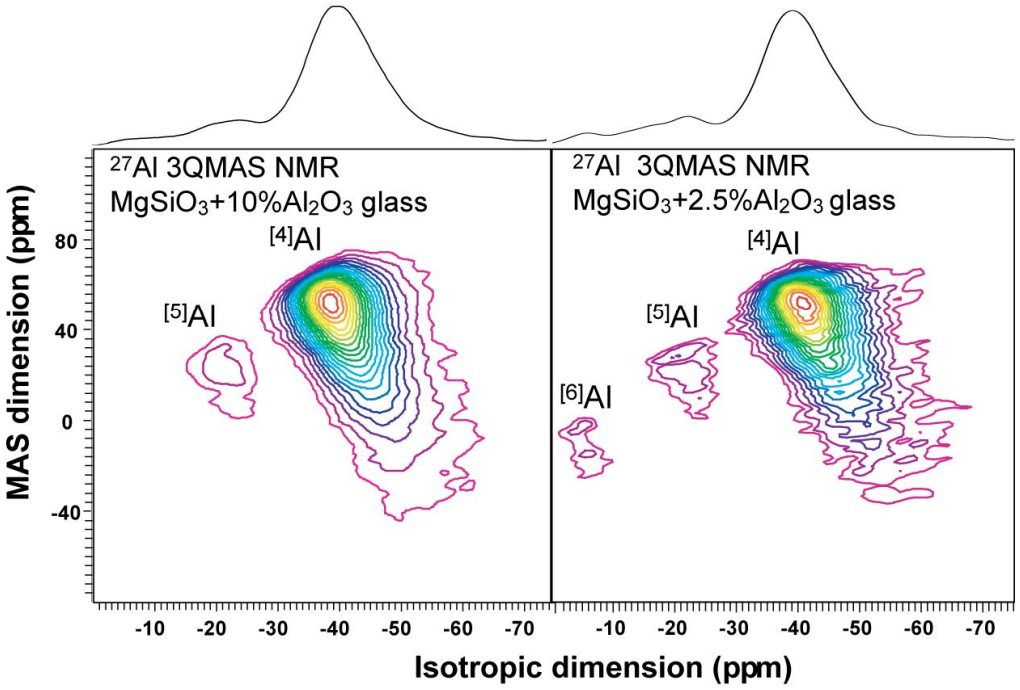

Figure A2. ^{27}Al 3QMAS spectra for Mg-aluminosilicate glasses at 9.4 T. Contour lines are drawn from 3% to 98% of relative intensity with a 5% increment.

APPENDIX 2

The atomic structure of Al_2O_3 thin film (Lee, S.K., Lee, S.B., Park, S.Y., Yi, Y.S., and Ahn, C.W., 2009, Physical Review Letter) While the structure of amorphous alumina has diverse industrial applications as catalyst, ceramics, and thin film devices, little is known about their atomic structures including its coordination states due to lack of suitable experimental probes. ^{27}Al MAS and 3QMAS NMR has proven to be extremely useful to resolve, otherwise overlapping Al species in amorphous materials. Here we extended these methods to explore the nature amorphous alumina in thin film and report the first high resolution ^{27}Al MAS and 3QMAS NMR spectra where the presence of distinct Al coordination species including $^{[4]}$Al, $^{[5]}$Al, and $^{[6]}$Al are for the first time demonstrated(figure A3. The calibrated fractions considering rotor background and other factor (i.e. C_q, quadrupolar broadening factor) for $^{[4]}$Al, $^{[5]}$Al, and $^{[6]}$Al are 55 ± 3, 42 ± 3, and 3 ± 2%, respectively. Study of alumina thin film with solid state NMR provides future directions to study single component glasses which are hard to synthesis.

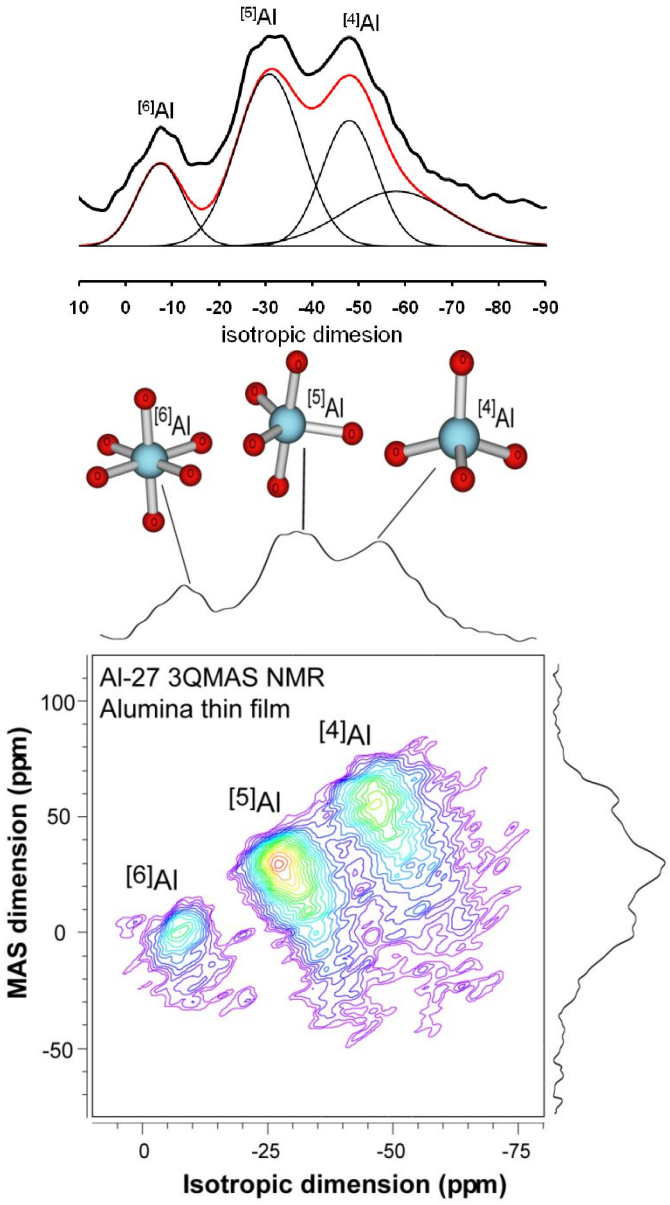

Figure A3. ^{27}Al 3QMAS NMR spectra for alumina thin film. Projections on the isotropic are also shown. (Lee et al., 2009) Contour lines are drawn at 5% intervals from 12% to 97% with added lines at 6% and 9%.

APPENDIX REFERENCE

Alvarez, L.J., Leon, L.E., Sanz, J.F., Capitan, M.J., and Odriozola, J.A., 1994, Surface-structure of cubic aluminum-oxide Physical Review B, v. 50, p. 2561-2565.

Bunker, B. C., Kirkpatrick, R. J., Brow, R. K., 1991, Local-structure of alkaline-earth boroaluminate crystals and glasses .1., crystal chemical concepts structural predictions and comparisons to known crystal-structures, Journal of the American Ceramic Society 74(6), 1425-1429.

Coster, D., Blumenfeld, A.L., and Fripiat, J.J., 1994, Lewis-acid sites and surface aluminum in alumina and zeolites- A high-resolution NMR-study, Journal of Physical Chemistry, v. 98, p. 6201-6211.

Eng, P.J., Trainor, T.P., Brown, G.E., Waychunas, G.A., Newville, M., Sutton, S.R., and Rivers, M.L., 2000, Structure of the hydrated alpha-Al2O3 (0001) surface, Science, v. 288, p. 1029-1033.

Fitzgerald, J.J., Piedra, G., Dec, S.F., Seger, M., and Maciel, G.E., 1997, Dehydration studies of a high-surface-area alumina (pseudo-boehmite) using solid-state H-1 and Al-27 NMR, Journal of the American Chemical Society, v. 119, p. 7832-7842.

Huggins, B.A., and Ellis, P.D., 1992, Al-27 nuclear magnetic resonance study of aluminas and their surfaces, Journal of the American Chemical Society, v. 114, p. 2098-2108.

Lee, S.K., 2004, Structure of silicate glasses and melts at high pressure: Quantum chemical calculations and solid-state NMR, Journal of Physical Chemistry B, v. 108, p. 5889-5900.

Lee, S.K., 2005b, Structure and the extent of disorder in quaternary (Ca-Mg and Ca-Na) aluminosilicate, American Mineralogist v. 90.

Kresse, G., Schmid, M., Napetschnig, E., Shishkin, M., Kohler, L., and Varga, P., 2005, Structure of the ultrathin aluminum oxide film on NiAl(110), Science, v. 308, p. 1440-1442.

Stierle, A., Renner, F., Streitel, R., Dosch, H., Drube, W., and Cowie, B.C., 2004, X-ray diffraction study of the ultrathin Al2O3 layer on NiAl(110), Science, v. 303, p. 1652-1656.

국 문 요 약

지구 구성 물질들은 성분의 수에 따라 단성분계에서 다성분계로 분류될 수 있다. 이 중 다성분계 비정질 규산염은 유리질, 세라믹, 내화물질의 주요 구성 물질이고 맨틀로부터 생성되는 초기 용융체(melt)의 주요 구성 성분이므로 다성분계 비정질 규산염의 원자구조와 물리 화학적 특성을 밝히는 것은 지구 내부의 마그마의 이동, 지구 시스템의 분화 등의 설명에 실마리를 제공해 준다. 특정 원자 중심의 정보를 제공해주는 고분해능 고상핵자기 공명 분광분석(NMR)은 현무암질 마그마를 포함한 대부분의 자연계의 다성분계 규산염 용융체의 원자 구조 분석에 적합하다. 본 연구에서는 일차원과 이차원 고상 NMR 을 이용하여 현무암질 마그마의 모델 시스템인 투휘석과 Ca-처마카이트를 단종으로 하는 CMAS ($CaO-MgO-Al_2O_3-SiO_2$) 비정질 규산염의 조성에 따른 원자 구조의 변화를 규명하였다. ^{27}Al MAS NMR 실험 결과 모든 조성에 대해 60 ppm 근처에서 $^{[4]}Al$ 피크가 지배적으로 나타나며 이는 Al^{3+}이 네트워크 형성 이온으로 작용한다는 것을 지시한다. 투휘석 성분이 증가함에 따라 피크 위치가 음의 방향으로 4.7 ppm 이동하는 것은 조성에서 Si 의 상대적인 양이 증가하면서 $Q^4(4Si)$가 증가하는 것을 의미하고 이를 통해 Al 주변의 산소가 모두 연결 산소(BO, bridging oxygen)임이 확인되었다. ^{27}Al 3QMAS NMR 실험 결과 1-D MAS NMR 스펙트럼에서는 구별되지 않던 $^{[4]}Al$ 와 $^{[5]}Al$ 의 피크가 분리되어 관찰되었다. 투휘석 성분이 증가하면서 $^{[5]}Al$ 의 상대적인 양이 증가하는 것이 관찰되며 이는 네트워크 교란작용을 일으키는 Mg^{2+} 가 증가하기 때문이다. Ca-Mg 알루미노규산염 내의 $^{[4]}Al$ 에 대한 C_q (quadrupolar coupling constant) 값은 투휘석 조성이 증가할수록 감소하는

경향을 보이며 이는 위상학적 무질서가 감소한 것을 의미한다. ^{17}O MAS NMR 실험 결과 Ca-Mg 알루미노규산염 내에 Ca-NBO (non bridging oxygen)인 Ca-O-Si 와 연결 산소가 ^{17}O MAS NMR 스펙트럼상에서 구별되며 투휘석 성분이 증가함에 따라 NBO 의 상대적인 양이 증가하는 것이 확인되었다. 고해상도 ^{17}O 3QMAS NMR 실험 결과 1D MAS NMR 상에서 확인되지 않던 Al-O-Al, Al-O-Si, Si-O-Si 와 Ca-NBO, {Ca, Mg}-NBO 가 부분적으로 구별되며 산소 주변의 원자환경은 투휘석과 Ca-Mg 알루미노규산염에 대해 이전에 알려지지 않았던 화학적 위상학적 무질서도에 대한 정보를 제공해준다. 투휘석과 Ca-처마카이트가 50:50 으로 섞여 있는 중간 조성에서 상당한 양의 Ca-NBO 가 -64 ppm 정도에서 분리되어 있는 것이 관찰되며 이는 Ca-NBO 와 Mg-NBO 가 생성될 때 랜덤 분포를 가지지 않고 Ca^{2+}가 NBO 를 선호한다는 것을 의미한다. Ca-Mg 알루미노 규산염 내에서 Mg^{2+}는 Si-O-Al 을 포함하는 BO 와 연결되어 전하 균형 양이온으로 작용하는 반면 Ca^{2+}는 네트워크 교란 양이온으로 작용한다. 본 연구에서의 Ca-Mg 알루미노 규산염에 대한 원자 구조는 조성에 따른 거시적 성질의 변화를 설명한다. 예를 들어 $^{[4]}Al$ 과 $^{[4]}Al\text{-}O\text{-}^{[4]}Si$ 의 존재는 비정질 투휘석과 Ca-처마카이트 유사이원계의 혼합 엔탈피가 음의 값을 가지는 것을 설명한다. 규산염 용융체의 점성도는 NBO 가 증가할수록 급격히 감소하는 것으로 알려져 있으나 투휘석과 회장석 이원계에 대해 실험적으로 NBO 의 변화를 밝힌 예는 없다. 본 연구에서는 Ca-Mg 알루미노 규산염의 산소 주변 원자환경을 통해 조성의 변화에 따라 NBO 의 상대적 양이 변하는 것을 실험적으로 증명하였으며 이는 투휘석의 상대적 양이 증가할수록 점성도가 감소하는 측정된 실험값과 일치하는 경향을 보인다.

NBO 와 BO 사이의 Ca^{2+}, Mg^{2+} 선호도는 CaO 와 MgO 의 활동도 계수에 영향을 주므로 궁극적으로 해양도와 중앙 해령에서 생성되는 용융체의 조성의 변화를 유도한다. 또한 지하수나 빗물에 의한 현무암의 용해과정에서 네트워크 교란 양이온과 NBO 사이의 강한 결합력으로 인해 Ca^{2+}에 비해 Mg^{2+}가 더 쉽게 용해된다. 본 연구에서의 결과는 다성분계 비정질 물질의 원자구조를 명확히 규명해 주며 원자구조와 성질 사이의 관계에 대한 새로운 연구 방향을 제시한다.

주요어 :현무암질 마그마, 다성분계 비정질 규산염, 투휘석−Ca−처마카이트 이원계, 핵자기 공명 분광분석, 원자구조